

# END SEAL DEFECTS IN COEXTRUDED REACTOR FUEL ELEMENTS

Keith G. Lakey

and

James B. Risser











44

END SEAL DEFECTS IN COEXTRUDED REACTOR  
FUEL ELEMENTS

by

Keith G. Lakey

B.S., United States Naval Academy  
(1946)

Nav. E., Massachusetts Institute of Technology  
(1951)

James B. Risser

B.S., United States Naval Academy  
(1949)

M.S. in Naval Architecture, Webb Institute of Naval Architecture  
(1954)

Submitted in Partial Fulfillment  
of the Requirements for the  
Degree of Master of Science  
at the

MASSACHUSETTS INSTITUTE OF TECHNOLOGY

July 1957



END SEAL DEFECTS IN COEXTRUDED REACTOR FUEL ELEMENTS

by

Keith G. Lakey and James B. Risser

Submitted to the Department of Chemical Engineering on July 9, 1957 in  
partial fulfillment of the requirements for the degree of Master of  
Science.

ABSTRACT

The coextrusion process for the fabrication of clad reactor fuel elements is investigated to determine methods of optimizing the typical extrusion "defect" between the core and end seal materials.

The influence of cone angle, conical preshaping, and relative material stiffness on the extrusion "defect" is studied under normal production conditions with copper base alloys.

The feasibility of the double extrusion technique with its considerable advantages over conventional methods is demonstrated and shown to be a valuable extension of the coextrusion process.

Several undesirable side effects of coextrusion are studied and their major causes isolated. Shift is shown to result primarily from the effects of uneven lubrication of the extrusion tools. The whiskering phenomenon is studied under various conditions; the conclusion is that the difference in flow velocity of the hard and soft materials in the billet is responsible for their formation. Whiskering is shown to be controllable to a degree by billet geometry.

Supervised by

Albert R. Kaufmann

Associate Professor of Metallurgy

35894



TABLE OF CONTENTS

	<u>page</u>
I. INTRODUCTION	1
II. GENERAL PROCEDURES	11
A. The Apparatus	11
B. Preparation of the Billet	11
C. The Extrusion Procedure	13
D. Preparation of the Specimens	13
E. Marking the Extrusion "Defect"	14
III. THE EXPERIMENTS, THE RESULTS, AND DISCUSSION	
OF RESULTS	15
A. Exploratory Experiments	15
B. The Effect of Cone Angle, Conical Preshaping, and Relative Material Stiffness ("Main Series")	19
C. The Double Extrusion Experiments	57
D. The Shift Experiments	76
E. The Whiskers Experiments	95
IV. CONCLUSIONS	116
V. RECOMMENDATIONS	118
VI. APPENDIX	119
A. Data Sheet	119
B. Determination of the Extrusion Constant, K.	134
C. Location of Original Data	139
D. Literature Citations	140



### LIST OF ILLUSTRATIONS

<u>Figure No.</u>	<u>Title</u>	<u>Page</u>
1.	Simple Billet Assembly (no preshaping).	3
2.	Typical Method of Direct Extrusion	3
3.	Typical "Defects" Produced by Extruding the Uncompensated Billet of Figure 1.	3
4.	The Double Extrusion Process Idealized to a Flat Interface in the Completed Rod.	7
5.	Typical Shift in an Extruded Rod.	9
6.	Typical Whiskers in an Extruded Rod.	9
7.	Typical Dog-Boning in an Extruded Rod.	9
8.	Typical Liner, Cone, and Die Construction.	12
9.	Main Series Billet Assemblies.	21
10.	Billet Components for Series 3.	25
11.	Quantities Measured in Evaluating Extrusion "Defects".	25
12.	Series 1 "Defects" (.5X)	27
13.	Comparison of "Defects" for Repeated Series 1 Extrusions (.5X).	28
14.	Series 2 Front "Defects" (.5X).	29
15.	Series 2 Rear "Defects" (.5X).	30
16.	Series 3 Front "Defects" (.5X).	31
17.	Series 3 Rear "Defects" (.5X).	32
18.	Series 4 Front "Defects" (.5X).	33
19.	Series 4 Rear "Defects" (.5X).	34
20.	Comparison of "Defects" for Reversed Billets and Conical Versus Spherical Preshaping (.5X).	35
21.	Comparison of "Defects" for Reversed Billets and Conical Versus Spherical Preshaping (.5X).	36
22.	"Defect" Length as a Function of $K_1/K_2$ and Interface angle for an Included cone angle of $90^\circ$ .	38
23.	"Defect" Length as a Function of $K_1/K_2$ and Interface angle for an Included Cone angle of $60^\circ$ .	39
24.	"Defect" Length as a Function of $K_1/K_2$ and Interface angle for an Included cone angle of $30^\circ$ .	40
24.1	"Defect" Length as a Function of $K_1/K_2$ and Cone angle for an Interface angle of $0^\circ$ .	41



24.2 "Defect" Length as a Function of $K_1/K_2$ and Cone angle for an Interface angle of $8^\circ$ .	42
24.3 "Defect" Length as a Function of $K_1/K_2$ and Cone angle for an Interface angle of $16^\circ$ .	43
24.4 "Defect" Length as a Function of $K_1/K_2$ and Cone angle for an Interface angle of $24^\circ$ .	44
25. "Defect" Area as a Function of $K_1/K_2$ and Interface angle for an Included Cone angle of $90^\circ$ .	45
26. "Defect" Area as a Function of $K_1/K_2$ and Interface angle for an Included Cone angle of $60^\circ$ .	46
27. "Defect" Area as a Function of $K_1/K_2$ and Interface angle for an Included Cone angle of $30^\circ$ .	47
28. Variation of "Defect" Length with absolute Value of $K$ for $K_1/K_2 = 1$ , $90^\circ$ Included cone angle, and $0^\circ$ Interface angle.	49
29. "Defect" Length for $90^\circ$ Included Cone angle, $0^\circ$ Interface angle, and Various Absolute Extrusion Constants.	50
30. "Defect" Area for $90^\circ$ Included Cone Angle, $0^\circ$ Interface angle, and Various Absolute Extrusions Constants.	51
31. "Defect" Length Comparison Between Three-Element Specimens in which Materials are Interchanged.	52
32. "Defect" Length Comparison Between Specimens having Conical and Spherical Preshaping.	53
33. Series 8 Billet Assembly Prior to First Extrusion.	59
34. Series 8 Billet Assembly Prior to Second Extrusion.	60
35. Components for Clad Double Extrusion, Series 9 and 10.	61
36. Extrusion Press Arrangement for First Extrusion in the Double Extrusion Process.	63
37. Exploded View of Billet Assembly for Series 10.	64
38. "Broken" Billets from Series 8 Showing the Preshape Resulting from First Extrusion.	67
39. Series 8 "Defects" (.5X).	68
40. Comparison of "Defect" Lengths in Double Extrusion and in Normal Extrusion of an uncompensated Billet.	69
41. Series 9 "Defects" (.5X).	72
42. Series 10 "Defect" (.5X).	72



43. Variation of "Defect" Length with Overall and First Area Reduction Ratios in Double Extrusion.	73
44. Cross Section of Naval Brass Billet Components for Series 11.	78
45. Series 11 "Defects" (.5X).	79
46. Series 12 "Defects" (.5X).	79
47. Cross Section of Billet Components for Series 12.	80
48. Series 13 "Defects" (.5X).	81
49. Cross Section of Naval Brass Billet Components for Series 14, 15, and 16.	83
50. Series 14 "Defects" (.5X).	84
51. Series 16 "Defects" (.5X).	84
52. Series 15 "Defects" (.5X).	85
53. Cross Section of Naval Brass Billet Components for Series 17 and 18.	87
54. Series 17 "Defects" (.5X).	88
55. Preparation of Cones for Series 18.	89
56. Series 18 "Defects" (.5X).	90
57. Shift Data from Series 1-4.	92
58. Billet Component Dimensions Common to Series 20-24.	96
59. Cross Section of Billet Components for Series 19.	97
60. Series 19 "Defects" (.5X).	98
61. Cross Section of Billet Components for Series 20.	100
62. Series 20 "Defects" (.5X).	101
63. Cross Section of Billet Components for Series 21.	102
64. Series 21 "Defects" (.5X).	103
65. Cross Section of Billet Components for Series 22.	105
66. Cross Section of Billet Components for Series 23.	106
67. Series 22 "Defects" (.5X).	107
68. Series 23 "Defects" (.5X).	107
69. Metal Flow During Whiskering (Series 23).	108
70. Cross Section of Billet Components for Series 24.	109
71. Series 24 "Defects" (.5X).	110
72. Line of Demarcation between Copper-Nickel Components in Series 24 (1X).	110



	vii
	<u>Page</u>
73. Cross Sections of Naval Brass Billet Components for Series 25.	112
74. Series 25 "Defects" (.5X).	113
75. Typical Graph of Ram Force vs. Ram Travel for a Three-Element Billet.	136



LIST OF TABLES

<u>Table No.</u>	<u>Title</u>	<u>Page</u>
I.	Materials Used in Main Series	19
II.	Materials in Series 2-4	20
III.	Series 5 Billet Composition	24
IV.	Series 6 Billet Composition	24
V.	Series 7 Billet Composition	24
VI.	Series 8 Unclad, Two-Element Billets	58
VII.	Second Extrusion Tool Dimensions, Series 8-10	64
VIII.	Series 9 Naval Brass-Cu Clad Billets	64
IX.	Series 10 U-Zr Core, Zircaloy Clad Billets	64
X.	Surface Finish Combinations for Series 19	99
XI.	O.D. of Core and End Seal Components for Series 20.	99
XII.	Chamfer Configurations for Series 21.	104
XIII.	Average K Values (tsi).	137



ACKNOWLEDGEMENT

The authors wish to express their appreciation to all the employees of Nuclear Metals, Inc. who assisted in the conduct of this investigation and particularly to Mr. Paul Loewenstein and Mr. Herbert F. Sawyer for their guidance and constructive criticism.

A special vote of thanks goes to Mr. Richard Billings, who performed all the extrusions and accomplished the many tasks incident thereto. His many helpful suggestions, his interest in and enthusiasm for the work, and his wholehearted support made this a pleasant and more productive experience for all.



### I. Introduction

Incident to the development of nuclear reactor technology in the past decade, much effort has been directed toward improving methods of fabricating clad fuel elements. The purpose of the cladding jacket is to protect the fuel element from the corrosive and erosive action of the reactor coolant, to contain the fission products, and to restrict dimensional change. The clad must also maintain a maximum rate of heat removal from the fuel element and have a minimum neutron capture cross section. Fabrication of the cladding jacket was accomplished in the beginning by drawing on or simply canning and welding closed.

A method of cladding the fuel in a protective shell by simultaneously extruding the two metals in one operation was first developed by Nuclear Metals Inc. and its predecessor, the M.I.T. Metallurgical Project(1,6). The term "coextrusion" has been applied to this process. At first the technique envisioned reducing the extruded rod by cold work to final size and shape, cropping each end, conditioning the end surfaces, and butt-welding end caps to complete the cladding envelope.

A new aspect of the coextrusion process was introduced when the core, cladding, and end seals (or end caps) were formed near to final size and shape in a single extrusion operation(10). The desirability of producing fuel elements with integral end seals was obvious for several reasons:

- a. No part of the fuel would be exposed during or after extrusion, thus minimizing accountability procedures and possible loss of fuel material
- b. The exact weight of fuel material could be measured in each fuel element prior to assembly of the billet.
- c. The surface of the fuel elements would be free of welded areas.
- d. The fuel elements would be extruded near to final size and shape, minimizing cold work procedures and heat treatment.



Refinement of this new technique and extension of its applicability to tubes and other fuel element sizes and shapes has progressed rapidly (13,8,7,9,11,2,14,16,17,3,15,4,5.)

In all of these investigations, much attention has been focused on the characteristic extrusion "defect" which is defined as the longitudinal departure of the core from a flat interface at the junction between the core and end seals. Figures 1,2, and 3 will help the reader visualize in simplified form how a typical extrusion "defect" is produced from a simple (uncompensated) billet. Figure 1 shows the elements of a typical billet assembly. All components are accurately machined, acid cleaned, and assembled in the copper can, which is then evacuated and sealed. This "canning" serves several useful purposes:

- a. It prevents direct contact between the cladding and the extrusion tools, thereby preventing galling of the cladding.
- b. It eliminates possible oxidation at extrusion temperature of the cladding and fuel alloy metals.
- c. The soft copper envelope serves as a lubricant during the extrusion process.
- d. It permits a vacuum to be maintained in the billet assembly which aids the formation of clean metallurgical bonds between the core and cladding during extrusion.

The nose plug is shaped to the angle of the cone shown in Figure 2 and helps induce steady state flow conditions. The end plug (or cut-off) shown at the rear of the billet prevents loss of cladding material since it forms the unextruded butt of material that remains in the liner; this must be cut off after the extrusion is completed.

After the billet is thoroughly lubricated and heated to extrusion temperature, it is placed in the press and extruded through the die by the force which is applied by the ram. The steel cone between the die and the billet directs the flow of metal to maintain uniform deformation and avoid areas of turbulent flow, thus producing a uniform thickness of cladding on the finished rod.



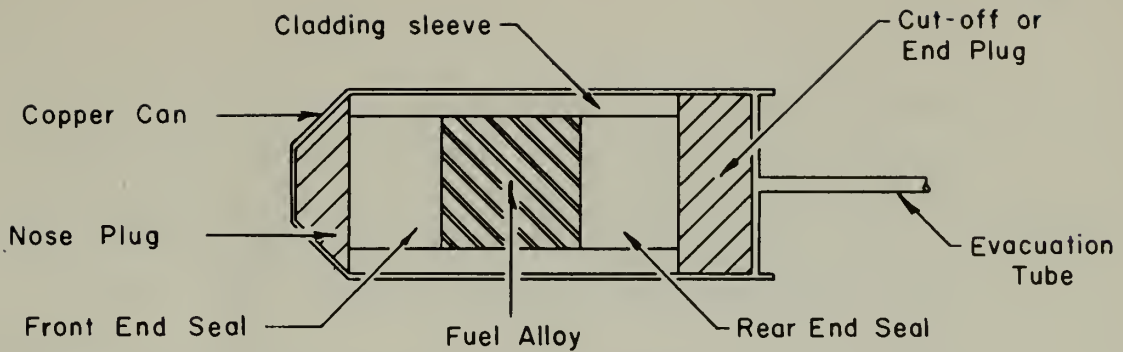


Figure 1 - Simple Billet Assembly (no Preshaping)

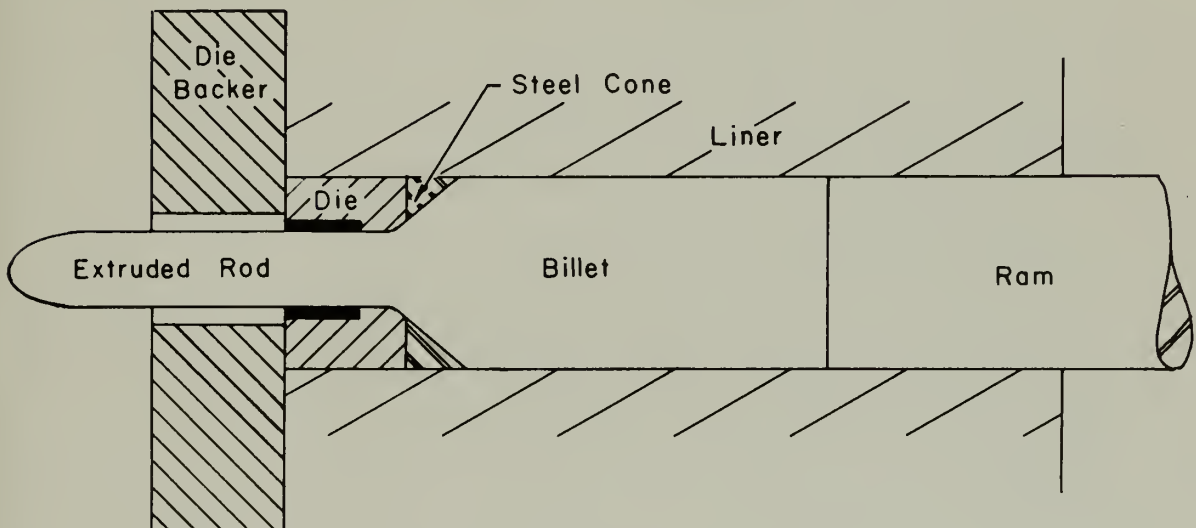


Figure 2 - Typical Method of Direct Extrusion

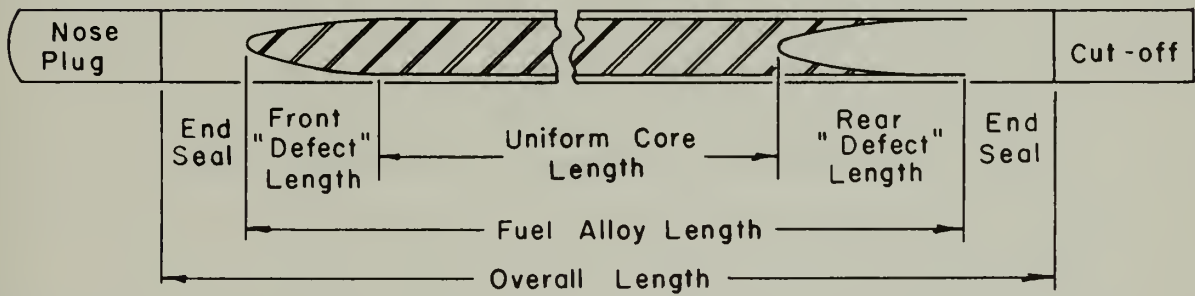


Figure 3 – Typical "Defects" Produced by Extruding the uncompensated Billet of Figure 1



In the "direct" extrusion process shown in Figure 2, the ram and billet move relative to the container in the direction of the die. In the "inverted" extrusion process, the ram and die move relative to the liner with the billet stationary while the extruded rod passes out through a hole in the ram. Only "direct" extrusions were performed in this investigation.

Figure 3 shows a cross section through a typical fuel rod which might result from the direct extrusion process just described. The extrusion "defect" occurs at the junction between the end seal material and the fuel alloy material. Although streamlined flow is present (i.e. all metal remains proportionately distant from center to outside) there is a difference in flow velocity over the cross section which results in greater movement of the central portion of the billet.

To meet the necessary conditions of fuel distribution and consequent neutron flux distribution in reactor design, it is obviously important that stringent restrictions be placed on the distribution of fuel alloy within the element itself. Thus a perfectly flat interface after extrusion, or what amounts to no "defect", is the optimum which is being sought. In actual practice, fuel element specifications will usually include the overall length, the end seal length, the uniform core length, and the longitudinal weight distribution. Although efforts to minimize the "defect" length in order to meet the above specifications have met with considerable success, most studies have been of a trial and error kind, only to optimize the fabrication procedure for a particular fuel element design.

Some of the factors which may conceivably affect the "defect" length are the cone angle, the relative stiffness of core and end seal (and cladding) materials, ram speed, liner temperature, billet temperature, area reduction ratio, cone material, position of the interface in the billet, cone opening, lubrication techniques, and geometry of the interface before extrusion, i.e. compensation or preshaping. It has been shown by previous investigators(11,15,19) that the "defect"



length increases appreciably with billet temperature and area reduction ratio, as would be expected. A number of exploratory experiments were performed to determine the effect of many of the above factors and thus establish the most suitable conditions for the primary experiments which followed.

Although the general practice has been to use cones with an included angle of  $90^{\circ}$ , the results of limited experiments with smaller cone angles (11,15) have indicated that an optimum "defect" length may be obtained with an included cone angle of around  $45-50^{\circ}$ . This possibility was investigated further by the present authors.

The effect of relative stiffness of material has been systematically investigated by Wegner(19), who used soft lead-antimony alloys under experimental extrusion conditions. These results were extended in the present investigation to materials having extrusion constants which more nearly match those of the usual reactor fuel element materials, and the extrusions were performed under production conditions.

In addition to varying the extrusion conditions in order to obtain a minimum "defect" length, the most profitable technique has been to preshape the interface between the core and end seal material in the billet so that a minimum "defect" length is approached as a final result. In the extrusion of rods, this is now accomplished by machining a concave segment of a sphere on the front of the core and a convex segment of a sphere on the rear of the core with matching shapes on the end seal surfaces. The same principle is applied to the fabrication of tubular fuel elements, in which case the preshape geometry becomes quite complicated. The necessary compensating volume can be determined roughly by the measured volume of metal involved in the extrusion "defect" from an uncompensated billet; however, this analogy relates only to the order of magnitude required for optimum compensation; the exact preshape required for a particular job must be arrived at by trial and error tempered by past experience. In the present work, the effects of a conical preshape were investigated in conjunction with the



experiments relating to the effects of cone angle and material stiffness.

In order to reduce machining losses, some consideration has been given to preshaping the billet components in a forging die(11); however, more work will be required to prove the feasibility of this technique.

One of the most interesting ideas for reducing the "defect" length was proposed by Wegner(19) as a result of his work at Nuclear Metals, Inc. in 1956. This "double extrusion" technique envisions extruding the billet twice in opposite directions, as shown schematically in Figure 4. Thus by giving the interface a "natural" preshape in the extrusion press, it is conceivable that this compensation will be exactly cancelled out during the second extrusion, producing a flat "defect" in the completed rod. The obvious advantages to be gained by the use of such a technique are:

- a. No loss of time and labor in machining compensation into the billet components.
- b. Realization of 100% yield from fuel alloy stock.
- c. Elimination of costly accountability procedures during machining operations.

For both the first and second extrusions in his double extrusion experiments, Wegner selected an area reduction ratio which was the square root of the final overall ratio. This produced a final "defect" which was much longer and in the opposite direction to that of the second extrusion. This "reversal" resulted simply from overcompensation in the first extrusion and can be eliminated by a combination of small reduction in the first extrusion to form the proper compensation with a much larger reduction in the second extrusion. Investigation of the feasibility of the double extrusion process and its application to the fabrication of an actual fuel rod was one of the primary objectives of the present work.

In addition to the extrusion "defect" itself, several undesirable side effects of the coextrusion process have assumed critical importance due to the rigid specifications which must be met in the fabrication of reactor fuel elements. These have been descriptively termed



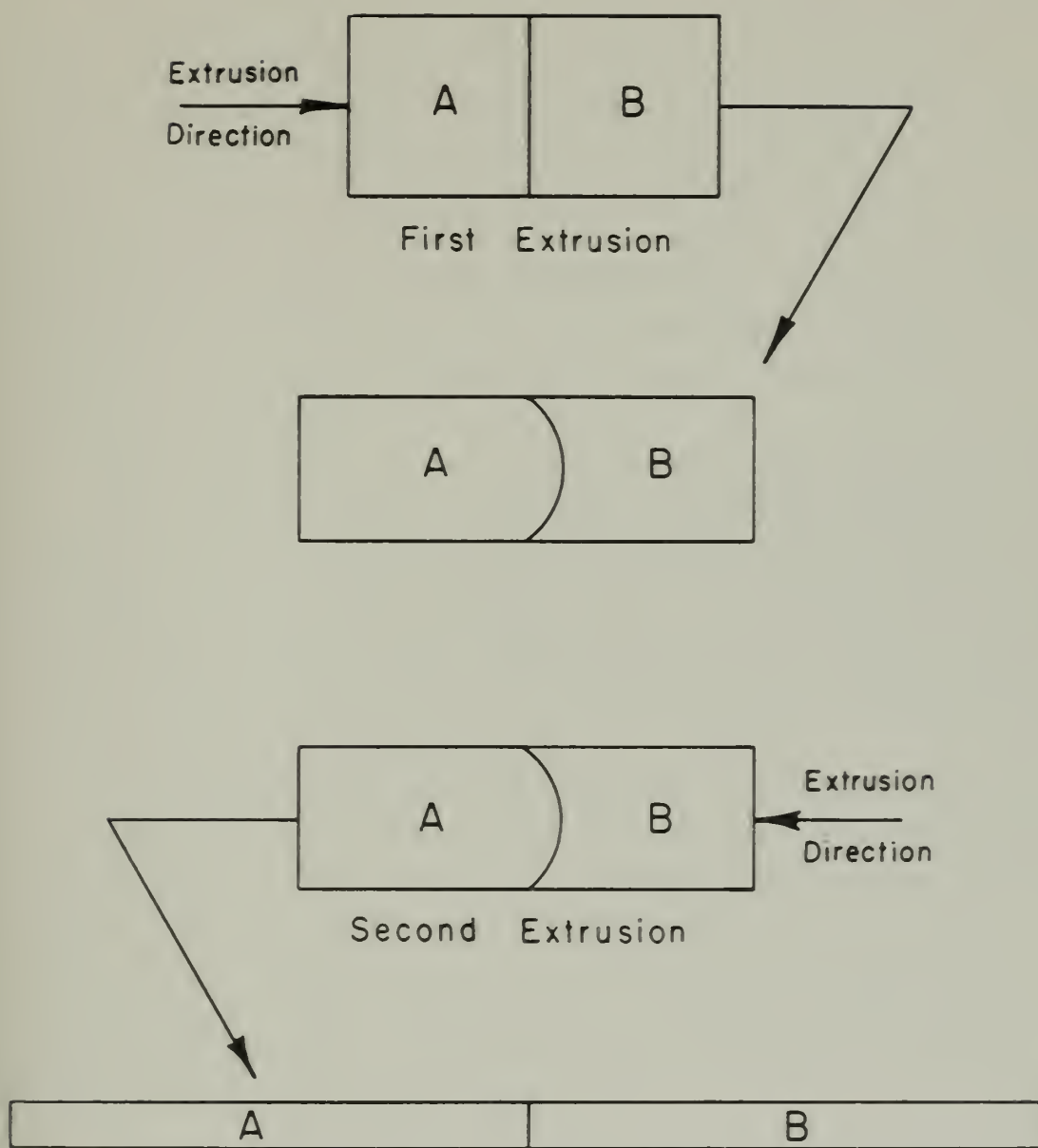


Figure 4 - The Double Extrusion Process Idealized to a Flat Interface in the Completed Rod



"shift", "whiskering", and "dog-boning".

The phenomenon of shift is illustrated in Figure 5. It results from unequal movement of the billet material during the extrusion process and is measured by the longitudinal displacement, or "shift", of points which occupied the same longitudinal position in the billet prior to extrusion. Shift becomes critical when its magnitude approaches that of the "defect" itself, in which case it comprises a significant portion of the total "defect" length. Although a number of possible explanations for the occurrence of shift have been offered, no objective appraisal of its causes was made prior to the present investigation.

The significance of the term "whiskering" can be seen from Figure 6. This extrusion phenomenon consists of hairlike projections of the core material toward the surface of the cladding, thus reducing the thickness of the cladding envelope, which is one of the most critical fuel element specifications. Whiskering has been observed to occur when a relatively soft fuel alloy is coextruded with a hard (or stiff) cladding and end seal material.

As indicated in Figure 7, "dog-boning" is a flattening or ballooning of the fuel alloy at the interface, and occurs when a hard core material is coextruded with a relatively soft cladding and end seal material. As was the case with whiskering, its undesirable effect is to reduce the cladding thickness and thus increase the probability of a fuel element casualty. Although no experiments were specifically designed to study dog-boning, it occurred a number of times and will be discussed briefly.

To summarize the above, the objectives of this investigation can be stated as follows:

- a. To perform a number of exploratory experiments in order to establish conditions for the work which would follow.
- b. To systematically investigate the variation of extrusion "defect" length as a function of cone angle, relative material stiffness, and conical preshaping.



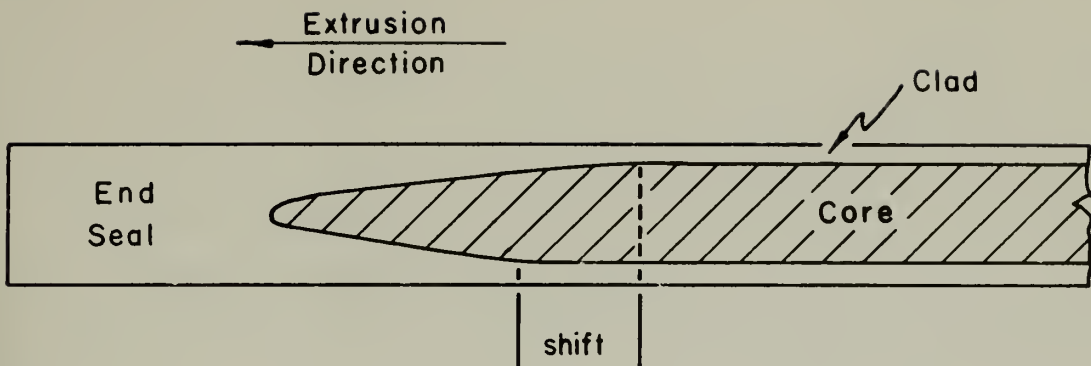


Figure 5 - Typical Shift in an Extruded Rod

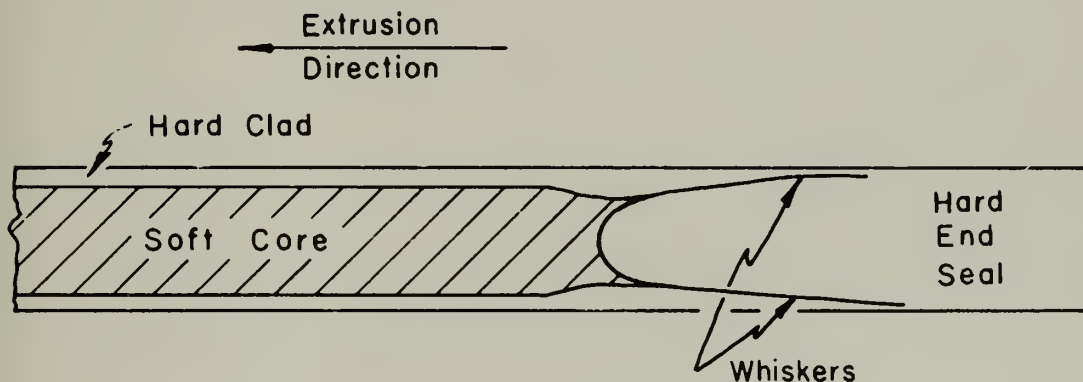


Figure 6 - Typical Whiskers in an Extruded Rod

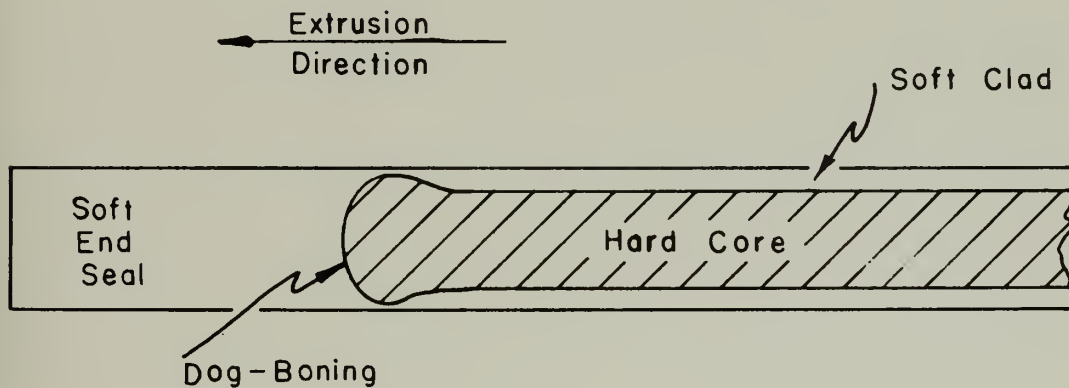


Figure 7 - Typical Dog-Boning in an extruded Rod



- c. To investigate the feasibility of the double extrusion process and its practical application to fuel element fabrication.
- d. To isolate the factors which contribute to shift.
- e. To investigate the mechanism of whisker formation and determine methods of controlling its effect.

The experimental work necessary to accomplish the above objectives required the extrusion of about 200 circular rods grouped into 33 distinct series. Each extrusion was performed under carefully controlled conditions with normal production equipment, techniques, and personnel at Nuclear Metals, Inc.



## II. GENERAL PROCEDURES

In this chapter the procedures which were generally applicable to the majority of experiments will be described in detail. When the information being sought, in a particular series, required other procedures a complete description will be found in the appropriate section of Chapter III.

### A. THE APPARATUS

All experiments were performed in a Watson-Stillman, 300 ton, horizontal, hydraulic extrusion press. The billets were heated to extrusion temperature in a electric furnace, and temperature control was accomplished by the use of Chromel-Alumel thermocouples and a calibrated potentiometer indicator.

The construction of the liner, cones, and dies used in most of the experiments is shown in Figure 8. The liner used throughout this investigation had a container constructed of hot work steel with a Rockwell hardness of 45C, and a tapered sleeve of high speed steel (18-4-1). All 90° cones were machined from cold rolled steel, while the 60° and 30° cones were of stainless steel.

The internal dies were made of high speed steel (18-4-1) with a Rockwell hardness of 45-50 C. The width of the die land varied from .125" to .150", and the die opening varied from .450" to .455".

### B. PREPARATION OF THE BILLET (the canning technique).

The cans were fabricated from 2" outside diameter copper tubing with 1/16" wall thickness. Where conical internal nose plugs were used, one end of the can was formed to a matching surface by flame heating and spinning over an appropriate mandrel.

All billet components were cleaned by pickling in a solution of equal parts nitric acid and water, rinsed in hot water, dried, and assembled with stainless steel tongs. Any excess can material was then cut off, and a copper cap containing the evacuation tube was welded on. The weld was ground, visually inspected, and air tested for leaks.

The billet was then evacuated by connecting the evacuation tube to a vacuum pump for about two hours. During the initial evacuation period,



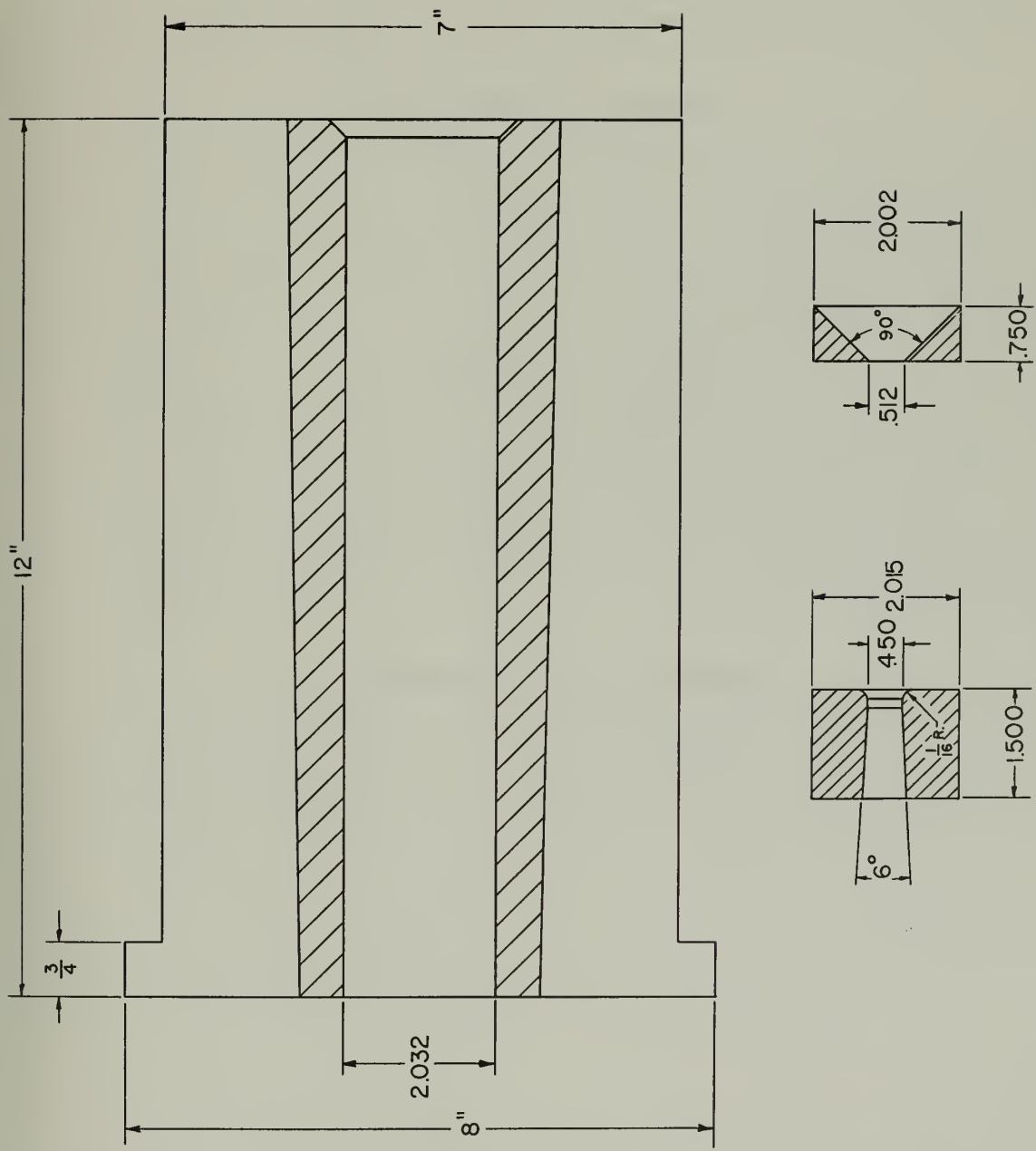


Figure 8 - Typical Liner, Core, and Die Construction. RC-164



flame heat was applied to the billet to help drive out any entrapped gas and air. After the evacuation period, the tube was heated to a cherry red, crimped in two places, and cut off between the crimps.

After cooling, the billet was lubricated by the application of several coats of "Aquadag" (colloidal graphite in water-22% solids) diluted with alcohol. Between coats the billet was dried and brushed to remove graphite scale. The billet was then placed in the electric furnace to heat for about two hours.

#### C. THE EXTRUSION PROCEDURE

Because of the lower temperature involved, the liner, cone, and die were generally heated in different furnace from the billets. When all components were at the proper temperature, the press was readied, the liner was placed in the press, and the proper cut-off (ram stopping point) and speed were set. The liner, cone, and die were then lubricated with "Oildag", a colloidal suspension of graphite in oil.

The billet was handled with tongs from the furnace and inserted in the liner. After insertion of the cone and die, the press door was closed, a catch tube was positioned, and the billet was extruded. Immediately after extrusion, the top of the rod was marked through a hole in the top of the catch tube, the butt was cut off, and the rod was put aside to cool.

#### D. PREPARATION OF THE SPECIMENS

The extrusion "defects" in each rod were studied by milling on the diameter which was vertical as the rod was extruded. The top of each specimen was indicated by an arrow stamped at the rear end. The five-digit extrusion number, and in some cases a two-digit prefix code number, was stamped at the forward end of the specimen. Thus the extrusion direction is always from right to left when the numbers are right side up. When more than one "defect" was contained in a rod, the letters A, B, etc. were stamped in front of the numerals to indicate the order of extrusion.

The specimens were then cut out of the rods, cleaned, etched, and photographed. The macroetching procedure for naval brass (see Chapter III, A. Exploratory Experiments for composition) consisted of thorough



cleaning followed by swabing with concentrated ammonium hydroxide for several minutes.

The copper-zinc alloys in Series 4 and 5 presented the most difficult etching problem. The following procedure gave the best results:

1. Clean in a solution of equal parts nitric acid and water.
2. Dry off and treat with equal parts hydrochloric acid and water.
3. Apply concentrated ammonium hydroxide thoroughly to the surface.
4. Wash off in cold water after film has formed on the surface.
5. Repeat as necessary to obtain uniformity and desired shade.

The Zircaloy clad, uranium-2 w/o zirconium alloy rod of Series 10 was flame heated and allowed to remain in air for several days. This allowed the core material to darken by surface oxidation.

In the photographs of the specimens presented in Chapter III, the darker material is always naval brass, except for Series 4 where the dark material is the copper-zinc alloy, and Series 10 where it is the uranium-zirconium alloy.

#### E. MARKING THE EXTRUSION "DEFECT"

When the billet components were identical materials, it was necessary to provide some method of indicating how the interface between the components was deformed during the extrusion process.

If the billet interface was flat, as it was in most cases, a 0.006" sheet copper shim was placed between the components. With the conical billet interfaces of Series 1, it became necessary to electro-plate .006"-.010" of copper on the male surface. This practice gave excellent results except in the cases of very long "defect" lengths, where the copper line was reduced considerably although still discernible to the naked eye.



### III. THE EXPERIMENTS, THE RESULTS, AND DISCUSSION OF RESULTS

For the purpose of discussion in this chapter, the experiments will be grouped into five major categories and subdivided into series as follows:

- A. Exploratory experiments: series a-h
- B. The effect of cone angle, conical preshaping, and relative material stiffness (main series): series 1-7
- C. The double extrusion experiments: series 8-10
- D. The shift experiments: series 11-18
- E. The whiskers experiments: series 19-25

#### A. EXPLORATORY EXPERIMENTS

##### Series a.

Objective: To determine the effect of ram speed on the "defect" length.

Six canned naval brass billets were extruded with ram speeds of about 1/4, 1/2, and 1 inch per second (full speed) under otherwise identical conditions.

No significant variation of "defect" length with ram speed was noted for materials of equal stiffness; a speed of 1/2 inch per second (half speed on the press) was arbitrarily selected for all the following experiments.

##### Series b.

Objective: To determine the effect of liner temperature on the "defect" length.

Six canned naval brass billets were extruded with the liner at room temperature, 500°F, and 900°F and otherwise identical conditions. No significant variation of "defect" length was noted with these extremes of liner temperature, and it was concluded that no special precautions were necessary to standardize the extrusion procedure in order to eliminate any effects of liner temperature. However, it is good practice to use a hot liner in order to minimize chilling of the billet and thus the



pressure necessary for extrusion. Accordingly, a liner temperature of 900°F was used generally throughout the remaining experiments.

Series c.

Objective: To determine the effect of billet temperature on the "defect" length.

Nine canned naval brass billets were extruded at temperatures of 900°F, 1150°F, and 1400°F and area reduction ratios of 4.93, 20.4 and 33.5.

The "defect" lengths increased significantly with billet temperature, with a much higher increase from 1150°F to 1400°F than from 900°F to 1150°F. For example, at an area reduction ratio of 20.4, the "defect" length increased from 4" to 5 1/4" as the temperature increased from 900°F to 1150°F, while it increased to 9 1/2" when the temperature was increased to 1400°F.

Since in practice the billet temperature is normally higher than that of the liner and other extrusion tools, a billet temperature of 1150°F was selected for the majority of remaining experiments. Another factor which influenced this choice was the desire to prevent overloading and possible stalling of the press in later experiments. At 1150°F, a sufficient reserve of press capacity was available to accommodate all conditions which could be foreseen.

Series d.

Objective: To determine the effect of area reduction ratio and billet size on the "defect" length.

Twelve canned naval brass billets were extruded from .900", 2.000", 3.625", and 4.800" liners. The three extrusions from each liner were at area reduction ratios of about 5, 20, and 30. As would be expected, the "defect length increased monotonically with area reduction ratio and liner diameter. However, a plot of the ratio of defect length to rod diameter versus liner diameter showed a minimum point at the 2" liner for each area reduction ratio. No explanation can be offered for this phenomenon.



A 2" liner and area reduction ratio of about 20 were selected for the remaining experiments because of the above and because they most nearly approached the typical conditions under which many reactor fuel rods are currently fabricated.

Series e.

Objective: To determine the effect of cone angle (see Figure 9) on the "defect" length for billets with a flat interface.

Twenty-eight canned naval brass billets were extruded, with included cone angles of 120°, 90°, 60°, and 30°. Seven area reduction ratios from 2.56 to 33.9 were used with each cone angle.

The results showed a continued lengthening of the "defect" with increasing cone angle at each area reduction ratio. A cone angle of 90° was selected for the remaining experiments, except in the cases where the effect of cone angle was being further investigated. This cone angle is used quite generally in the coextrusion of reactor fuel elements.

Series f.

Objective: To determine if the "defect" length is affected by the position of the interface in the billet.

Three 7-element (similar to Figure 66, with all components naval brass) canned naval brass billets were extruded at area reduction ratios of about 10, 20, and 30.

The "defect" was observed to decrease in length from the front to the rear of the rod. To confirm that this effect occurred in a typical coextrusion, three-element billets were prepared and extruded under similar conditions.

The rear defects were again found to be somewhat shorter than those in the front. This consideration will have some effect on the results of the following experiments and will be discussed further.



Series g.

Objective: To determine the effect of cone opening on the "defect" length.

Six canned naval brass billets were extruded through stainless steel cones with inside diameters ranging from .450" to .1075". The die size was constant at .450" for all extrusions.

The results showed that cone openings which fell within the die entrance radius (1/16") produced "defects" of approximately the same length. However, as the cone opening was increased beyond the entrance radius, the "defect" length increased rapidly.

A cone inside diameter of .512" was selected for the remaining experiments because this value was thought to blend in best with the die entrance radius and would have a minimum effect on the "defect" length as shown above.

Series h.

Objective: To determine the extrusion constants of stock copper and naval brass for use in later experiments.

A number of canned 2" billets were extruded under standard conditions for determination of the extrusion constants (see the Appendix, B. Determination of the Extrusion Constant, K). The results are summarized as follows:

Stock Copper-----12.0 tsi

Unleaded Naval Brass (60% Cu, 39.25% Zn, .75% Sn)-----11.5 tsi

Because it was inexpensive, readily available in bar stock, easy to machine, and easy to extrude, naval brass was selected as the basic metal for most of the experiments which follow.



B. The Effect of Cone Angle, Conical Preshaping  
and Relative Material Stiffness ("Main Series")

1. The Experiments

The objective of the Main Series was to determine the effect of cone angle, conical preshaping, and relative material stiffness upon the "defect" length and area when the extrusion takes place under production conditions. To this end, seven series were extruded under the following conditions:

Area Reduction Ratio:	20.4
Die Diameter:	0.450" to 0.455"
Cone	
O.D.:	2.002"
I.D.:	0.512"
Included Angle:	90°, 60°, 30°
Liner Dia.:	2.032"
Temperature	
Billet Assembly:	1150°F
Liner, Cone, Die:	900°F
Lubrication:	Normal
Canning:	Normal

In order to achieve the objective of the experiments, it was decided to use included cone angles of 90°, 60°, and 30°. On the basis of Wegner's results(19) with preshape (or interface) angles of 0°, 5°, 10°, and 15°, interface angles of 0°, 8°, 16°, and 24° were selected. Materials were chosen according to the following criteria:

- a. having extrusion constants covering a range of from 10 to 25 tsi, since this is the range of K's normally met in fuel element extrusion.
- b. easy to obtain.
- c. extrudable under the conditions of the experiments.

The materials selected are listed in Table I.

Table I. Materials Used in Main Series

Material	Estimated K at 1150°F, tsi
naval brass*	11.5**
Cu-5w/o Zn	17.5***
Cu-10w/o Ni	22.5****
Cu-16w/o Ni	26.0****



\*64% Cu, 39.25% Zn, 0.75% Sn.

\*\*Exploratory experiment average value.

\*\*\*From data by I.B. Roll, Nuclear Metals, Inc., 1953.

\*\*\*\*From data by P. Smoot and A. Block, Nuclear Metals, Inc., 1954.

Series 1-7 are described below: (see Figure 9 for billet geometry.)

#### Series 1

Objective: To determine the effect of cone and interface angles upon the "defect" in naval brass, i.e.,  $K_1/K_2 = 1$ .

Since Series e of A, Exploratory Experiments had accounted for the  $0^\circ$  interface angle case, nine billets, as in Figure 9a, were extruded, one for each combination of cone angle ( $90^\circ$ ,  $60^\circ$ ,  $30^\circ$ ) and interface angle ( $8^\circ$ ,  $16^\circ$ ,  $24^\circ$ ). Because the  $30^\circ$  and  $60^\circ$  cold-rolled steel cones cracked during extrusion, the six billets involved were rerun. After comparison of the "defects", two of the first six extrusions were discarded because the "defects" were strongly affected by the cone failures. The remaining 13 extrusions combined with one  $90^\circ$  cone angle- $8^\circ$  interface angle extrusion made in order to test the plated "shim", and the three extrusions from A, Exploratory Experiments, account for the 17 entries under Series 1 in the Appendix, A, Data Sheet.

#### Series 2, 3, and 4

Objective: To determine the effect of cone and interface angle upon the extrusion "defect" in three-element billets containing two materials of different extrusion constant.

Except for the materials involved, Series 2-4 were identical, each embodying 12 three-element billets (see Figure 9b), one for each combination of cone angle ( $90^\circ$ ,  $60^\circ$ ,  $30^\circ$ ) and interface angle ( $0^\circ$ ,  $8^\circ$ ,  $16^\circ$ ,  $24^\circ$ ). The billet components for Series 3 are pictured in Figure 10. The following table gives the composition of the billets of Series 2-4:

Table II. Materials in Series 2-4

Series	No. Elements	Material (Figure 9b)		
		1	2	3
2	3	naval brass	Cu-9w/o Ni	naval brass
3	3	naval brass	Cu-5w/o Zn	naval brass
4	3	Cu-9w/o Ni	Cu-5w/o Zn	Cu-9w/o Zn

0

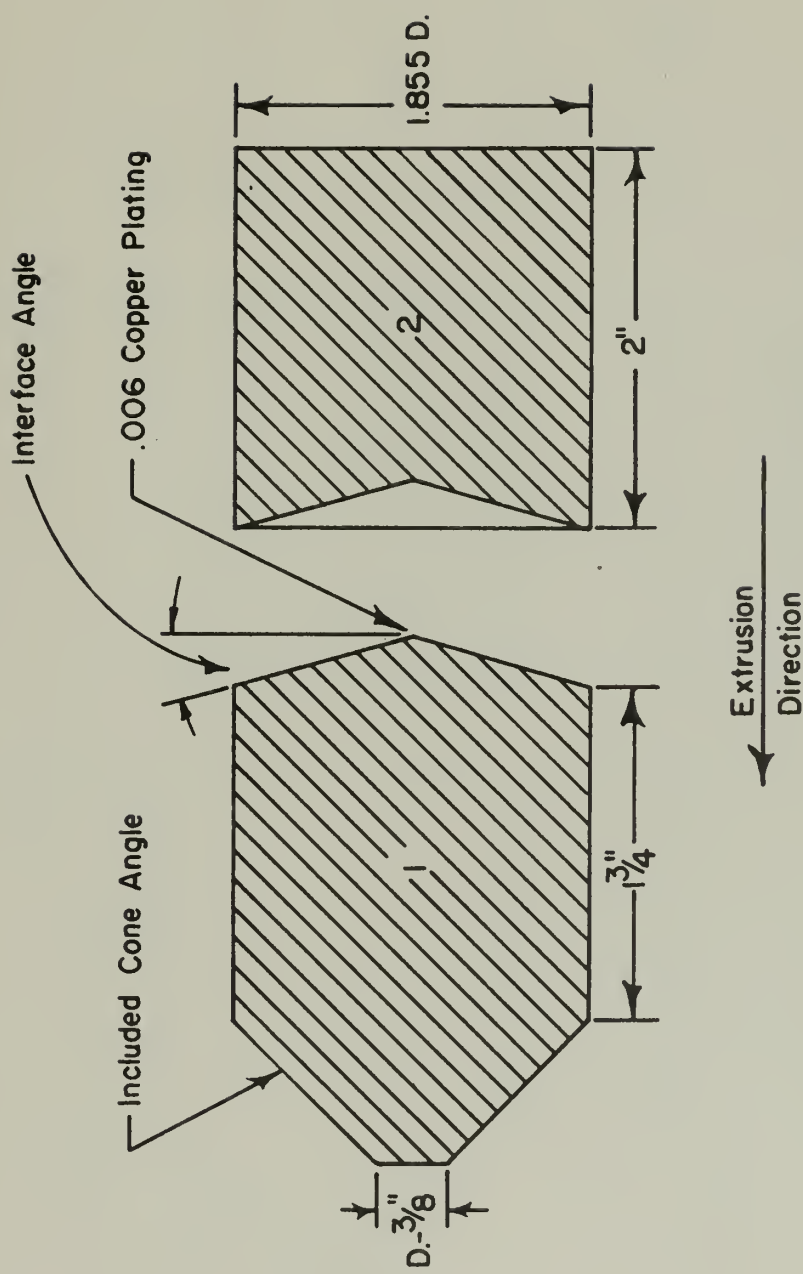


Figure 9a - Two Element Naval Brass Billet (Series 1, 5)



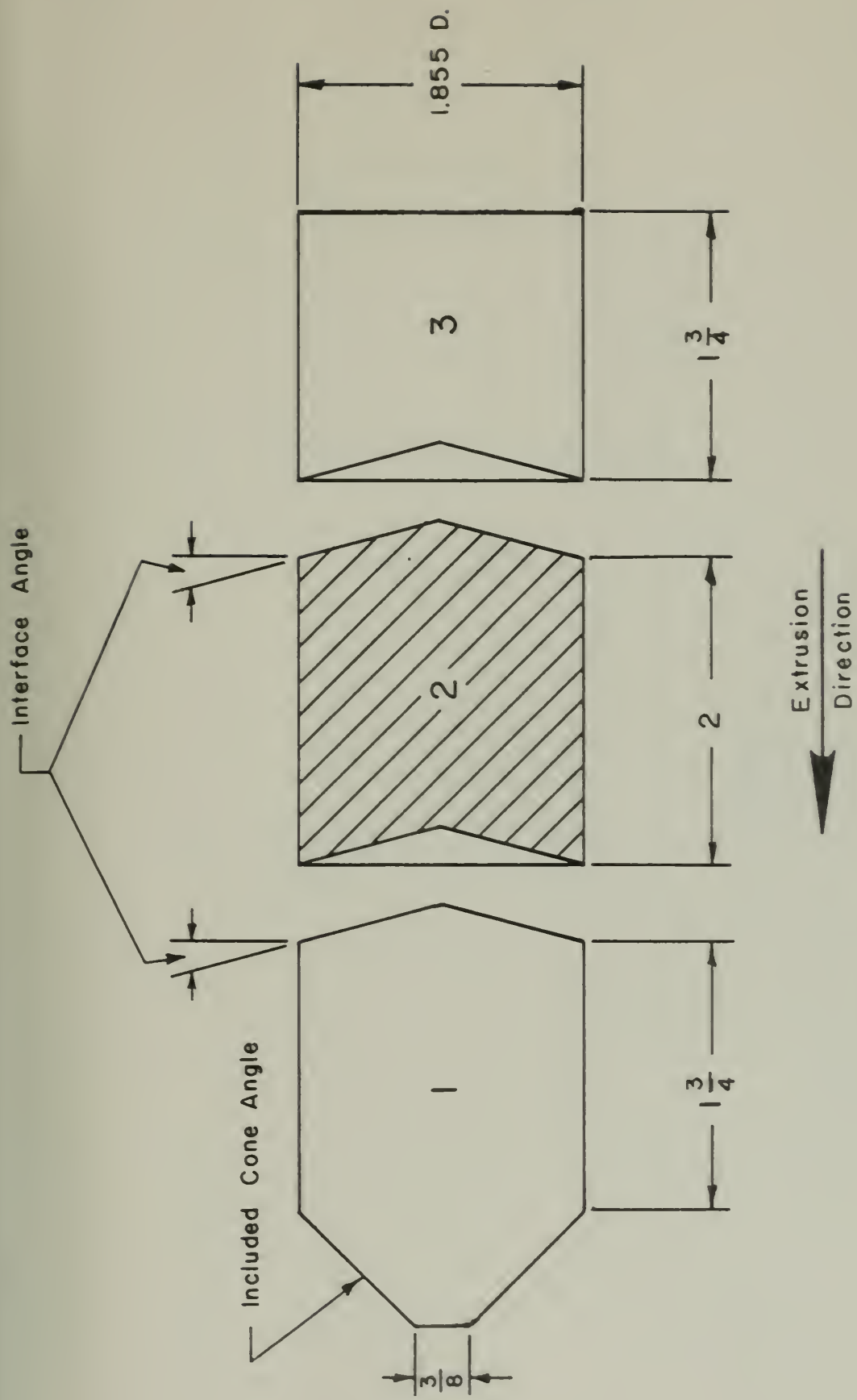


Figure 9A - Three Element Billet (Series 2-6).



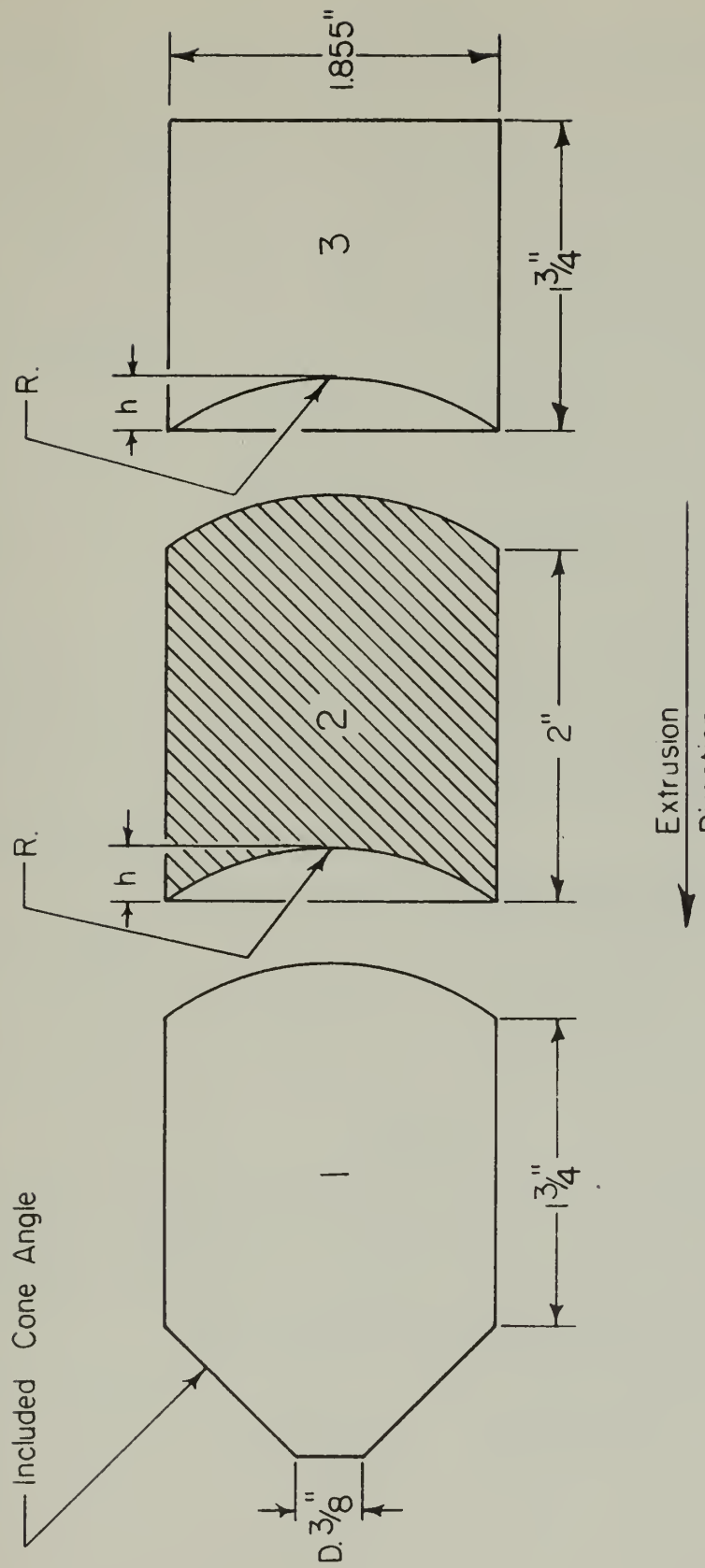


Figure 9c - Three Element Billet (Series 7)



Series 5

Objective: To determine the effect of the absolute value of the extrusion constant upon the "defect".

Series 5 consisted of 7 extrusions, each having 90° included cone angle and 0° interface angle. The following table gives the composition of each billet:

Table III. Series 5 Billet Composition

Extrusion No.	No. Elements	1	Material (Figures 9a and 9b)	2	3
14553	2	Cu-5w/o Zn	Cu-5w/o Zn	-	
14564	2	Cu-9w/o Ni	Cu-9w/o Ni	-	
14574	2	Cu-14w/o Ni	Cu-14w/o Ni	-	
14532	2	Cu-16w/o Ni	Cu-16w/o Ni	-	
14668	3	naval brass	Cu-16w/o Ni	naval brass	
14669	3	Cu-5w/o Zn	Cu-16w/o Ni	Cu-5w/o Zn	
14670	3	Cu-8w/o Ni	Cu-16w/o Ni	Cu-8w/o Ni	

Series 6

Objective: To determine the effect upon the extrusion "defect" of interchanging the arrangement of materials used in Series 2. In this series three three-element billets were extruded, all having a 60° cone angle and, as the following table shows, a material arrangement which is the opposite of Series 2.

Table IV. Series 6 Billet Composition

Extrusion No.	No. Elements	1	Material (Figures 9b)	2	3
14975	3	Cu-9w/o Ni	naval brass	Cu-9w/o Ni	
14976	3	"	" "	"	
14977	3	"	" "	"	

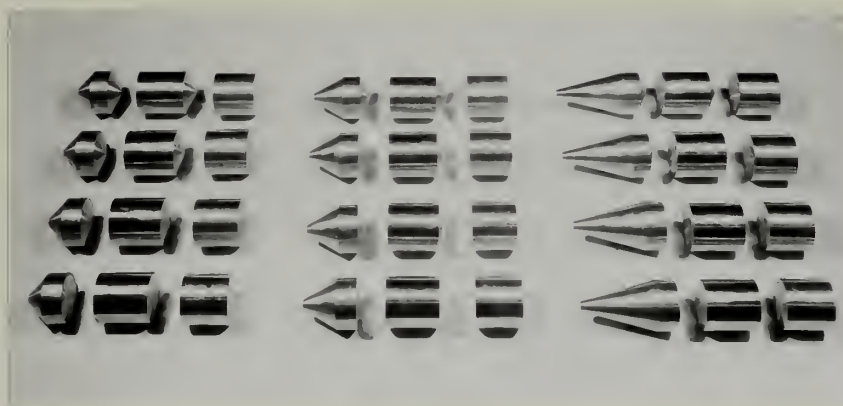
Series 7

Objective: To determine the effect upon the extrusion "defect" when spherical preshaping is substituted for conical preshaping, pre-shape volumes being equal. The table below gives the billet composition:

Table V. Series 7 Billet Composition

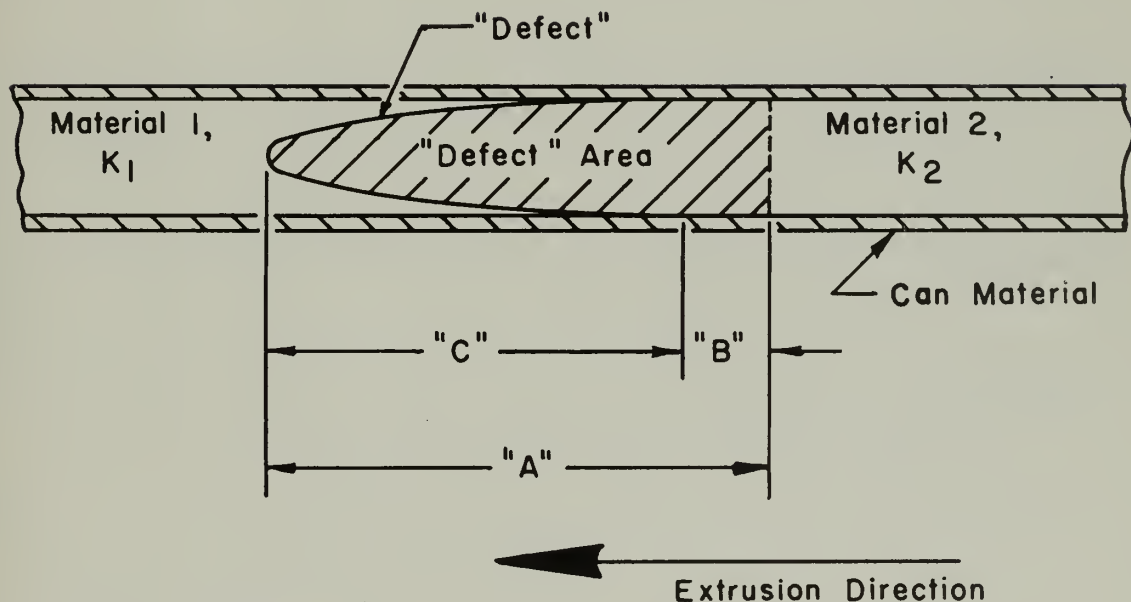
Extrusion No.	No. Elements	1	Material (Figure 9c)	2	3
15005	3	naval brass	Cu-9w/o Ni	naval brass	
15006	3	" "	"	" "	
15007	3	" "	"	" "	





RF 4602

Figure 10 - Billet Components for Series 3.



"A" Gross "Defect"

"B" Shift

"C" Net "Defect"

Figure 11 Quantities measured in evaluating Extrusion "Defects"



It was decided to use three-element billets in cases where different materials were extruded together because experience in fuel element extrusion indicates that with the three-element billet design adopted, there is no appreciable interaction between the front and rear "defects". In addition this procedure results in a considerable saving in time and money over the extrusion of corresponding two-element billets.

Also on the basis of accumulated experience, it was assumed that the position of the "defect" in the billet would not appreciably affect its character. Series 6 was designed to test this assumption. Only if the assumption were justified would direct comparison of front and rear "defects" be possible.

## 2. The Results

a. The Appendix, A. Data Sheet lists the observed results of Series 1-7.  $K_1$  and  $K_2$  are defined as shown in Figure 11.  $K_1$  is the extrusion constant of the first material to pass through the die where a given "defect" is concerned;  $K_2$  is associated with the second material to pass through the die.

The specimen numbering code is explained in the Appendix, A. Data Sheet. The gross "defect" length is measured from the extreme front of the penetration of the second material into the first to the point where the second material assumes a uniform cross section. The "defect" area is the area associated with the gross "defect" length. Net "defect" length is simply the gross "defect" length minus any effective shift. Judgment had to be used in many cases to assess the effect of shift on the net "defect" length, as may be seen in the Appendix, A. Data Sheet.

Figures 12-21 contain photographs of the "defects" produced in Series 1-4, 6 and 7. Series 5 "defects" were not photographed because of difficulty in etching the specimens.

The results of Series 1-7 may best be organized by considering these series as comprising a single body of data. On this basis, analysis of the Appendix, A. Data Sheet and Figures 12-21 yields the following:

(1) The front "defects" in Series 2 ( $K_1/K_2 = 0.584$ ) for interface angles of  $0^\circ$  and  $8^\circ$  show a progressive qualitative improvement as cone



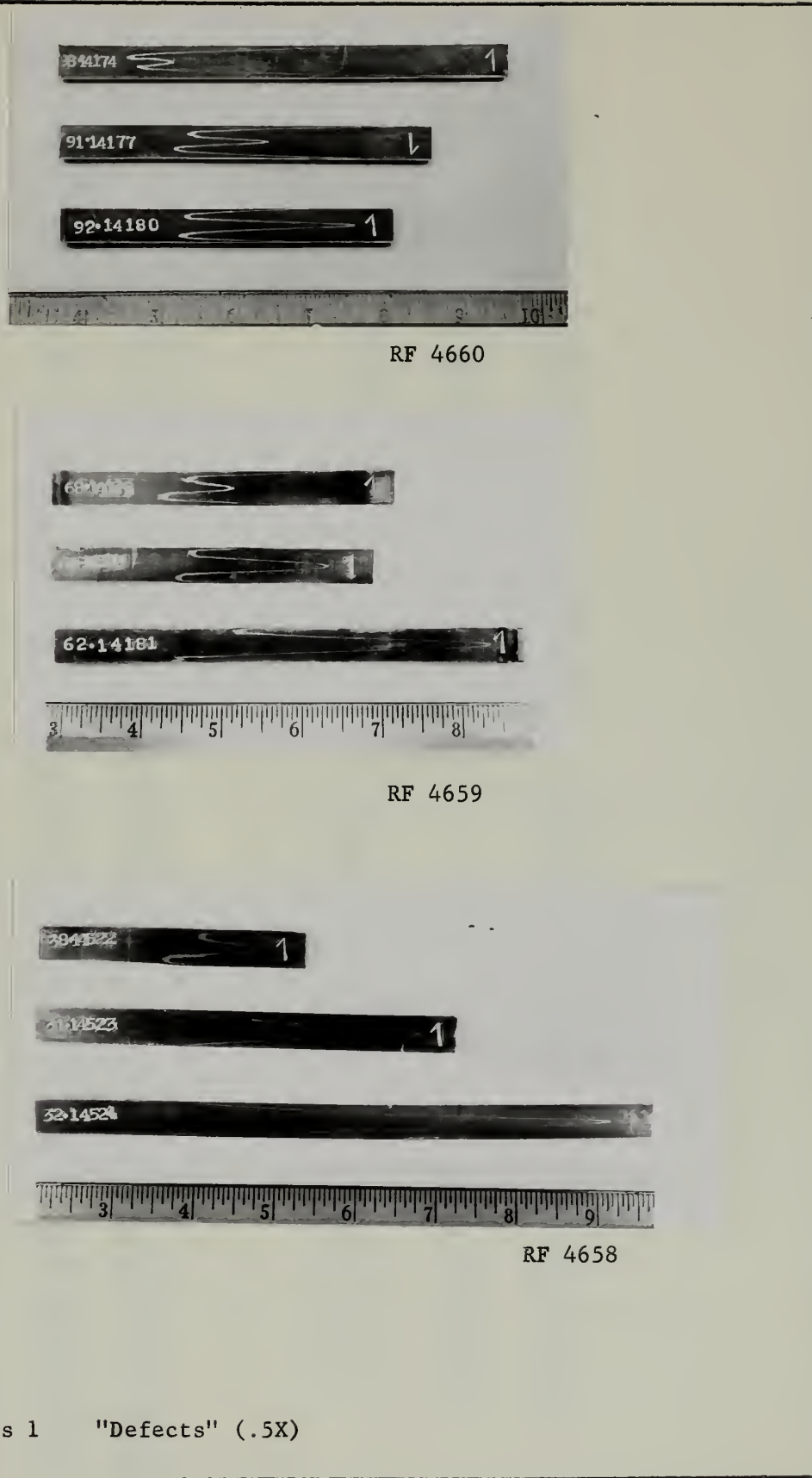


Figure 12 - Series 1 "Defects" (.5X)



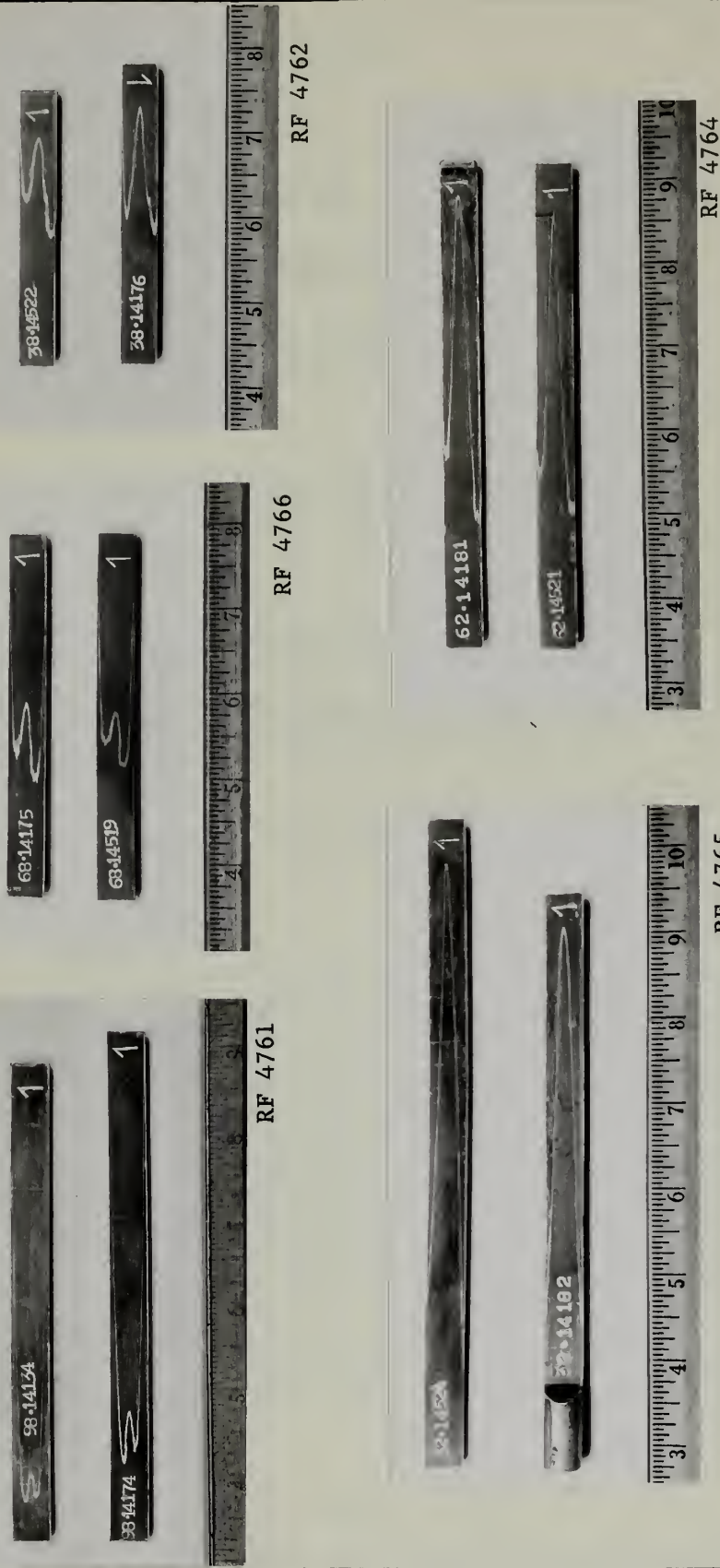


Figure 13 - Comparison of "Defects" for Repeated Series 1 Extrusions (.5X)



A 90-14432 1

A 98-14433 1

A 91-14434 1

A 92-14435 1

1 1 1 2 1 3 1 4 1 5 1 6

RF 4636

A 60-14436

A 68-14437 1

A 61-14438

A 62-14439

1 2 1 3 1 4 1 5 1 6 1 7 1 8

RF 4635

A 30-14440 1

A 28-14441

A 21-14442 1

A 22-14443

1 1 1 2 1 3 1 4 1 5 1 6 1 7 1 8 1 9

RF 4634

Figure 14 - Series 2 Front "Defects" (.5X)



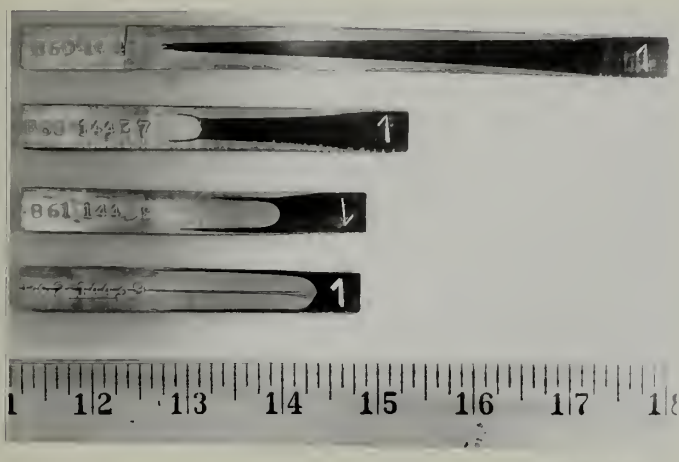
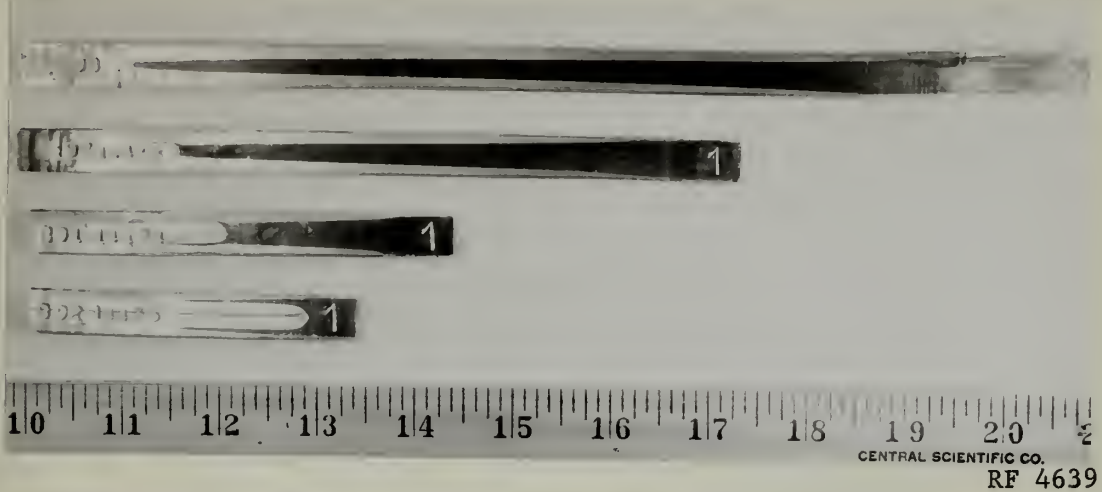


Figure 15 - Series 2 Rear "Defects" (.5X)



A90-14646

A98-14647

A91-14648

A92-14649



RF 4711

A60-14650

A68-14651

A61-14652

A62-14653



RF 4710

A30-14654

A38-14655

A31-14656

A32-14657



RF 4709

Figure 16 - Series 3 Front "Defects" (.5X)

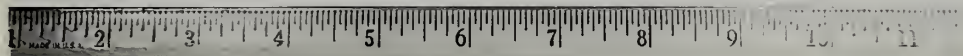


890-14646

898-14647

891-14648

892-14649



RF 4708

893-14650

894-14651

895-14652

896-14653



RF 4707

897-14654

898-14655

899-14656

900-14657



RF 4706

Figure 17 - Series 3 Rear "Defects" (.5X)



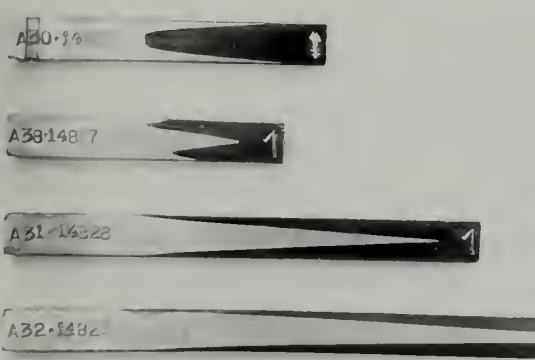
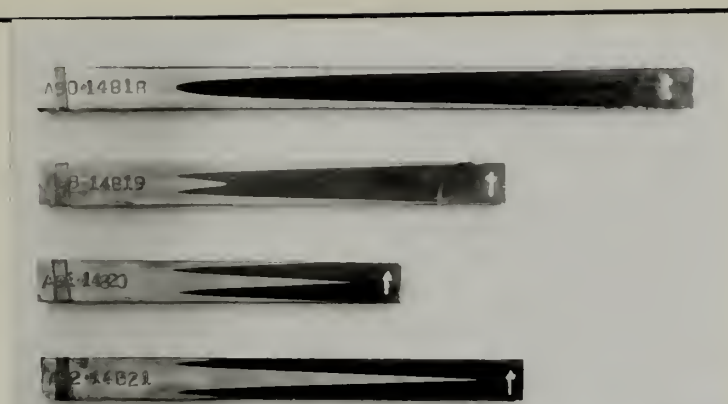


Figure 18 - Series 4 Front "Defects" (.5X)





RF 4782



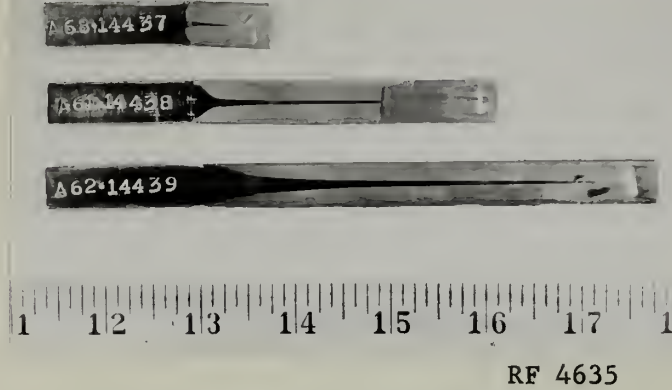
RF 4783



RF 4784

Figure 19 - Series 4 Rear "Defects" (.5X)

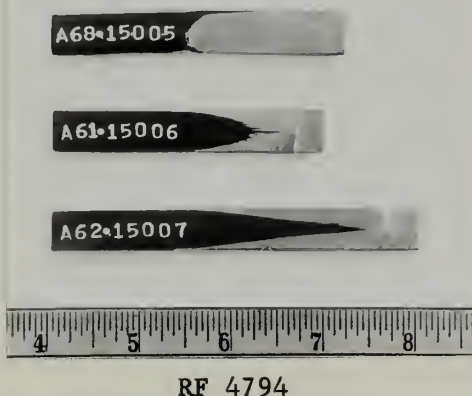




a. Front "Defects" from Series 2



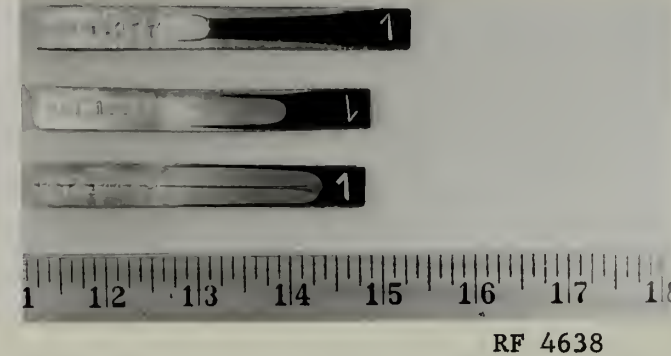
b. Rear "Defects" from Series 6



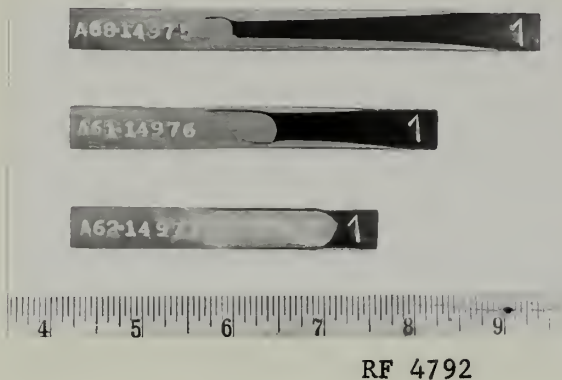
c. Front "Defects" from Series 7

Figure 20 - Comparison of "Defects" for Reversed Billets and conical versus Spherical Preshaping (.5X)





a. Rear "Defects" from Series 2



b. Front "Defects" from Series 6



c. Rear "Defects" from Series 7

Figure 21 - Comparison of "Defects" for Reversed Billets and Conical versus Spherical Preshaping (.5X)



angle decreases. Though the can wall thickness was greatly reduced in the vicinity of the front "defect" in all 0° and 8° specimens in Series 2, reference to Figure 11 clearly shows the decrease in voids and shortening of "defect" length as cone angle decreases. Series 3 shows this same tendency, though "defects" for this series are more satisfactory as the result of the K ratio being nearer to 1.0 ( $K_1/K_2 = 0.667$ ). Front "defects" in both Series 2 and 3 show the typical "dogbone" form associated with extrusion of billets in which the K ratio is less than 1.0, to the point where appreciable overcompensation or reversal of the direction of the "defect" begins. Beyond this point of overcompensation the dogboning tendency diminishes as overcompensation increases. Series 4, of course, has front and rear "defects" clearly akin to those of Series 1, since the K-ratios are near 1.0.

(2) The rear "defects" in Series 2 and 3 show the following tendency: as interface angle increases, for a given cone angle, the tendency of the "defect" to take on the appearance of a whiskers-dogbone "defect" increases. As cone angle decreases this tendency also increases. Series 4 rear "defects", again since the K-ratio is near 1.0, closely resemble those of Series 1.

(3) As Figure 13 shows, reproducibility of the "defects" in Series 1 repeated billets is fair. The maximum variation in "defect" length is about 20%.

b. Figures 22-24.4 are plots of net "defect" length against K-ratio for various cone and interface angles. The K-ratios used are bases upon average K's, for reasons explained in the Appendix, B. Determination of Extrusion Constant, K. Similarly, Figures 25-27 are plots of "defect" area against K-ratio for various cone and interface angles. Data upon which these plots were based are from Series 1-5.

Analysis of these ten plots yields the following:

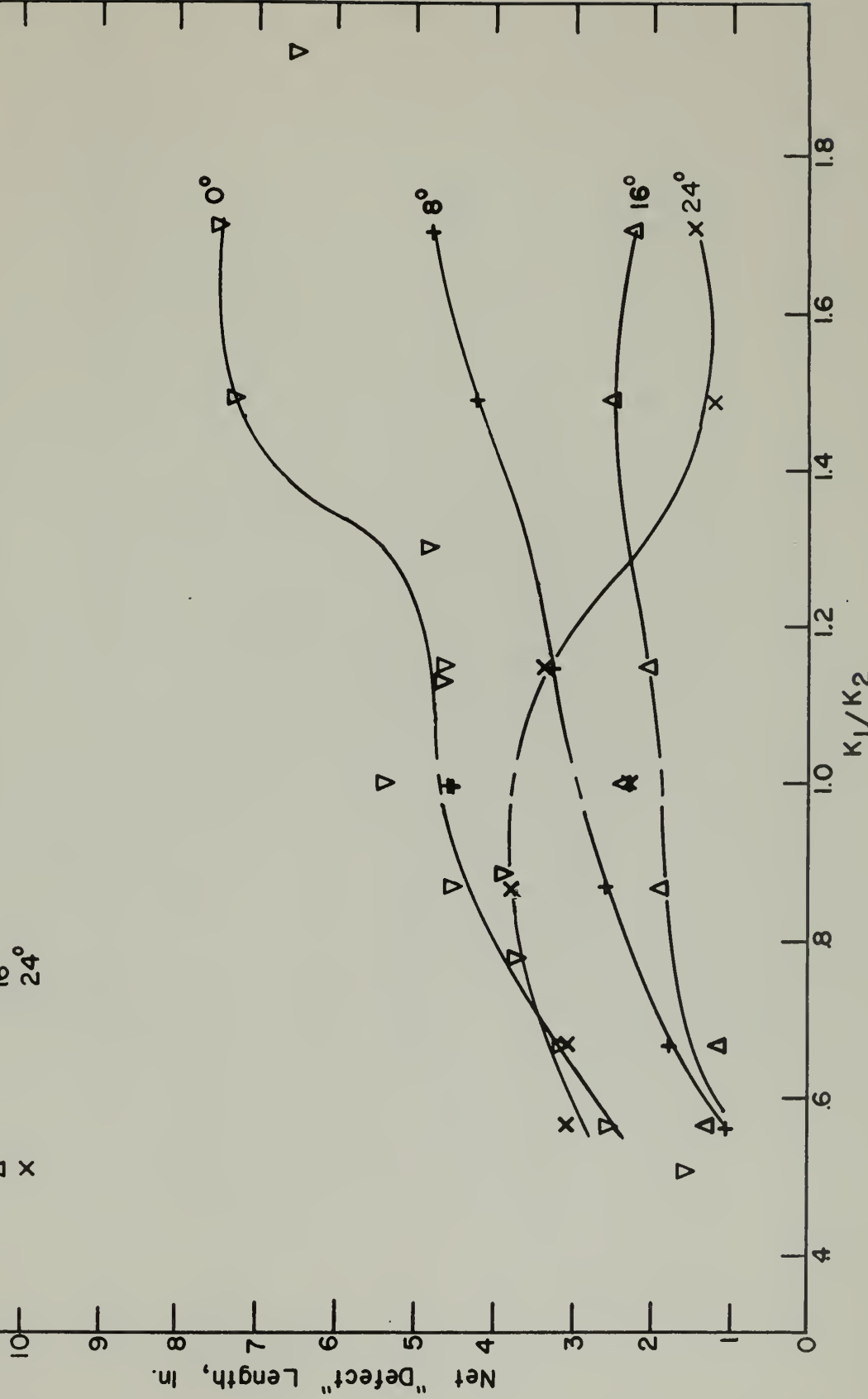
(1) The area and length plots show a good qualitative correspondence, that is, the variation of "defect" area and length have the same general trend for increasing K-ratio.



Symbol

	<u>Interface Angle</u>
▽	0°
+	8°
△	16°
×	24°

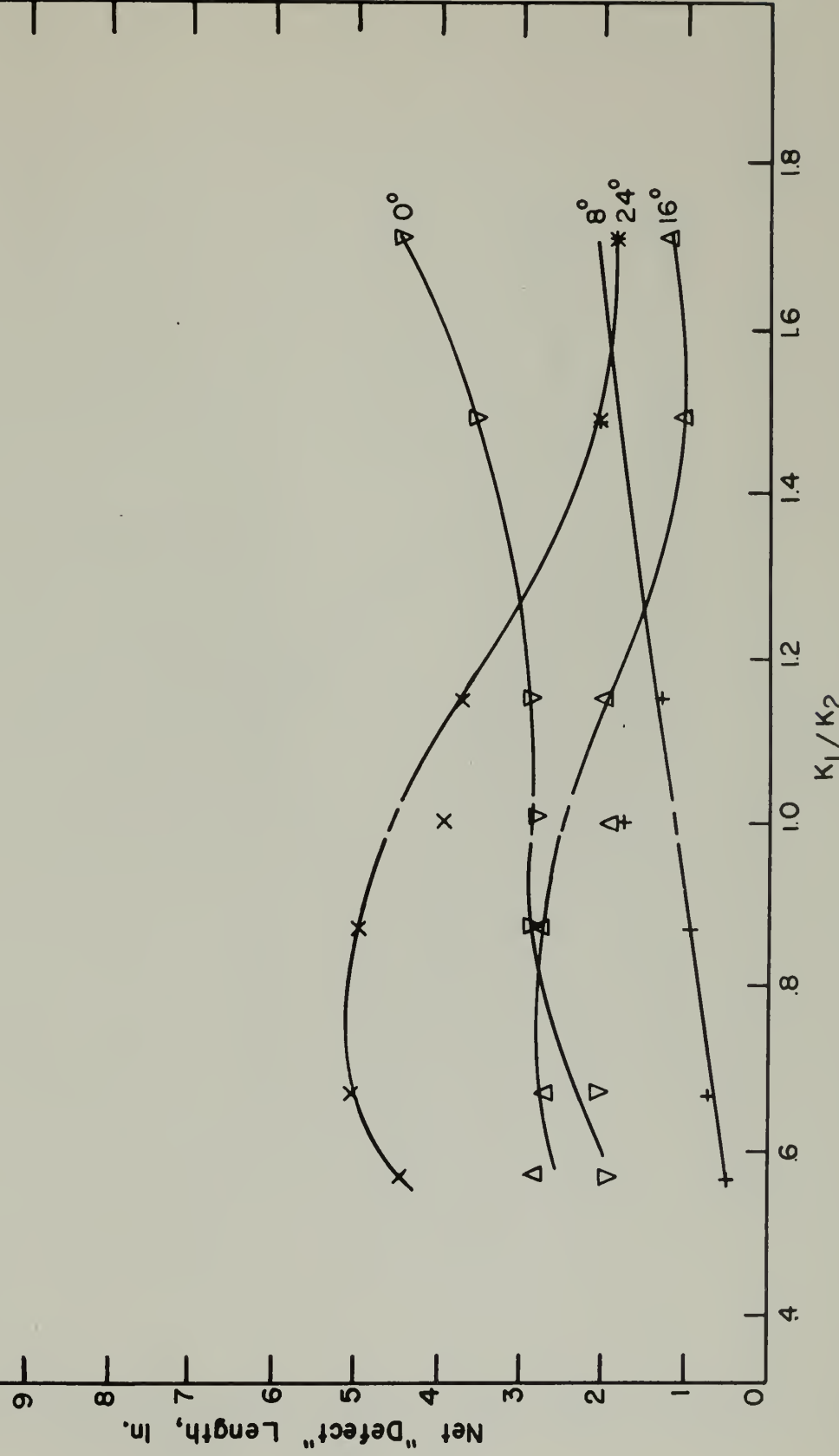
Figure 22 - "Defect" Length as a Function of  $K_1/K_2$  and Interface angle for an Included cone angle of 90°.



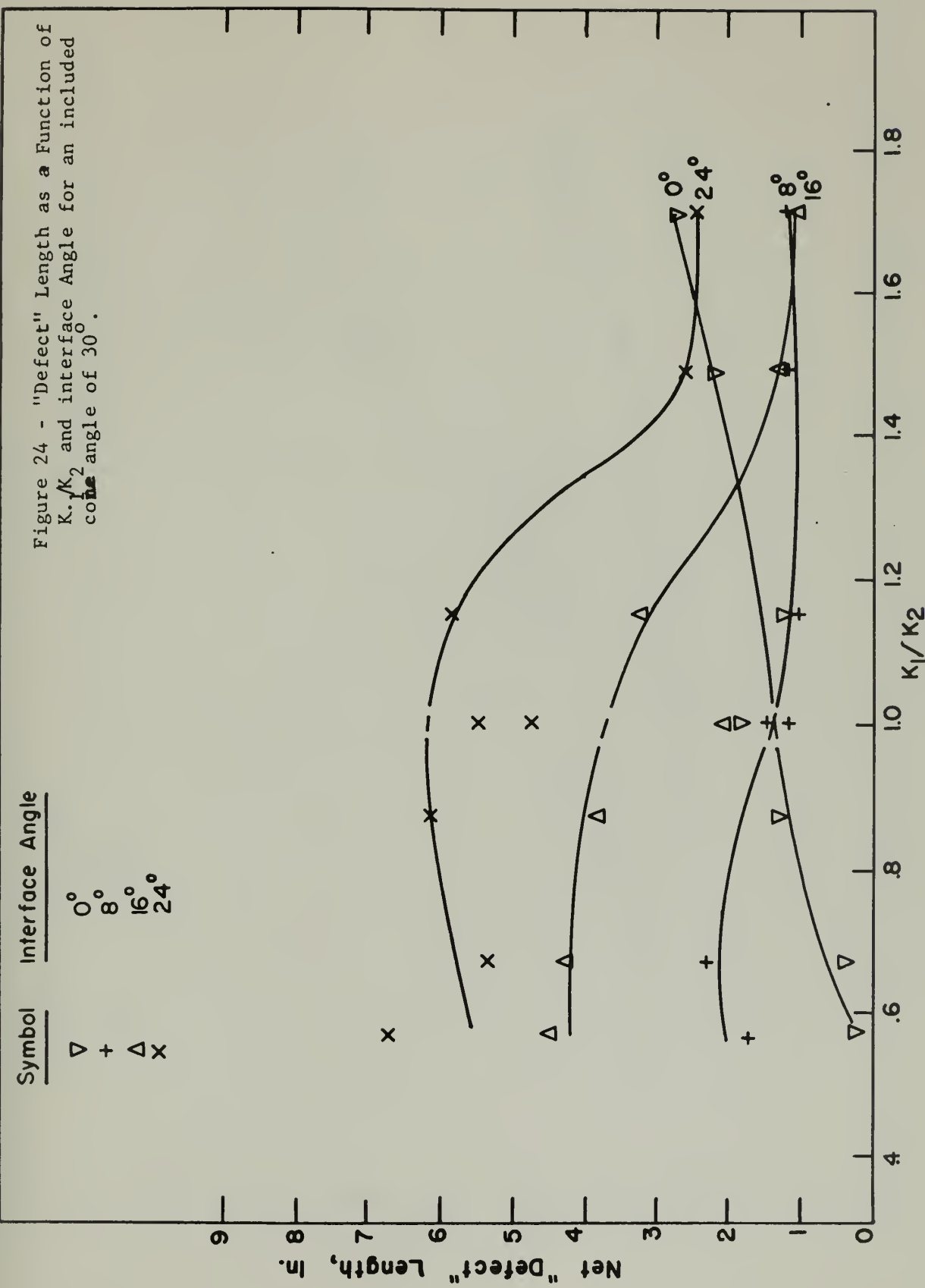


Symbol	Interface Angle
$\nabla$	0°
+	8°
$\Delta$	16°
$\times$	24°

Figure 23 - "Defect" Length as a Function of  $K_1/K_2$  and Interface angle for an Included cone angle of 60°.



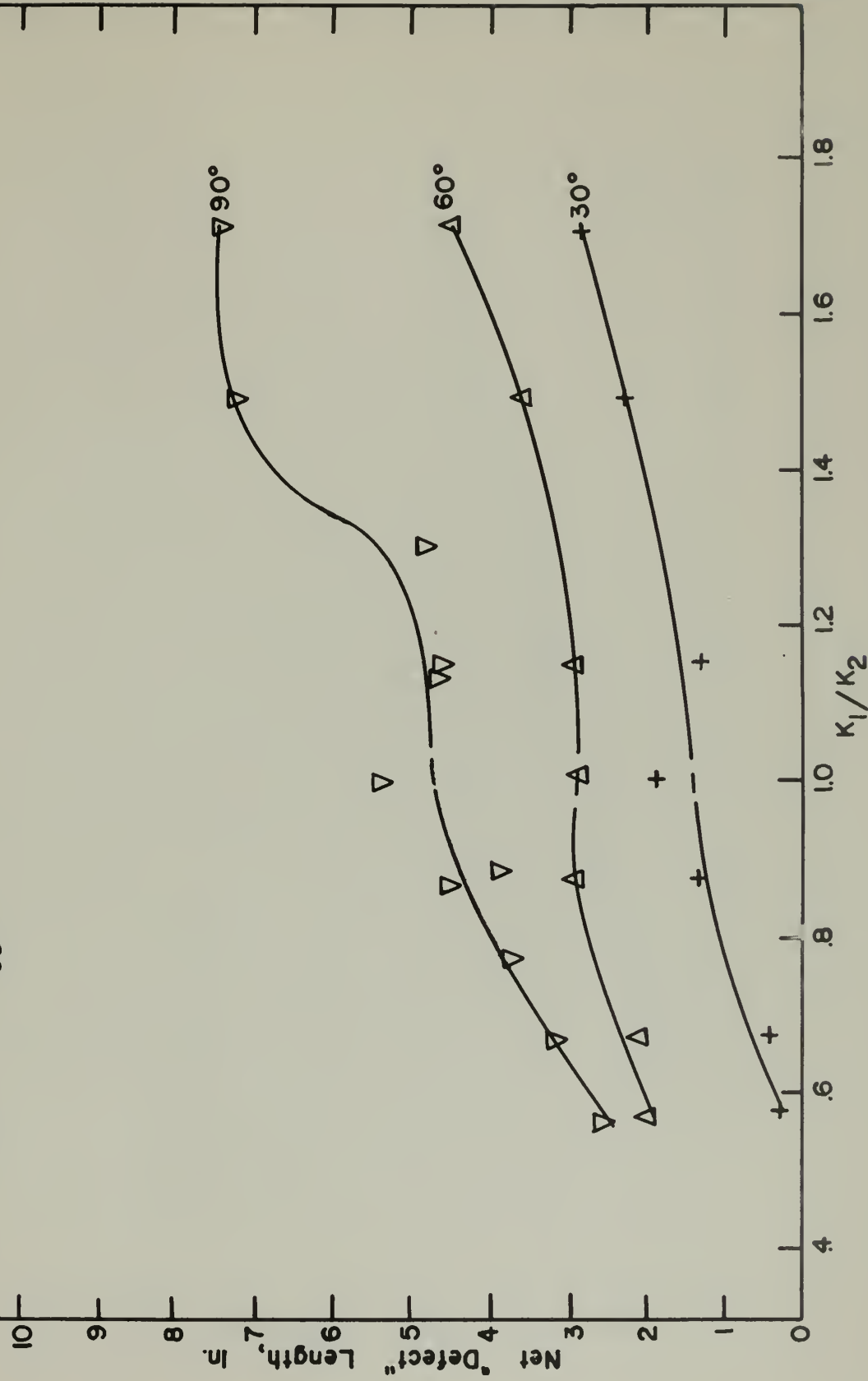






<u>Symbol</u>	<u>Cone Angle</u>
▽	90°
△	60°
+	30°

Figure 24.1 - "Defect" Length as a Function of  $K_1/K_2$  and cone angle for an Interface angle of 0°





Symbol	Cone Angle
▽	90°
△	60°
+	30°

Figure 24.2 - "Defect" Length as a Function of  $K_1/K_2$  and cone angle for an Interface angle of 8°.

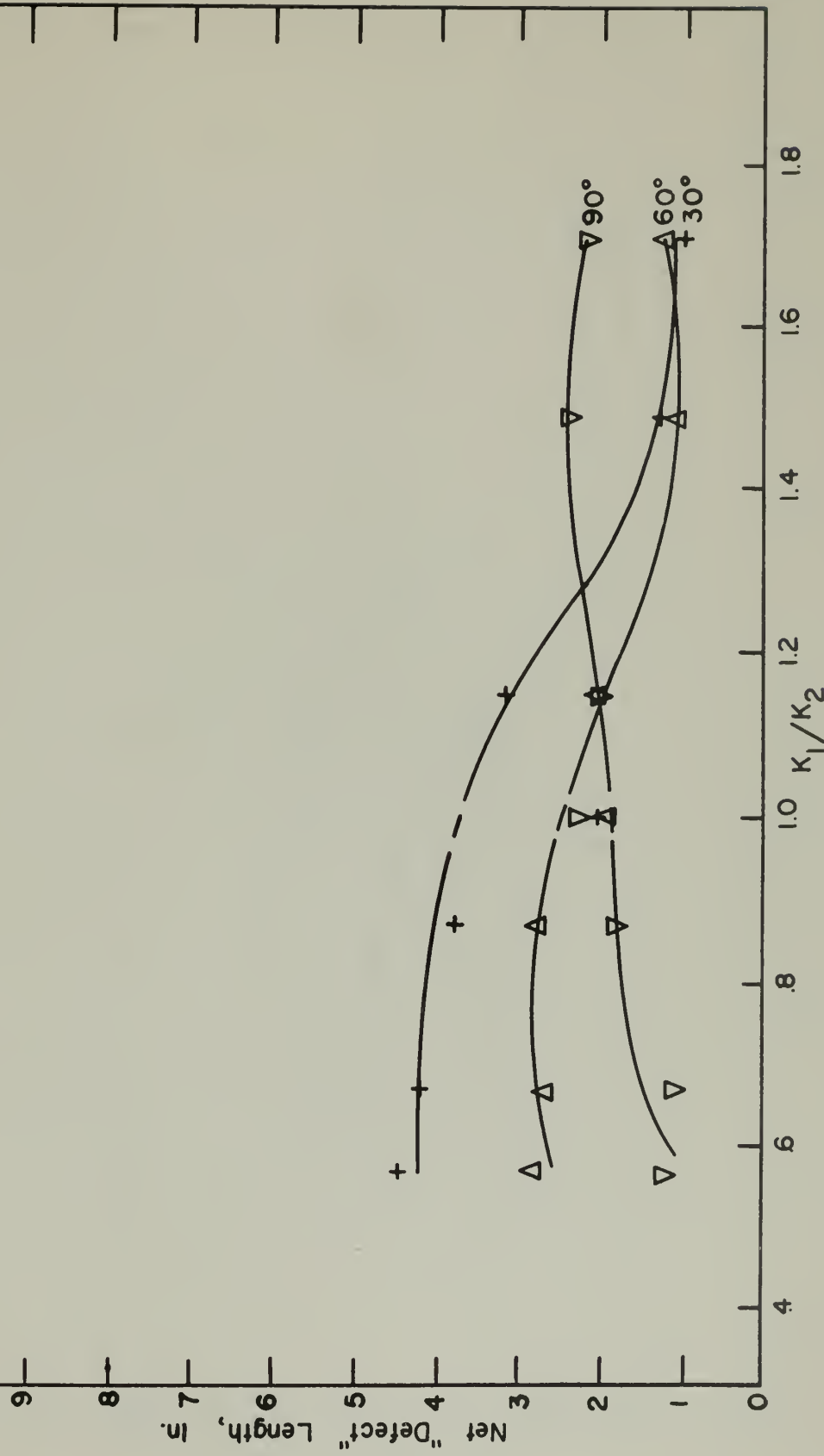




Symbol

	<u>Cone Angle</u>
$\nabla$	90°
$\Delta$	60°
+	30°

Figure 24.3 - "Defect" Length as a Function of  $K_1/K_2$  and cone angle for an Interface angle of 16°.



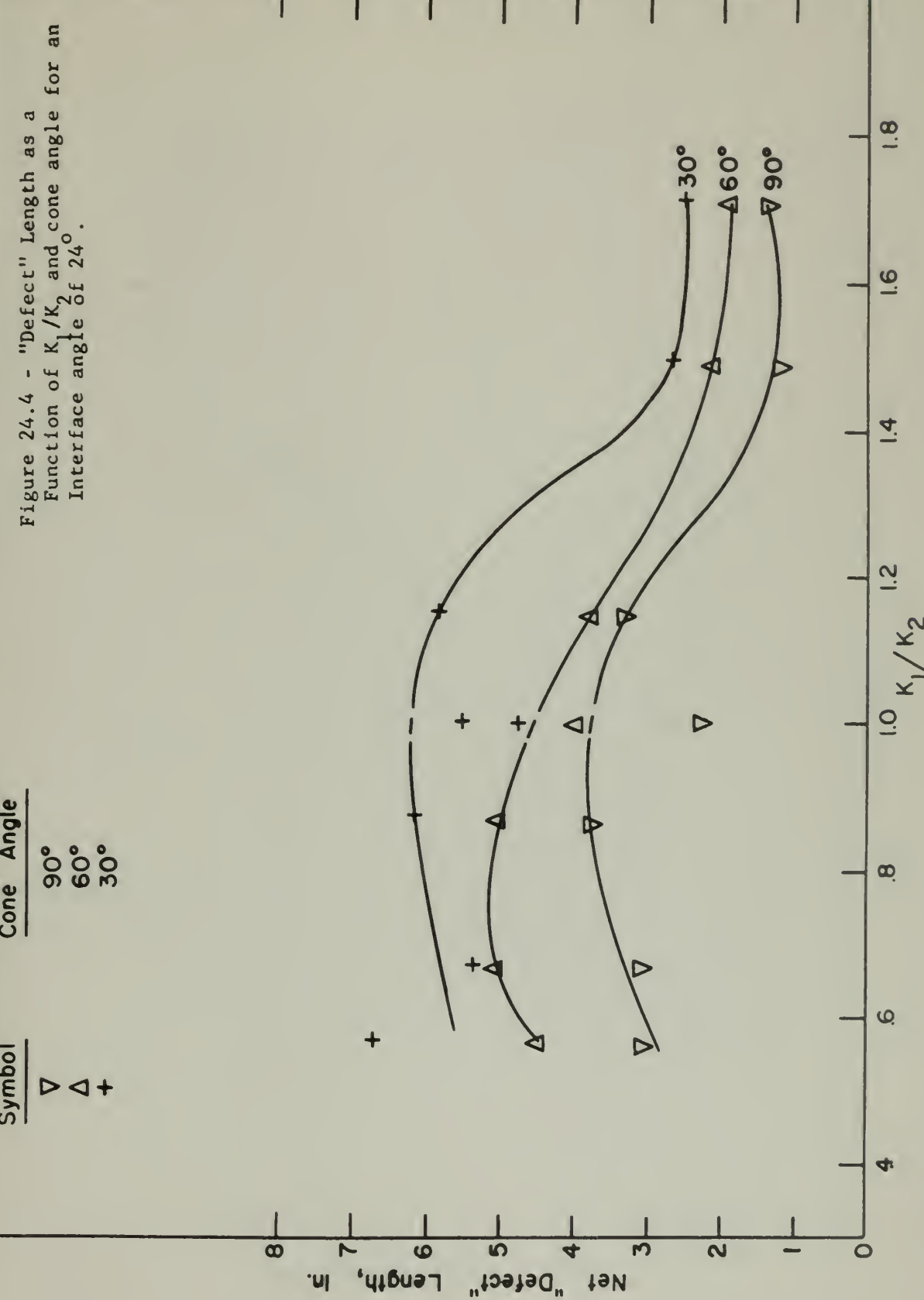


Symbol

$\nabla$   
 $\Delta$   
 $+$

Cone Angle

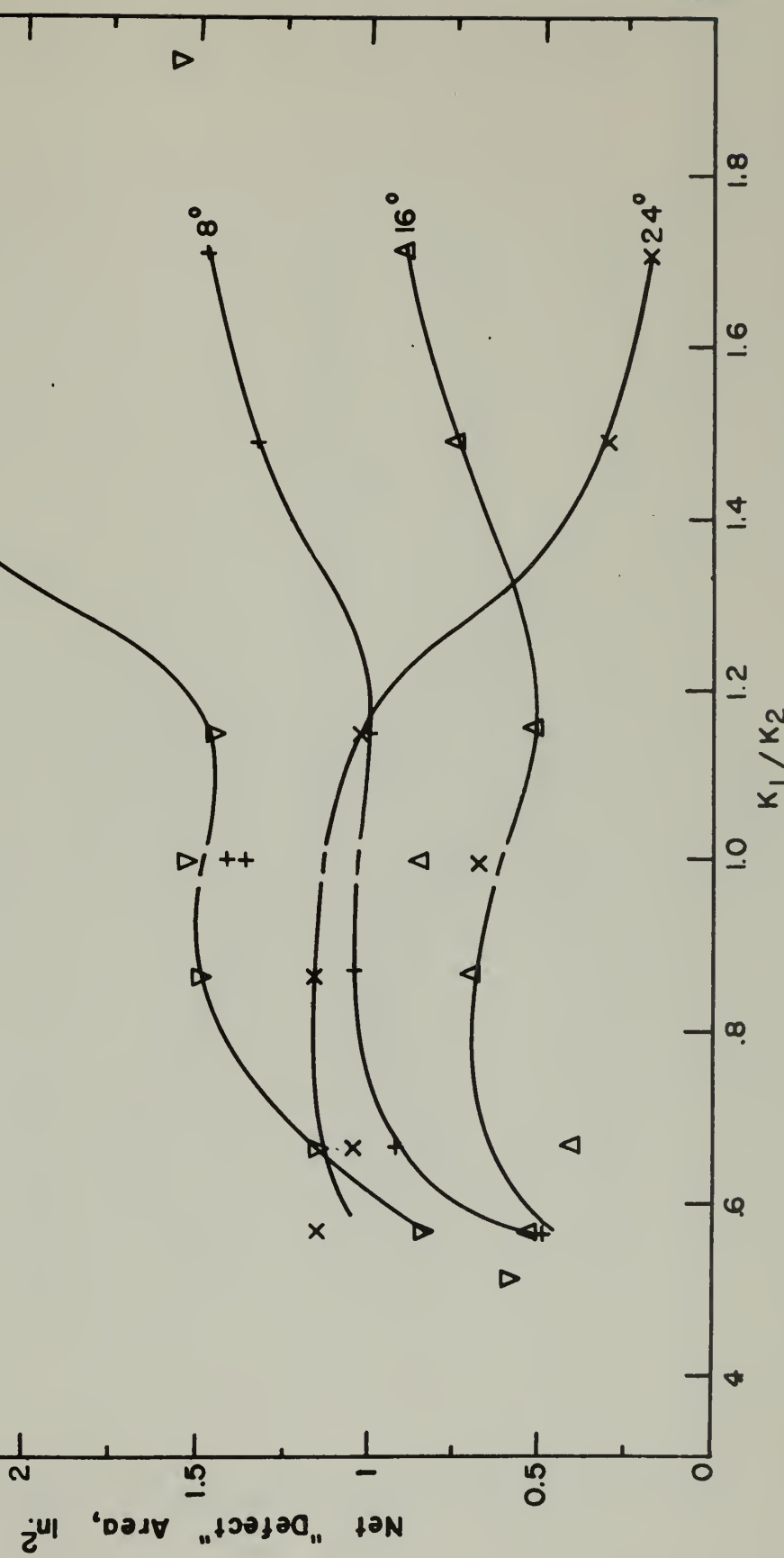
90°  
60°  
45°  
30°





Symbol	Interface Angle
$\nabla$	0°
+	8°
$\Delta$	16°
$\times$	24°

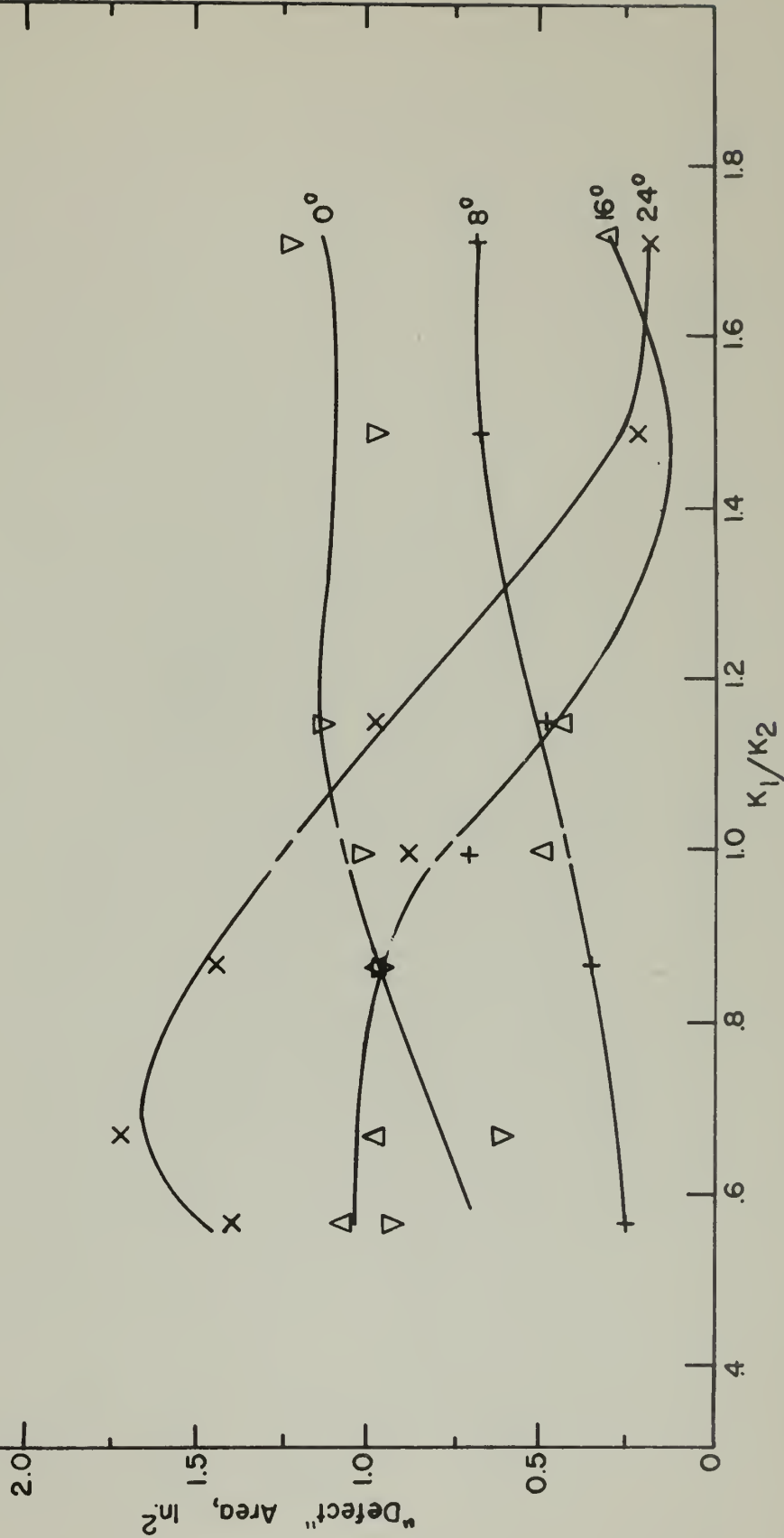
Figure 25 - "Defect" Area as a Function of  $K_1/K_2$  and Interface angle for an Included cone angle of 90°.



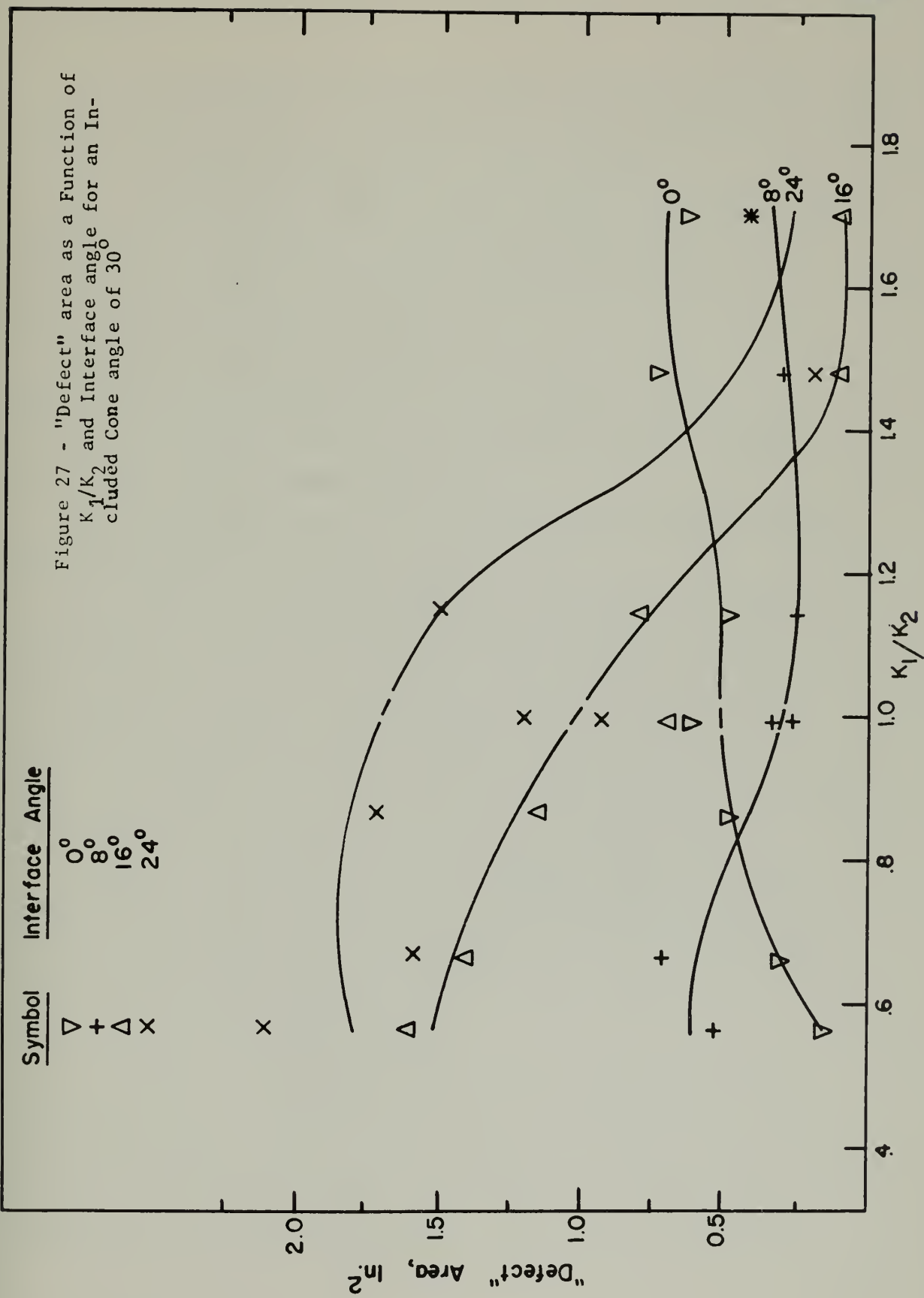


Symbol	Interface Angle
$\nabla$	$0^\circ$
+	$8^\circ$
$\Delta$	$16^\circ$
$\times$	$24^\circ$

Figure 26 - "Defect" area as a function of  $K_1/K_2$  and Interface angle for an included cone angle of  $60^\circ$ .









(2) Decreasing the included cone angle decreases the "defect" length and area below the point of overcompensation; above this point, decreasing the cone angle increases "defect" length and area.

(3) Increasing the interface angle decreases the "defect" length and area below the point at which overcompensation begins; above this point "defect" length and area increase with interface angle.

(4) Decreasing the included cone angle decreases the interface angle required for optimum compensation.

(5) For K-ratio less than unity, at any cone angle, the interface angle yielding the experimentally smallest "defect" length and area is about  $8^{\circ}$  less than that yielding the smallest "defect" length and area for a K-ratio of greater than unity.

(6) The curves plotted do not in general pass through, or near, the points plotted from Series 1 ( $K_1/K_2 = 1.0$ ).

c. Figure 28 is derived from Series 1 and 5; in it is plotted the effect of K upon net "defect" length for a K-ratio of unity, cone angle of  $90^{\circ}$ , and  $0^{\circ}$  interface angle. Figure 28 shows the result one might expect: "defect" length, under given extrusion conditions, decreases as K increases. Referring now to Figure 22, in which the remainder of Series 5 results are plotted with the  $0^{\circ}$  interface angle results from Series 2-4, we see that the Series 5 points are reasonably close to the plotted curve except for  $K_1/K_2 = 0.88$  and 1.30.

Figures 29 and 30 contain plots of "defect" lengths and areas, respectively, for  $90^{\circ}$  cone angle,  $0^{\circ}$  interface angle and varying K values. The unbroken lines are the curves plotted in Figures 22 and 25, while the dotted lines represent the estimated variation of "defect" length and area with absolute K value.

d. Figure 31 shows the relation of net "defect" length for billets of Series 6 in which the locations of the two materials were interchanged. It would appear from the random differences in "defect" lengths that there is no systematic variation in "defect" length with location in the billet. However, the difference in "defect" lengths between the billets is as much as 30%. Figures 20 and 21 show the



Figure 26 - Variation of "Defect" Length with absolute Value of  $K$  for  $K_1, K_2$  1, 90° Included cone angle, and 0° Interface angle.

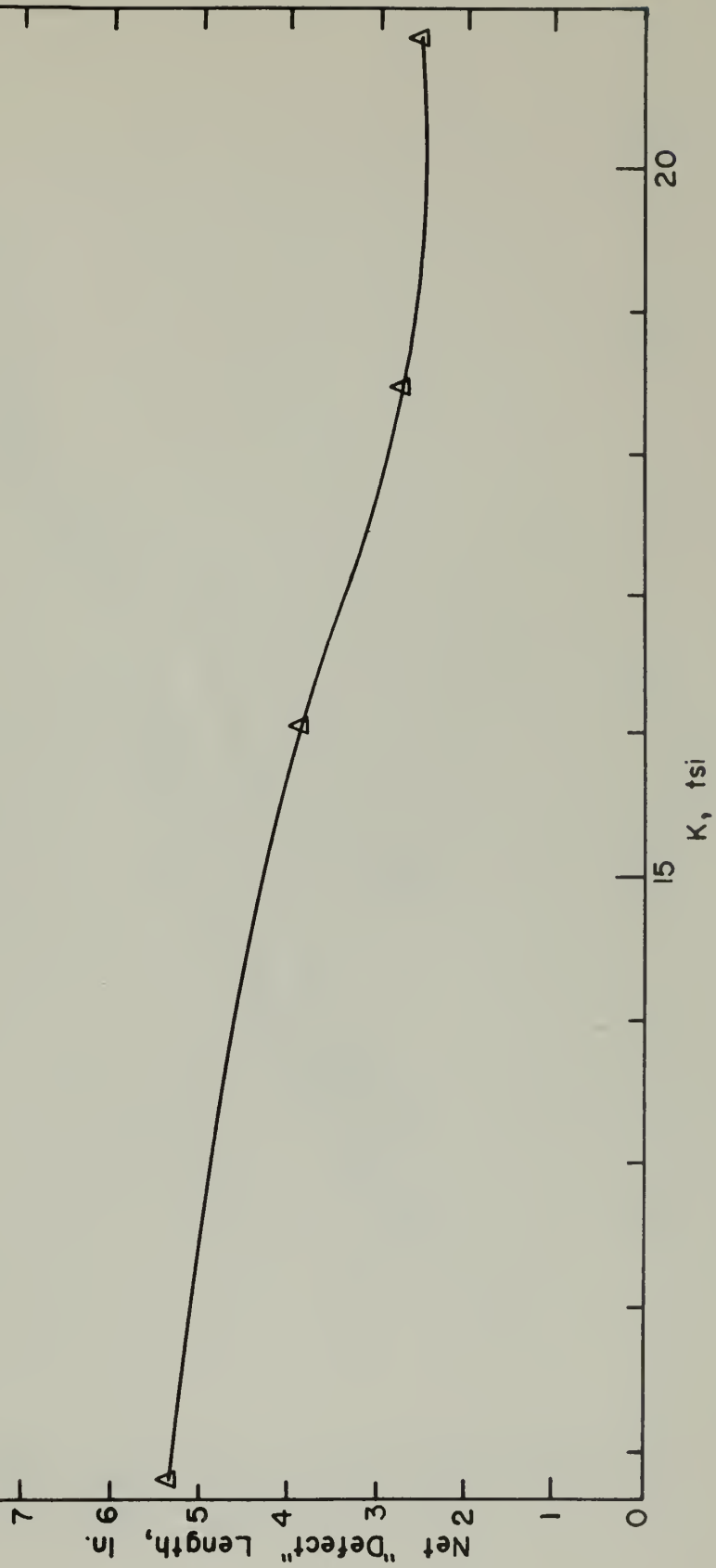
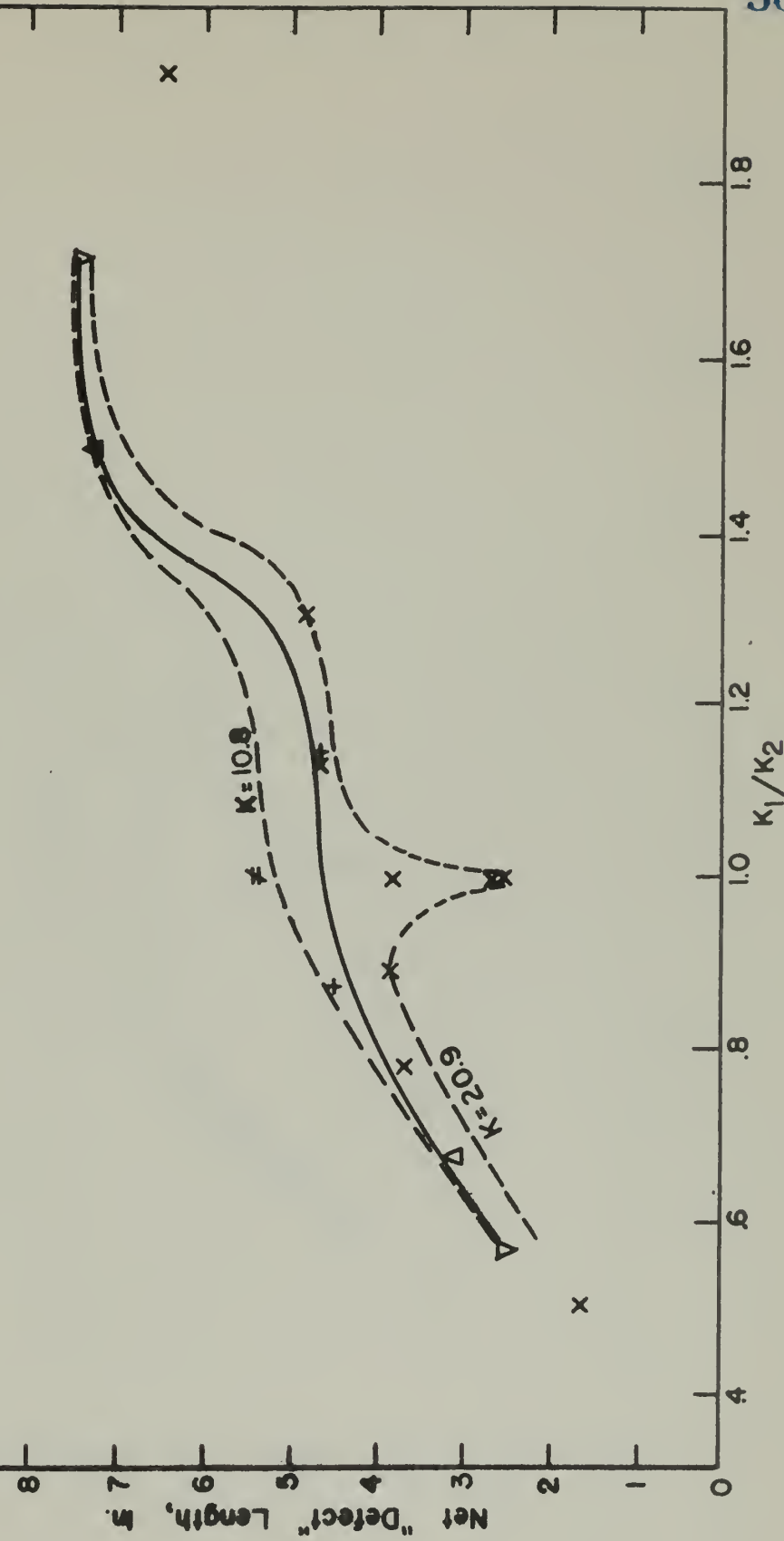


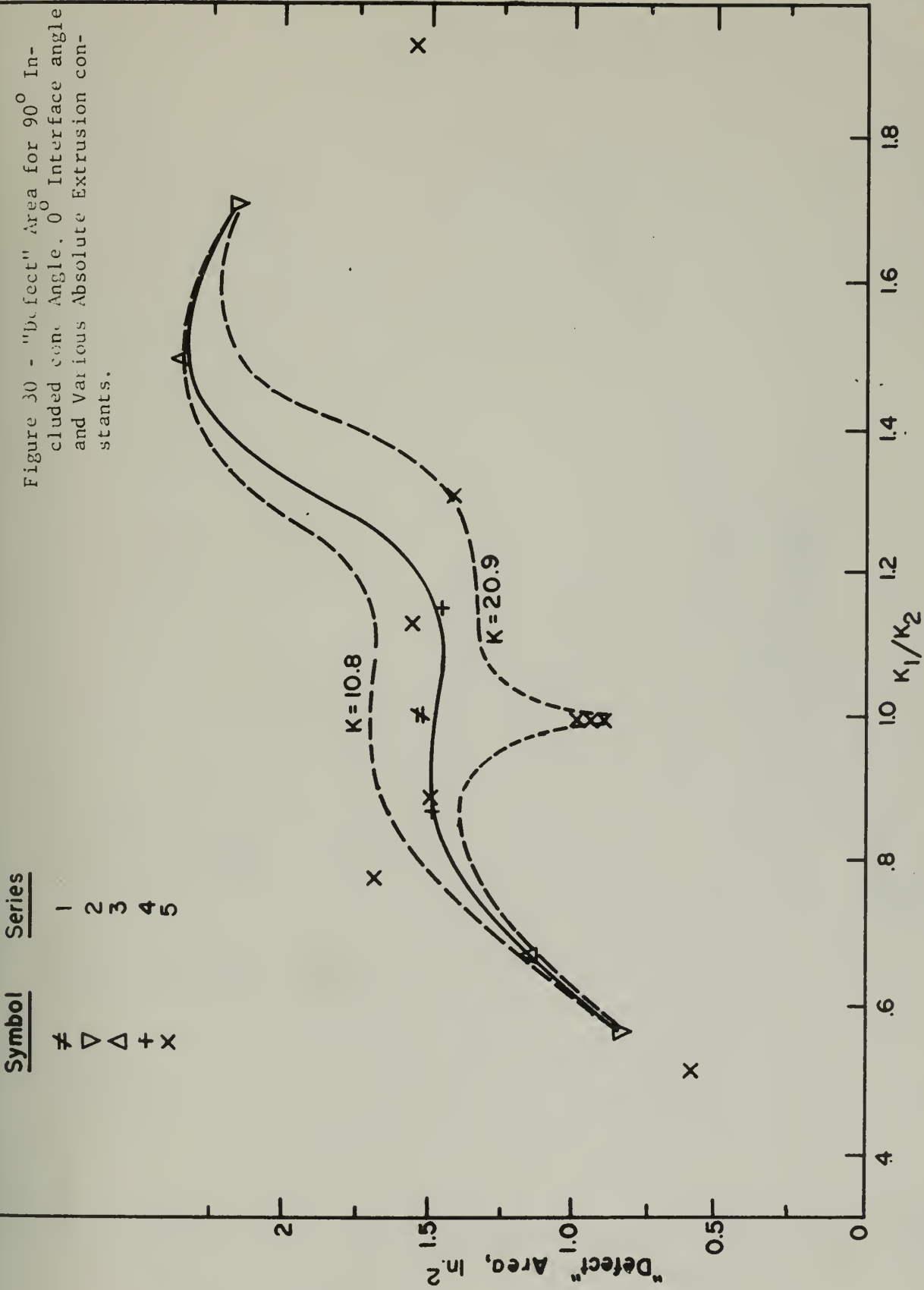


Figure 9 - "Defect" Length for  $90^\circ$  Included  
Crank angle,  $0^\circ$  Interface angle, and  
various absolute Extrusion constants.

Symbol	Series
*	1
▽	2
△	3
+	4
×	5



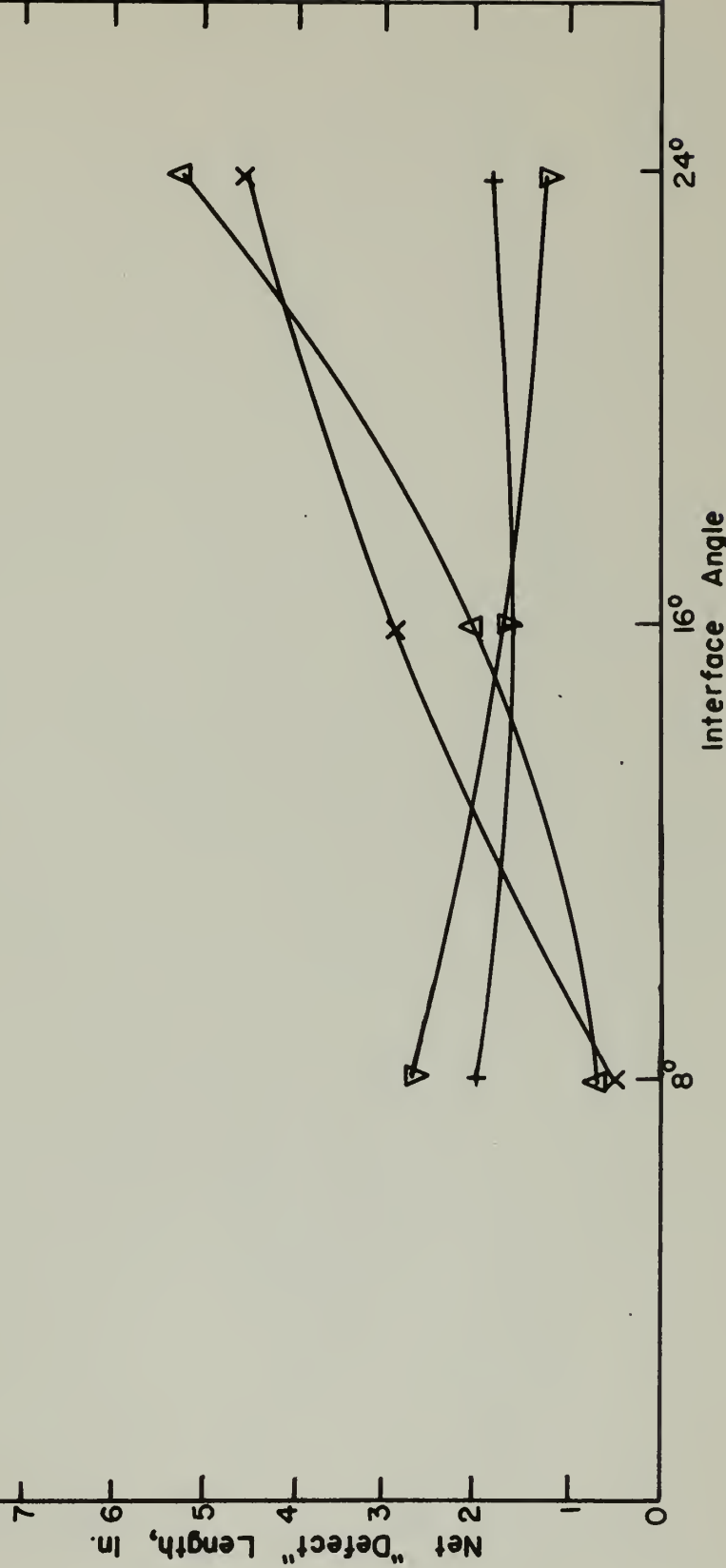






<u>Symbol</u>	<u>Series</u>	<u>"Defect"</u>
X	2	Front
+	2	Rear
▽	6	Front
△	6	Rear

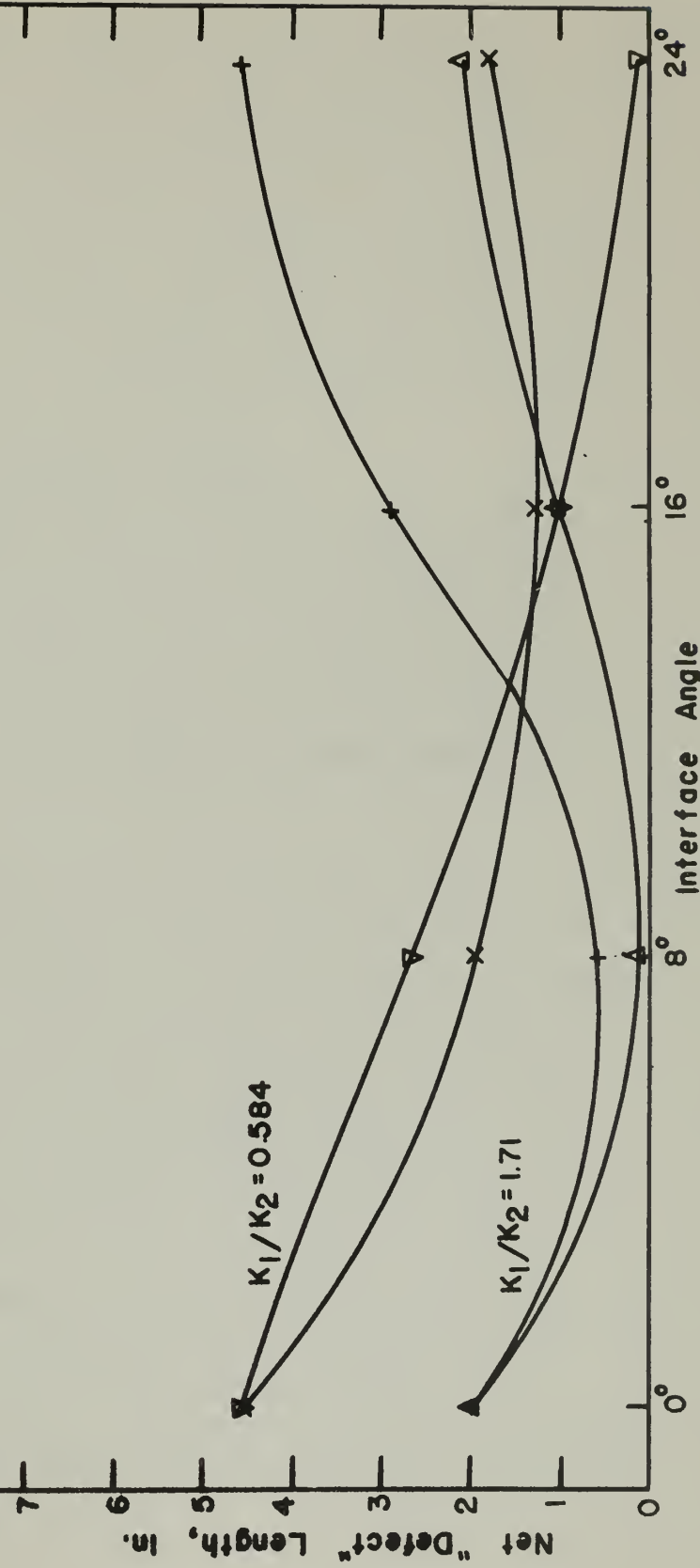
Figure 31 - "Defect" Length Comparison between Three-element Specimens in which Materials are Interchanged.





<u>Symbol</u>	<u>Preshape</u>	<u>"Defect"</u>
Δ	Spherical	Front
▽	"	Rear
+	Conical	Front
×	"	Rear

Figure 32 - "Defect" Length comparison between Specimens having Conical and Spherical Preshaping. (60° Included Angle.)





appearance of the corresponding "defects" of Series 2 and 6.

e. Figure 32 compares the "defect" length resulting from billets with conical and spherical preshapes of equal volume, as a function of interface angle, with a cone angle of  $60^\circ$ . It will be noted that for front "defects", in all cases, conical compensation produces longer "defects" than spherical compensation. In the case of rear "defects", on the other hand, for an  $8^\circ$  interface angle the conical "defect" is smaller; for  $16^\circ$  the "defects" are identical; and for  $24^\circ$  the conical "defect" is clearly the larger. Figures 20 and 21 show the appearances of corresponding "defects" from Series 2 and 7.

### 3. Discussion of Results

a. As noted by Wegner(19), when the K-ratio is low, voids are formed at the "defect" interface. From the results of Series 2 and 3, it appears that a modest amount of conical preshaping (or, from specimens A61.15006 and A62.15007 of Series 7, spherical preshaping) will result in elimination of both voids and the severe dogboning noted in many of the Series 2 and 3 front "defects". Should preshaping be impossible, then reducing the cone angle will help to reduce void formation and dogboning.

The explanation for "defect" behavior under these conditions is readily arrived at. Overcompensation leads to the inclusion of soft material (naval brass) in the "defect", and the ability of this inclusion to deform readily relative to the harder CuNi ( or CuZn) results in lessening the tendency toward dogboning. Reducing the cone angle, which is equivalent to providing a more gradual deformation of the billet as it approaches the die, allows the stiffer material to keep up with the naval brass during extrusion, thus minimizing void formation and dogboning.

b. The increasing tendency of the rear "defect" to show dogboning as interface angle increases is actually the result of increasing compensation, ending in overcompensation of the "defect". As the included cone angle is decreased, the uncompensated "defect" decreases in length. Since increasing the interface angle leads to increasing



compensation, the result is that the stiffer material, as cone angle decreases and/or interface angle increases, is left behind in the naval brass. The relatively high extrusion constant of the stiffer material causes the dogbone shape of the overcompensation.

c. Increasing compensation (interface angle) and decreasing cone angle lead to the same result -- a shorter "defect". Since a small included cone angle leads to reduced defect length, as the cone angle is reduced the compensation required may be expected to be reduced. The "defect" length and area plots show exactly this tendency.

The plots also show that as  $K_1/K_2$  increases, the compensation required for minimum "defect" length and area increases. This phenomenon may be explained on the basis of the increasing stiffness of material 1 (Figure 9). As material 1 stiffens, its ability to elongate in the direction opposite to that of extrusion decreases.

Thus it appears that the trend of the results is explainable on the basis of the demonstrable inability of stiff materials to flow as readily as less stiff materials during extrusion.

d. Figures 12, 18 and 19 show the decided similarity between the "defects" resulting when  $K_1/K_2$  is 1.0, .87 or 1.15. This similarity is, at first approximation, quantitative ("defect" length) as well as qualitative, as examination of the data sheet will show.

e. The reproducibility evident in the Series 1 extrusions is believed sufficient to allow reasonably accurate conclusions as to "defect" length on the basis of only one experiment at a given condition. Cost considerations make this procedure necessary.

f. In considering the results of Series 6, as compared with the 60° cone specimens of Series 2, at first glance the correspondence may seem doubtful. A close look at the form of the "defects" compared indicates that the long, thinned-out form of the "defects" could easily vary considerably in the extrusion process with only small variation in billet dimensions, or extrusion procedure. Further, slight variations in billet diameter or milling accuracy will have a disproportionately great effect upon "defect" length.



g. Net "defect" length was used in evaluating the variation of "defect" with cone angle and interface angle because it seemed most logical not to charge shift to "defect" formation, as shift is a side effect. "Defect" area, in order to compare with Wegner's results, was taken to include shift. The correspondence between "defect" length and area led to the abandonment of area measurements for Series 6 and 7 of the "Main Series" and in all Double Extrusion experiments.

h. Wegner(19), developed "S-curves" for "defect" areas plotted against  $K_1/K_2$ . No variation of "defect" area (or length) of this nature was developed in this work, as may be seen in Figures 25-27.

However, these plotted curves require careful interpretation if they are to be useful. The billets used in Series 2, 3, 4, which constitute the major part of the "Main Series", do not contain a single common material, as may be seen from Table II. Since "defect" length and area in general increases with decreasing  $K$ , for a given  $K_1/K_2$ , it is plain that with the experimental plan which was followed, the points on the "defect" length and area plots do not properly belong to the same line, but are rather individual points of a family of curves. Each individual curve in the family will be composed of a single material with a given  $K$ , extruded with materials of different  $K$  to obtain a range of  $K$ -ratios.

Figures 29 and 30 were constructed with this in mind. On the basis of extrusions in Series 1-5, an envelope is indicated in each of the plots within which "defect" lengths and areas should lie. From the lack of relevant points on the two dotted lines on each figure, it is clear that the envelopes are no more than poorly educated guesses. Nevertheless it is plain from the data plotted that something of this nature does occur in extrusion under these experimental conditions.

Points whose  $K$ -ratio is 1.0 do not lie consistently on the length and area vs  $K_1/K_2$  curves in any of the figures, and for this reason the curves are broken in the vicinity of  $K_1/K_2 = 1.0$ . It will be noted that Figures 29 and 30 show a steep valley in the vicinity of  $K_1/K_2 = 1.0$



for  $K = 20.9$ . This reflects the fact that at or near  $K_1/K_2 = 1.0$ , a wide variety of absolute  $K$  values may be extruded. The wide variety of  $K$  values leads to a wide variation in "defects" and hence to the local variation plotted. Conversely, for  $K$ -ratios not in the vicinity of 1.0 a smaller range of absolute  $K$ 's is extrudable, and the envelope lines, as shown, become less widely separated. It is believed that Wegner's plots, reevaluated in the light of the above observations, might yield results more in agreement with the results of this experiment.

i. Comparison of the corresponding "defects" in Series 1 and 6 shows that the assumption that front and rear "defects" are independent in a three-element billet is justified within experimental error.

j. Results of Series 7 show that spherical compensation yields shorter front "defects" at interface angles of  $16^\circ$  and  $24^\circ$ . This is due to lack of a "point" on the spherical compensation as it is this "point" which accounts for the greater length of the conically-compensated "defect". In both the spherical and conical preshaping, there is overcompensation at these interface angles.

Rear "defects", on the other hand, are shorter only when spherically compensated by a " $24^\circ$  interface angle", and in this case because the spherical interface prevented the whisker-like inclusion of naval brass which is noticeable in the conically-compensated "defect". This is to be expected in view of the greater compensation required for  $K_1/K_2$  large than for  $K_1/K_2$  small.

### C. The Double Extrusion Experiments

#### 1. The Experiments

The objective of the double extrusion experiments was to establish the feasibility of double extrusion as a fuel element fabrication technique, and to apply this technique to the production of representative fuel elements. To this end three series of experiments were set up: Series 8 as a feasibility study, Series 9 as the application of double extrusion to the fabrication of clad fuel elements, and Series 10 as the fabrication by double extrusion of a uranium-2 w/o zirconium fuel core with zircaloy cladding.



Series 8 embodied 13 two-element naval brass billets, as shown in the table below:

Table VI. Series 8 - Unclad, Two-Element Billets

Extrusion Extrusion	Extrusion Numbers	First Area Reduction Ratio, $R_1$	Overall Area Reduction Ratio
1*	14247/—	1.54	—
2*	14248/—	2.16	—
3*	14389/—	3.58	—
4	14296/14328	1.54	20.4
5	14346/14367	1.54	9.9
6	14384/14503	1.54	33.2
7	14347/14368	2.16	20.4
8	14385/14505	2.16	33.2
9	14386/14504	2.16	9.9
10	14348/14506	3.58	9.9
11	14387/14507	3.58	20.4
12	14388/14508	3.58	33.2
13**	14559/14565	1.54	20.4

\*Broken open for inspection

\*\*Rerun of extrusion 4

All Series 8 extrusions were at  $1150^{\circ}\text{F}$  with full lubrication. The dies, liners and cones were at room temperature to facilitate handling (see A. Exploratory Experiments, for the effect of liner temperature.)

The billet assembly finally arrived at is shown in Figure 33. The nose piece and cut-off are separate from the "fuel assembly" proper because it is necessary to discard or rework the nose and cut-off to prepare the assembly for the second extrusion, while also maintaining the copper can intact in order to insure a good bond in the finished product. In Figure 33 the nose piece and cut-off are shown with shoulders. This was done in order to eliminate voids so that the billet assembly would upset evenly. It should also be noted that a hole was drilled into the cut-off to accommodate the evacuation tube. Subsequent experiments with shift indicated that this was an unnecessary precaution, so long as the evacuation tube was bent over prior to extrusion.

Figure 34 shows schematically the appearance of the billet assembly before second extrusion. The shape of the shim indicates the deformation which resulted from the first extrusion; the exact shape



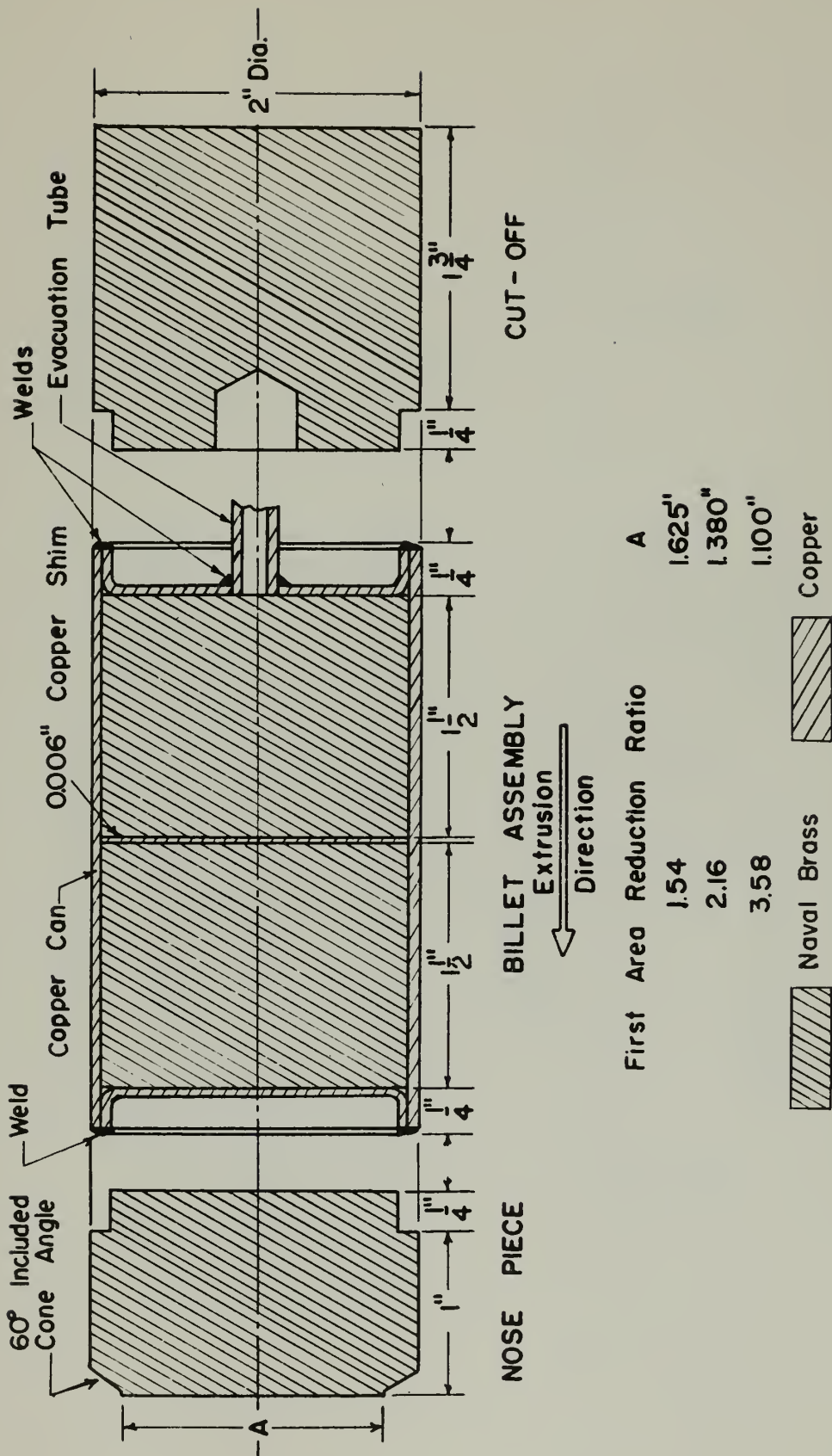


Figure 33 - Series 8 Billet Prior to First Extrusion



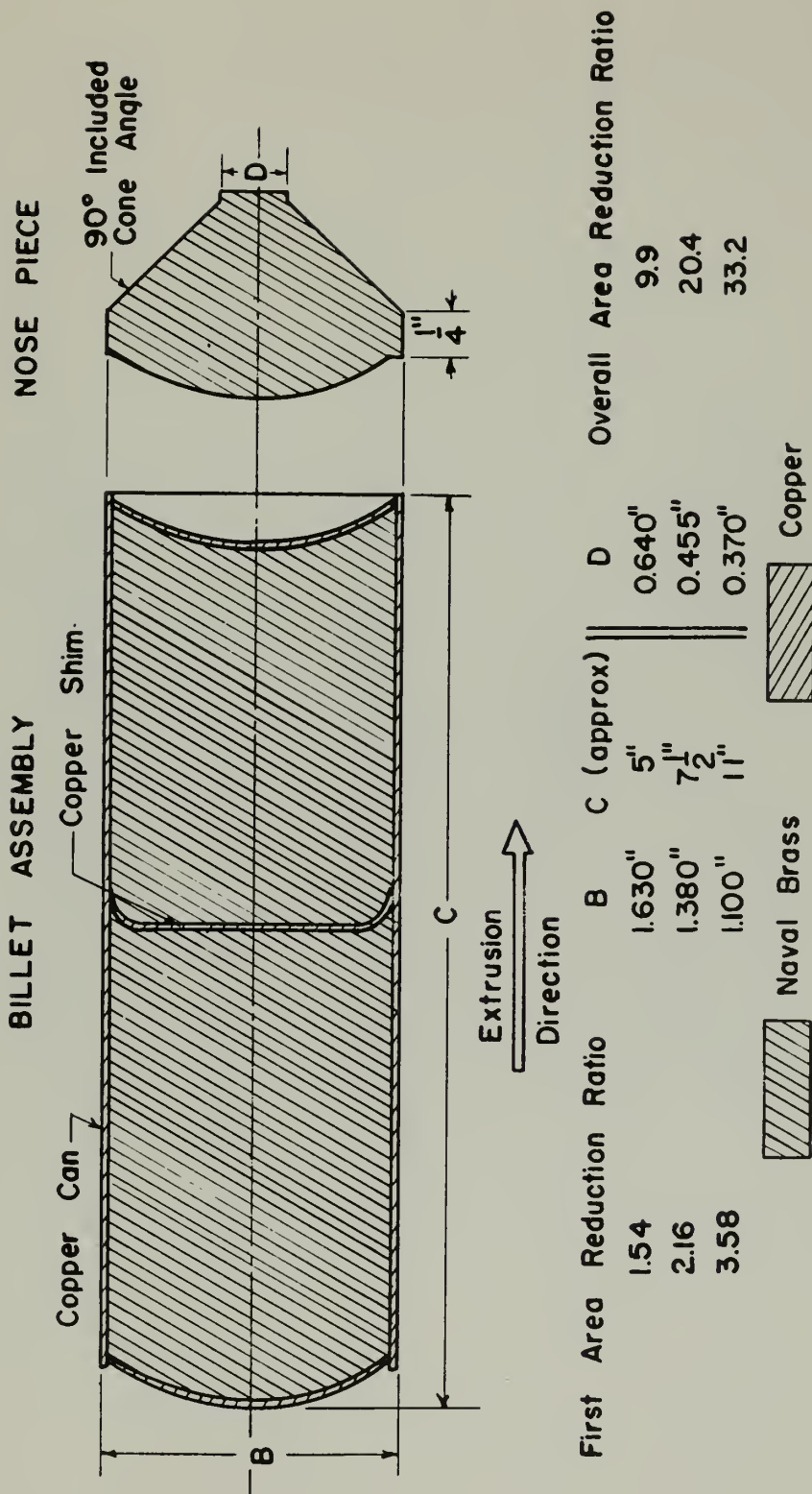


figure 34 - Series 8 Billet Prior to Second Extrusion



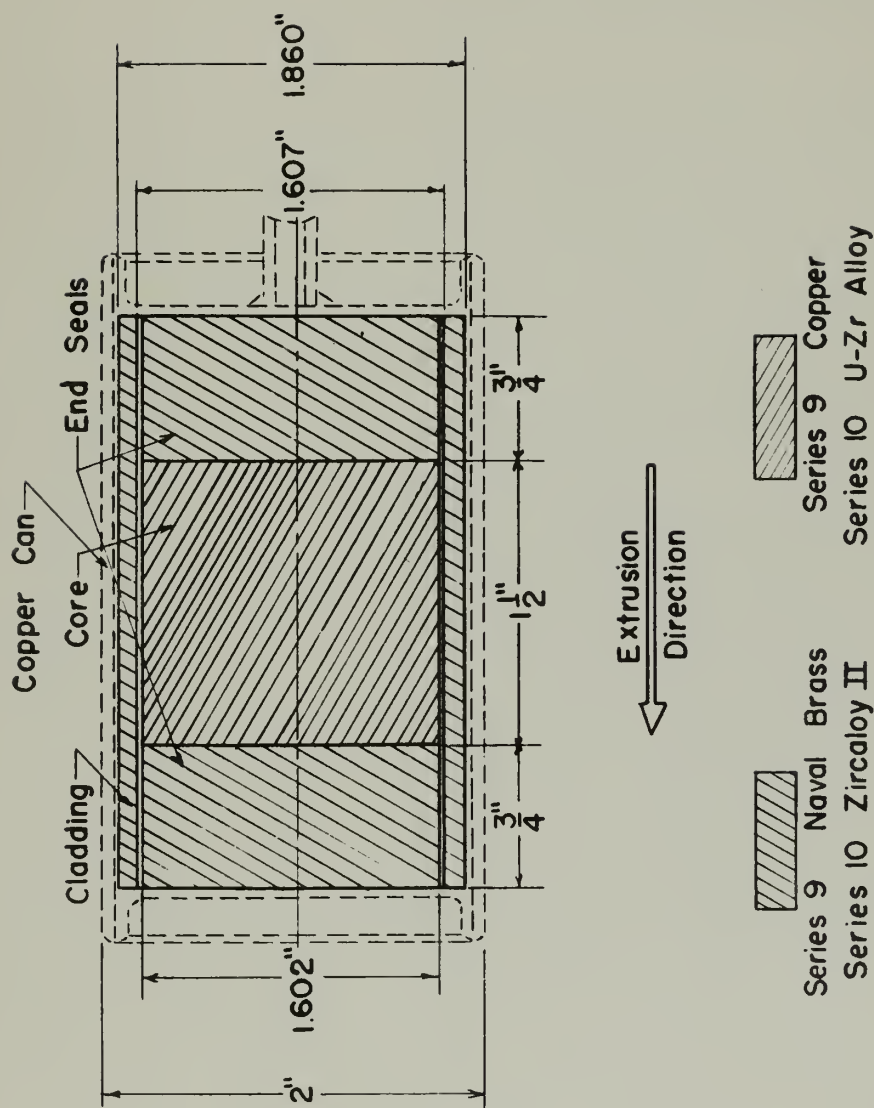


Figure 35 - Components for Clad Double Extrusion (Series 9,10)



for each first reduction ratio may be found in Figure 38. The former cut-off has now been machined to a nose piece which mates with the billet assembly; the former nose piece has been discarded, and the ram will bear directly upon the end of the billet assembly during the second extrusion.

Figure 36 shows the press arrangement for Series 8, 9, and 10 first extrusions. An external die was required because the extremely light first reduction would have made the wall thickness of an internal die impractically thin. As it was, the dies used for the 2.16 and 3.58 first reductions cracked when first used, and after two extrusions they broke into several pieces. However, this did not interfere with die usefulness to any appreciable extent. All three external dies were machined with a shoulder to aid in centering them relative to the liner, thus avoiding eccentric extrusion of the billet.

First extrusion was at the outset attempted without use of the catch tube. The resulting billets were bent sufficiently to prevent re-extrusion. Straightening proved impossible because of the billets' low mechanical strength. Therefore, a catch tube was constructed for each reduction ratio and attached to the die backer plate as shown in Figure 36. Before extrusion the catch tube was lubricated with oildag to minimize the chance of jamming the billet. The marking hole shown in the catch tube was used to mark the tops of the extruded billets.

Second extrusion was performed according to normal procedure, using internal dies and 90° cold rolled steel cones. As noted above, billet temperature was 1150°F, while the liner, cone, and die were at room temperature. Table 7 gives the liner, cone and die dimensions for second extrusions. Specimens were second-extruded with the top of the first extrusion at bottom of the liner, to determine whether such placement had any effect upon shift.



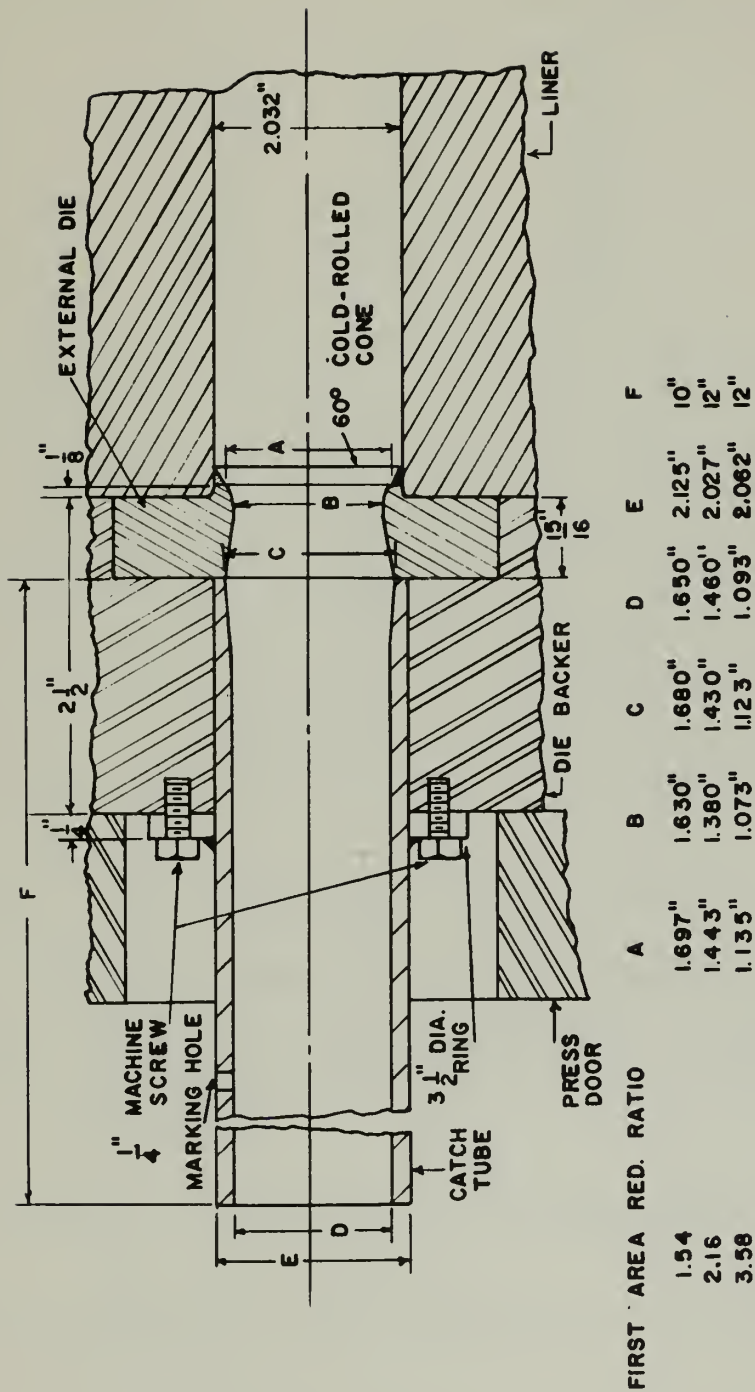


Figure 36 - Extrusion Press Arrangement for First Extrusion in the Double Extrusion Process.



Table VII. Second Extrusion Tool Dimensions, Series 8-10

First Area Red. Ratio	Overall Area Red. Ratio	Liner Dia., In.	Die Dia., In.	Cone I. D. In.
1.54	9.9	1.660	.640	.702
1.54	20.4	1.660	.455	.517
1.54	33.2	1.660	.370	.432
2.16	9.9	1.406	.640	.702
2.16	20.4	1.406	.455	.517
2.16	33.2	1.406	.370	.432
3.58	9.9	1.100	.640	.702
3.58	20.4	1.100	.455	.517
3.58	33.2	1.100	.370	.432

A word needs to be said about the selection of cone angles. It was anticipated that the first area reduction ratio of 1.54, which was the minimum possible with existing equipment, would lead to over-correction in the final product. Therefore, a first extrusion cone angle of  $60^\circ$  was selected in order to reduce the "defect" (compensation) introduced by the first extrusion, and a second extrusion cone angle of  $90^\circ$  was specified to maximize the tendency to form a "defect" in the final product. By this device it was hoped to avoid over-compensation. It is interesting to note that the same result might have been achieved by selection of different billet temperature for the two extrusions.

Series 9 and 10 were composed of similar three-element clad billets. Details are set forth in the tables below:

Table VIII. Series 9 - Naval Brass-Cu Clad Billets

Extrusion	Extrusion Numbers	First Area Reduction Ratio, $R_1$	Overall Area Reduction Ratio
1	14645/14667	1.54	9.9
2	14758/14764	1.54	9.9
3	14793/14805	1.54	20.4

Table IX. Series 10 - U-Zr Core, Zircaloy Clad Billets

Extrusion	Extrusion Numbers	First Area Reduction Ratio, $R_1$	Overall Area Reduction Ratio
1	14994/14996	1.54	20.4

The nose pieces and cut-offs for Series 9 were exactly the same as for Series 8, except that they were of copper (see Figure 33), and



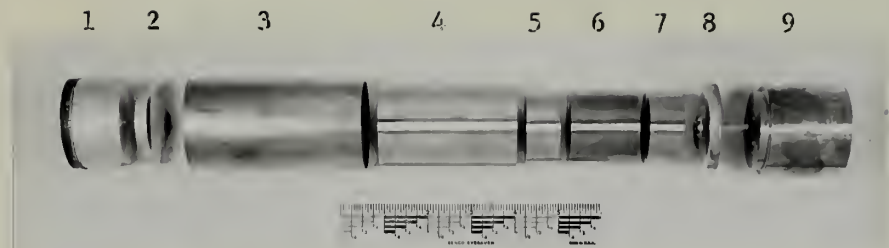
the billet components are shown in Figure 35. Copper and naval brass were chosen for the core and cladding respectively because they were readily available and had about equal K's (11 tsi), which is also true of the K's of U-2w/o Zr and Zircaloy II (K = 17.5 tsi). Extrusion procedure was identical with that set forth above with only two exceptions. The forward end of extrusion 2, after first extrusion, was cut off to give the ram better bearing for second extrusion and thus reduce "defect" length. In extrusion 3, first extrusion, the billet assembly and nose piece were heated to 1200°F, while the cut-off was heated to 1400°F. The hope here was to: (a) increase compensation "defects" in first extrusion by increasing the billet assembly temperature; (b) increase compensation in the rear "defect" of the first extrusion by increasing cut-off temperature.

The Series 10 billet assembly was arranged exactly the same as in Series 9, and is also shown in Figure 35. U-2w/o Zr and Zircaloy II were used as core and cladding respectively in order to duplicate the extrusion of an actual reactor fuel element. For first extrusion Cu-9w/o Ni was used for the nose piece and Cu-5w/o Zn for the cut-off. The desire here was to minimize the "defect" in the front of the first extrusion by using a hard nose and to maximize the rear "defect" by using a soft cut-off. Cu-9w/o Ni was used for the nose piece and cut-off in second extrusion, in order to minimize "defect" length in the final product.

Extrusion procedure was identical with that of Series 8, except that billet temperature was 1200°F, and the liner, die and cone were heated to 900°F for second extrusion in order to ease the fitting of the ram to the liner.

In Figure 37 the components of the Series 10 billet are shown as they were prior to assembly.





RF 4767

<u>Number</u>	<u>Component</u>
1	Nose piece with cone in place
2	Can end
3	Can
4	Cladding
5	End seal
6	Core
7	End seal
8	Can end with evacuation tube
9	Cut-off

Figure 37 - Exploded View of Billet Assembly for Series 10.

## 2. The Results

### a. Series 8

(1) The feasibility of reducing "defect" length in co-extruded clad fuel elements by use of double extrusion was clearly established for materials of equal or nearly equal K. The observed data for the double extrusion experiments are in the Appendix, A. Data Sheet.

(2) For the extrusion procedure used, a first area reduction ratio of 1.54 produced a "defect" length 20-25% of that observed in a similar uncompensated billet which was conventionally co-extruded. This is shown in Figure 40. Increasing  $R_1$  (area reduction ratio for first extrusion) increases "defect" length; when  $R_1$  is 2.16, "defect" length is about the same as for an uncompensated conventional extrusion, and above this ratio, "defect" length is greater than in the uncompensated case, but in the opposite direction, as may be seen in Figure 40.

(3) "Defect" length resulting from double extrusion is relatively insensitive to overall area reduction ratio at or near the





a.  $R_1 = 1.54$

RF 4555



b.  $R_1 = 2.16$

RF 4556



c.  $R_1 = 3.58$

RF 4554

Figure 38 - "Broken" Billets from Series 8 Showing the Preshape Resulting from First Extrusion.





a.  $R_1 = 1.54$  RF 4661



b.  $R_1 = 2.16$  RF 4662



c.  $R_1 = 3.58$  RF 4663

Figure 39 - Series 8 "Defects" (.5X).



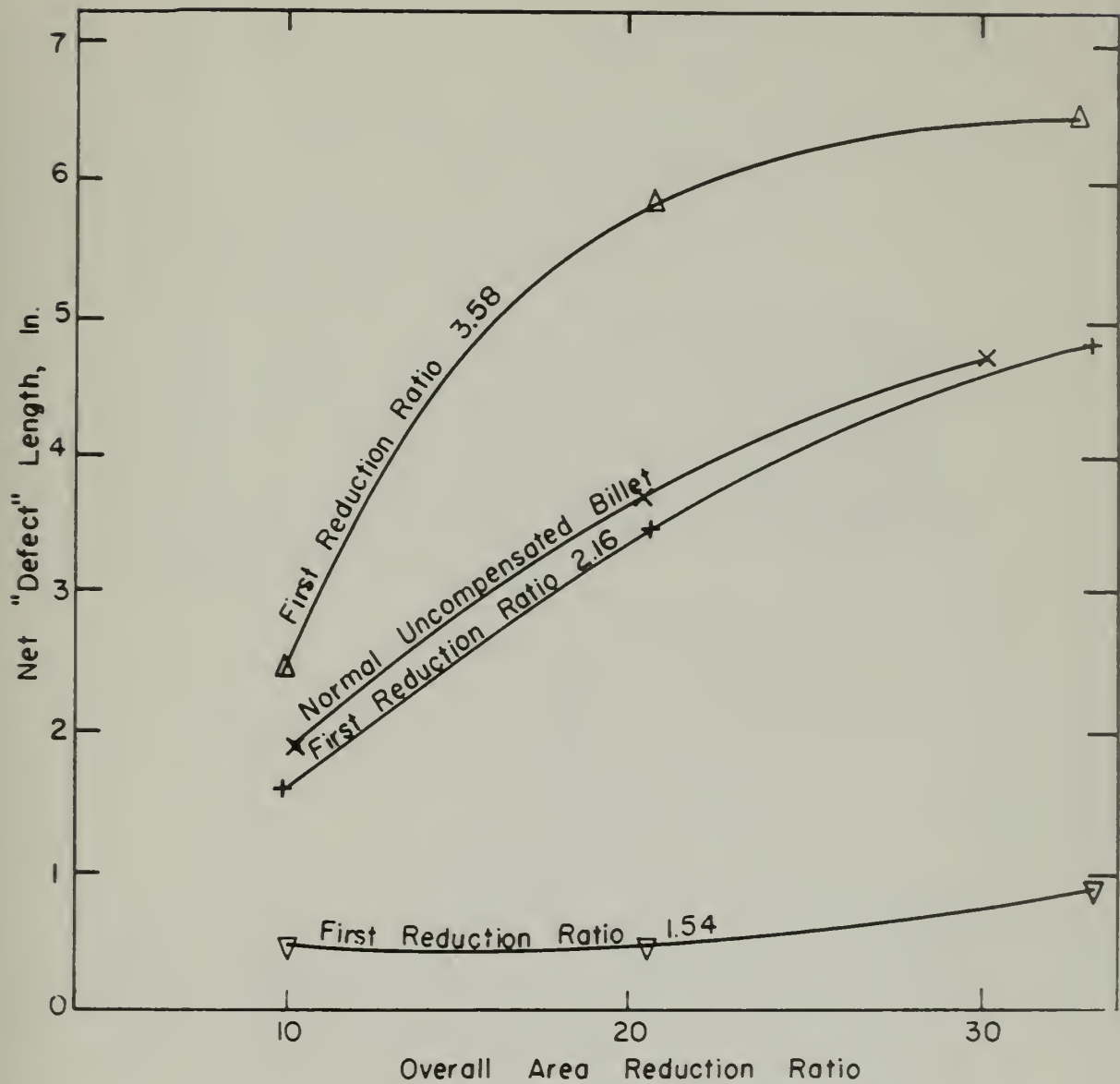


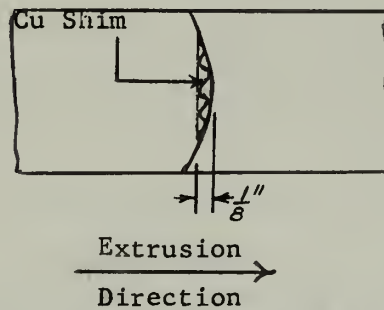
Figure 40 - Comparison of "Defect" Lengths in Double Extrusion and Normal Extrusion of an Uncompensated Billet.



optimum extrusion condition ( $R_1$  for optimum preshaping).

(4) Except for extrusion 1, all extrusions of Series 8 compared favorably with conventionally coextruded rods in bonding and uniformity of can thickness. See Figure 39. On the other hand, though the "defects" resulting from double extrusion in which  $R_1$  is 2.16 and 3.58 closely resemble the usual "defect" in an overcompensated rod, where the first area reduction ratio is 1.54, the "defect" shows great irregularity, though "defect" length is short.

(5) Figure 38 shows extrusions 1-3 opened up for inspection after first reductions of 1.54, 2.16 and 3.58. The length of the "defect" (compensation) increases rapidly with increasing values of  $R_1$ . Close inspection of extrusion 1 disclosed an extensive void between the mating surfaces of the "defect". The copper shim had deformed so as to occupy this void as the sketch below shows. This void was not seen in extrusions 2 and 3.



(6) Extrusion 13 is a rerun of extrusion 4. From the Appendix, A. Data Sheet, the "defect" length of 13 is half that of 4, though their appearance is otherwise about the same. The only difference in the extrusion procedure for these specimens was the grooving of the nose piece and cut-off prior to first extrusion of 13, in order to eliminate voids in the billet.

(7) Shift in doubly extruded specimens was not appreciably greater than in conventional coextrusions. All first extrusions were marked to indicate the top of the extruded billet as a part of the extrusion process. Examination of the first extrusions showed shift to be randomly distributed around the billet circumference. As noted



above, the top of the billet after first extrusion was placed at the bottom of the liner for second extrusion. This had no appreciable effect upon shift in the final product.

b. Series 9

(1) As Figure 41 shows, the front "defect" was undercompensated in all extrusions, while the rear "defect" showed a greater degree of compensation.

(2) Clad thickness was uniform in all extrusions, and there was no evidence of excessive shift.

(3) "Defects" in all cases were characterized by clearly defined separation of the copper core and naval brass cladding.

(4) The net length of the front "defect" was about the same for all three extrusions; the net length of the rear "defect" in extrusion 3 was appreciably longer than in extrusions 1 and 2, as the result of undercompensation.

c. Series 10

(1) As Figure 42 shows, the front "defect" was undercompensated, though comparable in length with the front "defects" in Series 9. The rear "defect" was undercompensated and slightly longer than in extrusion 3 of Series 9.

(2) Cladding thickness was uniform and bonding appeared satisfactory.

(3) Shift was not excessive, but affected both "defects".

3. Discussion of Results

a. The feasibility of the double extrusion process has been demonstrated by Series 8, 9, and 10, at least so far as rods in which core and clad have about the same K are concerned. These results are not readily applicable to the fabrication of a rod wherein the K's are widely different, because of the effects of whiskering and dogboning. It is doubtful that double extrusion will lessen these effects, though this point should be demonstrated by further experiment.

b. As might be expected from the "Main Series" results, the "defect" length in double extrusion is radically affected by the



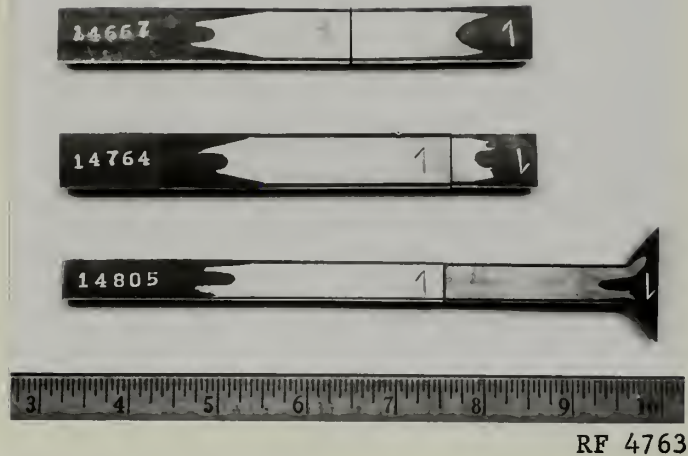


Figure 41 - Series 9 "Defects" (.5X).



Figure 42 - Series 10 "Defect" (.5X).



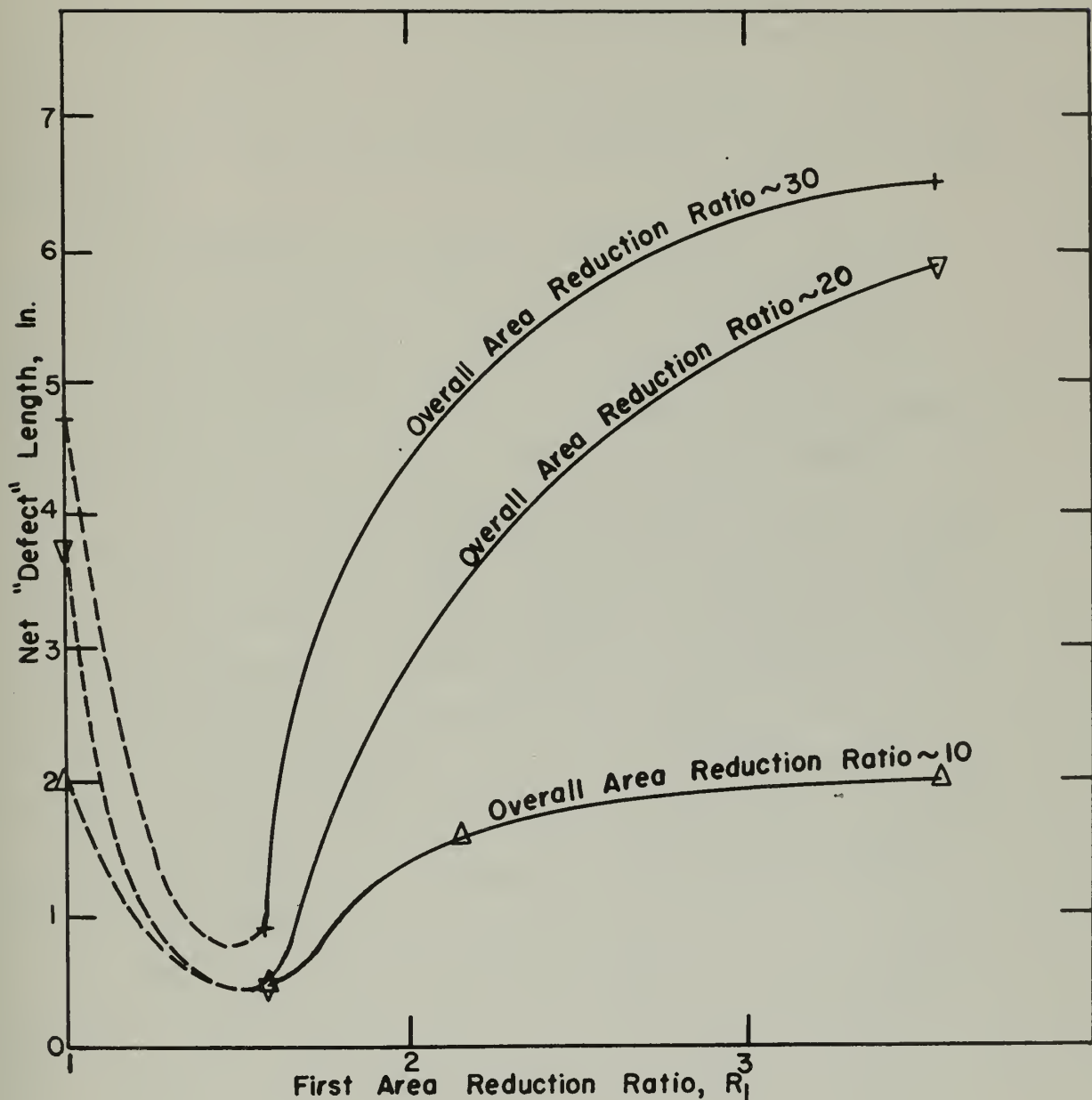


Figure 43 - Variation of "Defect" Length with Overall and First area Reduction Ratios in Double Extrusion.



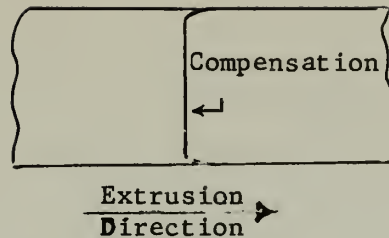
value of  $R_1$ , as may be seen in Figure 43. Unfortunately the available equipment did not permit the extrusion of a billet at an  $R_1$  of less than 1.54. The absence of data in the less-than 1.54 domain accounts for the dotted lines in Figure 43; further study of the double extrusion process should include experiments on the effects of extrusion at a first reduction of less than 1.54. On the basis of the above results however, it is believed that nearly minimum "defect" lengths were obtained in these experiments.

c. The insensitivity of "defect" length to overall reduction ratio at  $R_1 = 1.54$  is shown in Figure 40. This phenomenon, which was evident in Series 8 and 9, has no ready explanation. Further experiments will be required to verify the possibility that the low first area reduction ratio is the cause, or that the particular conditions of these experiments lead to a compensation which somehow "adjusted" itself to varying overall reduction ratios.

d. It can be fairly said that double extrusion results in considerable reduction in "defect" length. On the other hand, it is clear that under the conditions of these experiments, double extrusion does not yield the desired flat interface between core and end seals. It does not seem likely that any practical double extrusion technique will yield perfect compensation. But since it is unlikely, from experience to date, that any other method of compensation will produce flat interfaces, this is not a fatal flaw. The advantage of double extrusion is the simplicity of preparing billets combined with the minimization of "defects".

e. Comparison of the "defect" and the shape of the compensation introduced by first extrusion at  $R_1$  of 1.54 leads to the following conclusions. The compensation resembles a very shallow parabola, while the final "defect" shows undercompensation near the outside of the rod, and, typically, a greater degree of compensation toward the center. This would indicate that the ideal compensation would be somewhat as sketched below.





f. From the results of extrusions 4 and 13 of Series 8, the elimination of voids between the nose piece, cut-off and billet assembly leads to appreciable reduction in "defect" length, as the result of more even initial upset. The elimination of voids in the billet used for second extrusion is a difficult problem because of the irregularities that result from first extrusion. An attempt was made to weld the nose piece and cut-off to the billet assembly in extrusions 1 and 2 of Series 9, but the welds pulled apart during extrusion, and it was thus impossible to conduct the second extrusion under ideal conditions of billet arrangement. The rear end of the billet in extrusion 2 of Series 9 was cut off flat to give the ram a good bearing for second extrusion; the front and rear "defects" were shorter in this case than in extrusion 1, in which the ram bore against the rounded billet end. It is not certain, of course, that voids or other irregularities in the billet assembly will adversely affect "defect" length to the extent indicated in these few experiments, but the point seems worth further attention.

g. As far as appearance is concerned, the final product of double extrusion appears to be satisfactory in respect to bonding and uniformity of core and cladding. As Figure 38 shows, the "defects" of extrusions in Series 8 for which  $R_1$  was 1.54 present an irregular appearance. This is the result of the crinkling of the copper shim during first extrusion, when a void between the billet components was formed. This irregular appearance was not present in the "defects" of Series 9 and 10, where no shim was used.

h. In spite of the fact that double extrusions undergo "double jeopardy" where shift is concerned, excessive shift was not observed in any of the double extrusion "defects". Randomness of shift is no doubt the cause for this; there is always the chance, of course, that first and second extrusion shifts will coincide, with the result that an



unsatisfactory "defect" will be produced.

i. The persistent difference in the degree of compensation of front and rear "defects" in the Series 9 and 10 extrusions is the result of inequality of "defect" lengths in the front and rear of the billet. After first extrusion, the front "defect" (compensation) is longer than that in the rear. For second extrusion the billet is reversed, but again the tendency is to form a longer "defect" in the front than in the rear. The net result of the two extrusions, then, is to produce an under-compensated front "defect" and a nearly correctly compensated rear "defect". Since the length difference in front and rear "defects" is small, this effect is striking evidence of the sensitivity of final "defect" to the compensation put into the billet. The effect may be controlled by using a soft cut-off to increase rear "defect" length in first extrusion, and a hard nose piece to reduce front "defect" length in both extrusions.

This technique was tried in extrusion 3 of Series 9, and met with some success in that the front "defect" showed a fair degree of compensation, and the "defect" lengths were comparable. It was not so successful in Series 10, probably because the cut-off was too stiff.

#### D. The Shift Experiments

##### 1. The Experiments and the Results.

All shift experiments were performed at an area reduction ratio of 20.4 with die, cone, and liner construction exactly as shown in Figure 8. Cold rolled steel cones were used throughout. In the discussion to follow, the term "top shift" will be used to indicate that the "defect" was longer at the top of the specimen than at the bottom as shown in Figure 5. "Bottom shift" will be used to indicate the opposite effect. Arrows are used in the photographs to indicate the top and bottom terminus of the "defect" in each specimen. All shift data is listed in the Appendix, A. Data Sheets.

#### Series 11

Objective: to determine if uneven initial upset of the billet was a contributing factor to shift.



Procedure: Three canned billets were extruded with slanting flat surfaces milled on the after ends of the rear components to exaggerate any possible effects of initial upset. (See Figure 44.) The billets were inserted in the liner with the longer dimension on top.

The dies, cones, and liner were at 900°F and the billets at 1150°F. Normal lubrication procedures were used.

Results: The results are shown in Figure 45. The specimen numbers and corresponding slant angles are:

14695 - 5°  
14696 - 10°  
14697 - 15°

#### Series 12

Objective: To determine if the position of the billet relative to the cone and die prior to upset was a contributing factor to shift.

Procedure: Three uncanned billets with centering projections were extruded under identical conditions (see Figure 47). The purpose of the projections was to maintain the billet, cone, and die in line during upset. The dies, cones, and liner were at 900°F and the billets at 1150°F. Normal lubrication procedures were used. The projections were quenched in water just prior to loading in the press in order to provide a solid backing during upset.

Results: The results are shown in Figure 46. Shift was randomly distributed both in length and position.

#### Series 13

Objective: To determine if the relative fit between liner and billet was a contributing factor to shift.

Procedure: Six undersize canned billets were extruded under identical conditions. Three of the billets contained 1.730" O.D. components in a 1 7/8" O.D. can and three contained 1.605" O.D. components in a 1 3/4" O.D. can. Other billet dimensions were the same as shown in Figure 49. The dies, cones, and liner were at 900°F and the billets at 1150°F. Normal lubrication procedures were used.

Results: The results are shown in Figure 48. The specimens from the 1 7/8" cans show consistent top shift of about equal magnitude.



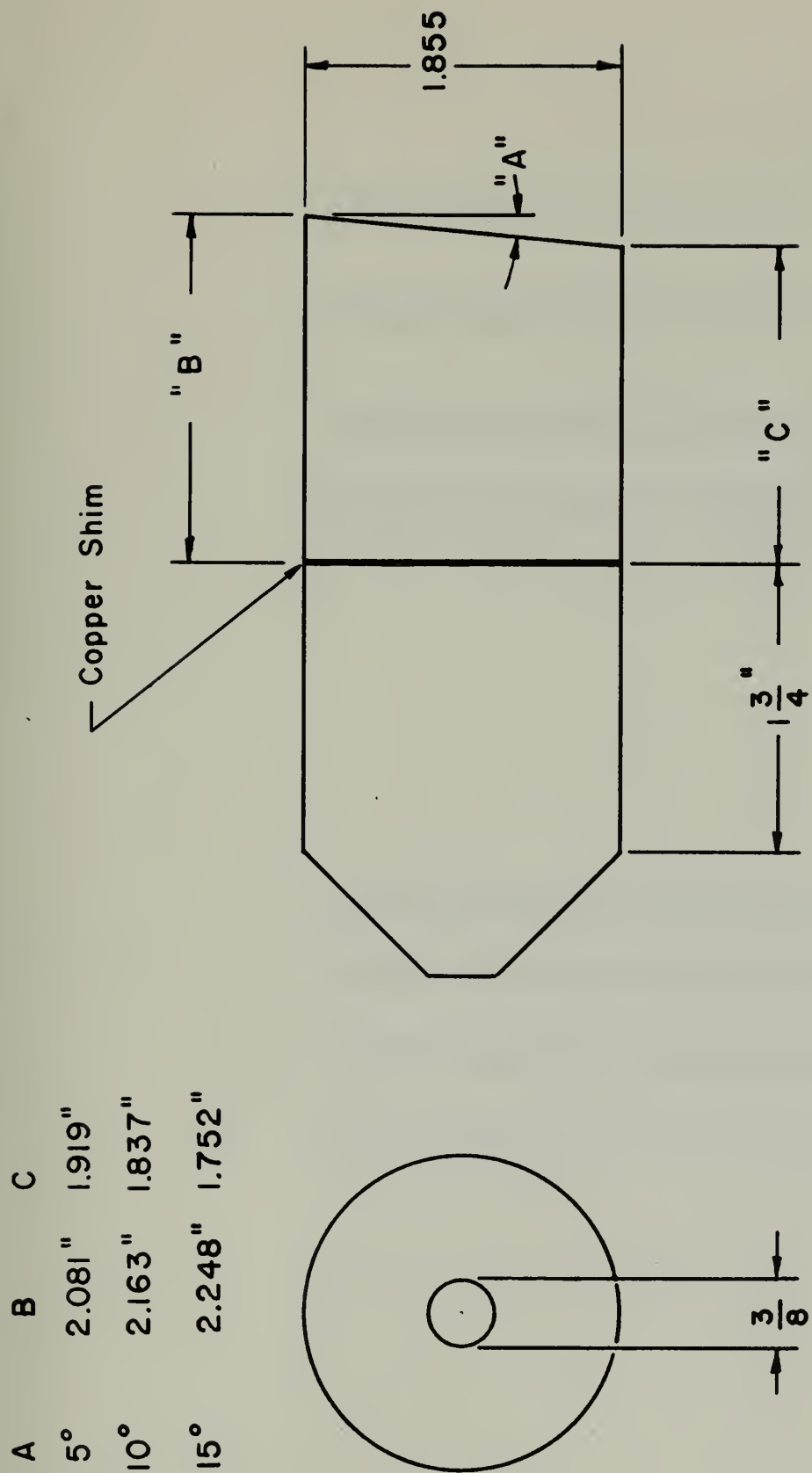


Figure 44 - Cross Section of Naval Brass Billet Components for Series 11





Figure 45 - Series 11 "Defects" (.5X).

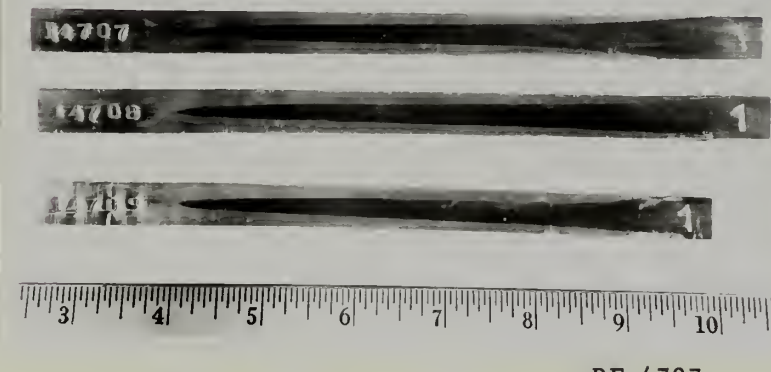


Figure 46 - Series 12 "Defects" (.5X).



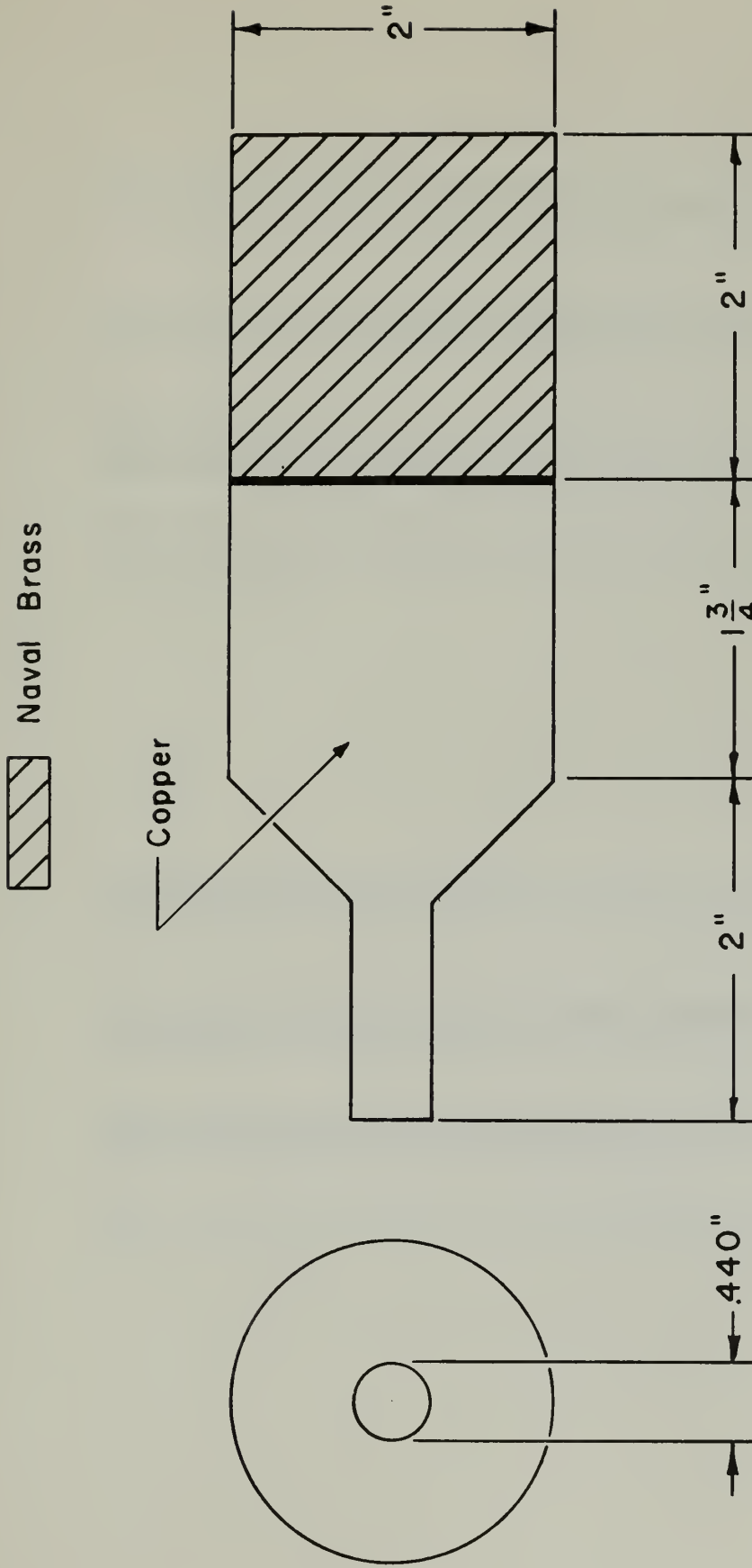


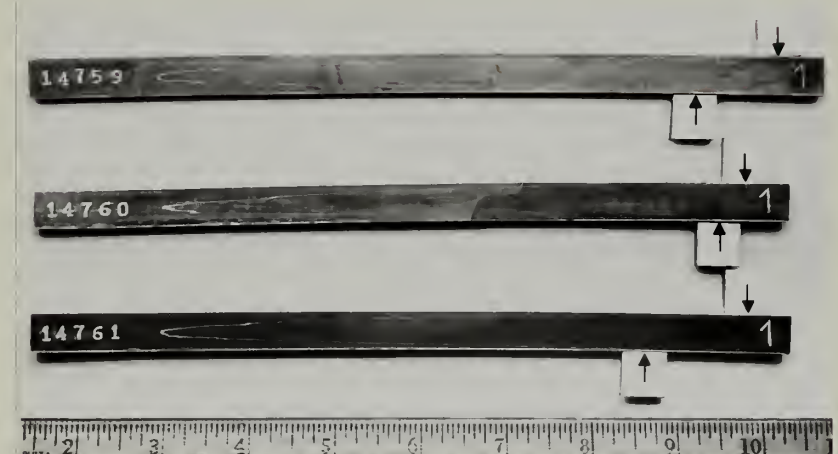
Figure 47 - Cross Section of Billet Components for Series 12.





a. 1 7/8" O.D. can

RF 4728



b. 1 3/4" O.D. can

RF 4729

Figure 48 - Series 13 "Defects" (.5X).



All those from the 1 3/4" cans show top shift but of random magnitude. The irregularity near the forward end of the "defect" in the latter specimens was apparently formed by upset of the extremely undersized cans.

#### Series 14

Objective: To determine if cooling of the billet in the liner just prior to extrusion was a contributing factor to shift.

Procedure: Three canned billets were extruded under identical conditions except that the interval of time between insertion in the liner and beginning of extrusion was varied.

The billet components are shown in Figure 49. The dies and cones were at 900°F and the billets at 1150°F. The liner was at room temperature to induce cooling of the bottom of the billet and any possible shift effects. Normal lubrication procedures were used.

Results: The results are shown in Figure 50. Specimen 14700 cooled for 15 seconds, 14698 for 30 seconds, and 14699 for 1 minute. The extrusion pressure increased with cooling period, showing that the desired cooling was induced, but the resulting shift showed no correlation with cooling period.

#### Series 15

Objective: To determine if the type of lubricant used on the liner, cone, and die has any effect on shift.

Procedure: Six canned billets were extruded under identical conditions except that two different types of lubricant were used.

The billet components are shown in Figure 49. The dies, cones, and liner were at 900°F and the billets at 1150°F. Normal lubrication procedures were used except for the type of lubricant. Ore-Lube is a product of the Ore-Lube Company of 11 Front St., New York. Hot Die Lube No. 4 is a product of the Fiske Brothers Refining Company of Newark, New Jersey and Toledo, Ohio.

Results: The results are shown in Figure 52. The extrusion pressure required for Ore-Lube was essentially the same as that for normal lubrication with Oil-dag, and the "defect" lengths were also comparable.



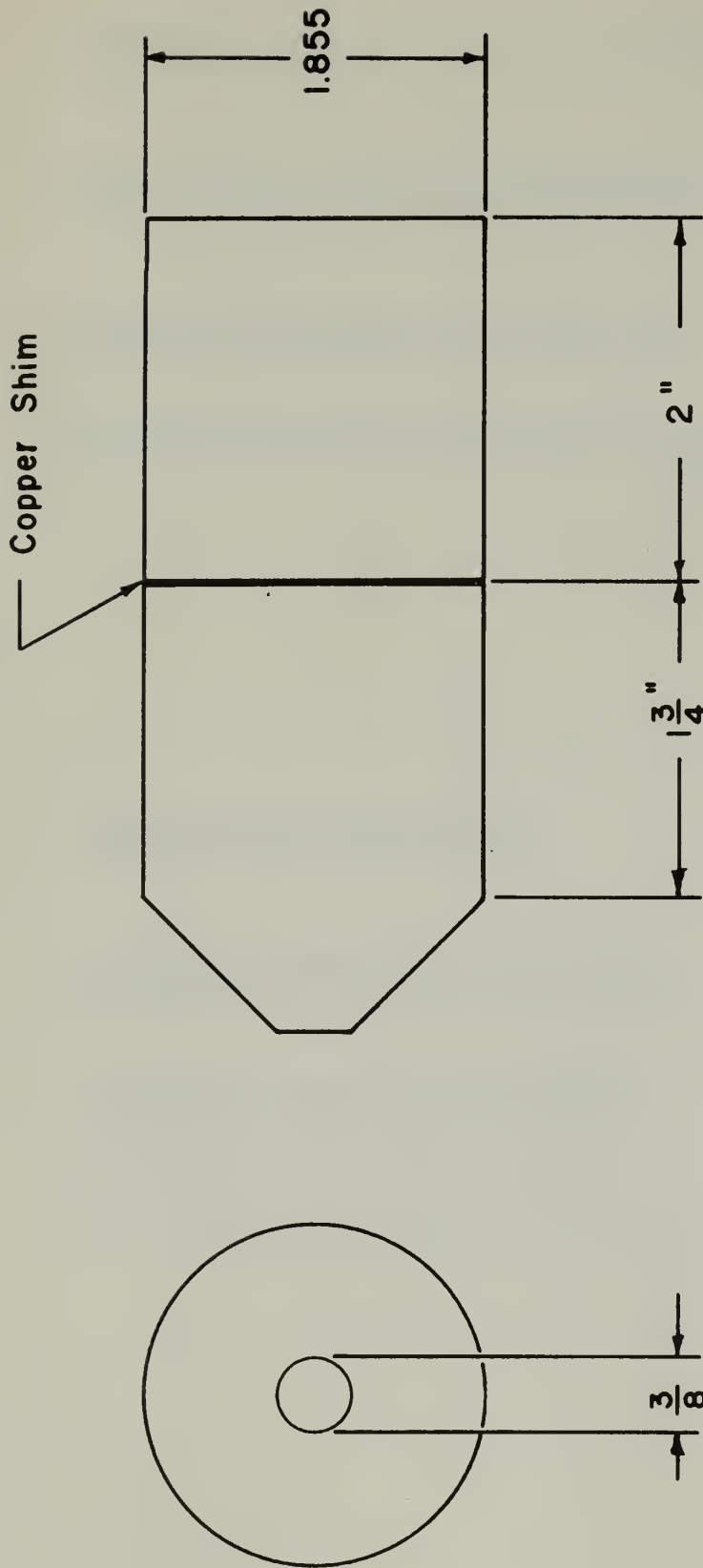


Figure 49 - Cross Section of Naval Brass Billet Components for Series 14,15, and 16.





Figure 50 - Series 14 "Defects" (.5X).

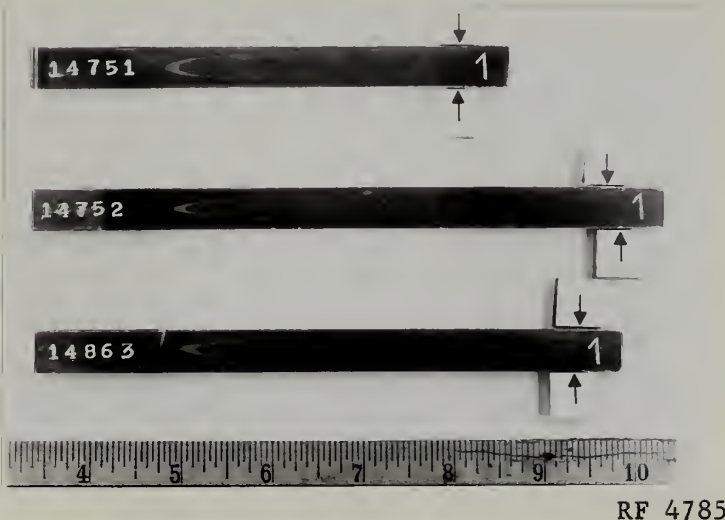


Figure 51 - Series 16 "Defects" (.5X).





a. Ore-Lube

RF 4730



b. Hot Die Lube No. 4

RF 4731

Figure 52 - Series 15 "Defects" (.5X).



However, Hot Die Lube No. 4 required higher pressures and produced considerably longer "defects". The Ore-Lube specimens show either no shift or slight bottom shift while those from Hot Die Lube No. 4 show consistently large top shift.

#### Series 16

Objective: To determine if shift can be eliminated by distributing the lubricant evenly on the billet and all extrusion tools.

Procedure: Three canned billets were extruded under identical conditions with great care taken to approach "ideal" lubrication.

The billet components are shown in Figure 49. The liner, cones, dies, and billets were coated evenly with aquadag and thoroughly dried out. The billet, cone, and die were assembled in the liner which was then sealed with graphite plugs. The liner was heated to 900°F for three hours to insure that all components inside reached the same temperature. The graphite plugs were then removed, the liner inserted in the press, and the billets extruded with every precaution to maintain the lubricant coating intact.

Results: The results are shown in Figure 51. The shift was negligible compared to that which is obtained under normal conditions. The variation in "defect" length is attributed to a difference in billet temperature attained inside the liner, and should not influence the shift results.

To verify the amount of shift in these specimens, they were sectioned through the axis at several points, etched, and examined at a magnification of 30 times. The results showed the copper shim line to be perfectly concentric about the rod axis for specimens 14752 and 14863, thus confirming little or no shift. In specimen 14751, however, there was actually about 3/8" shift at an angle of 120° from the top of the rod, although no shift was indicated by examining the milled diameter.

#### Series 17

Objective: To study the shift phenomenon during the extrusion process.

Procedure: Three canned multi-element billets were extruded under



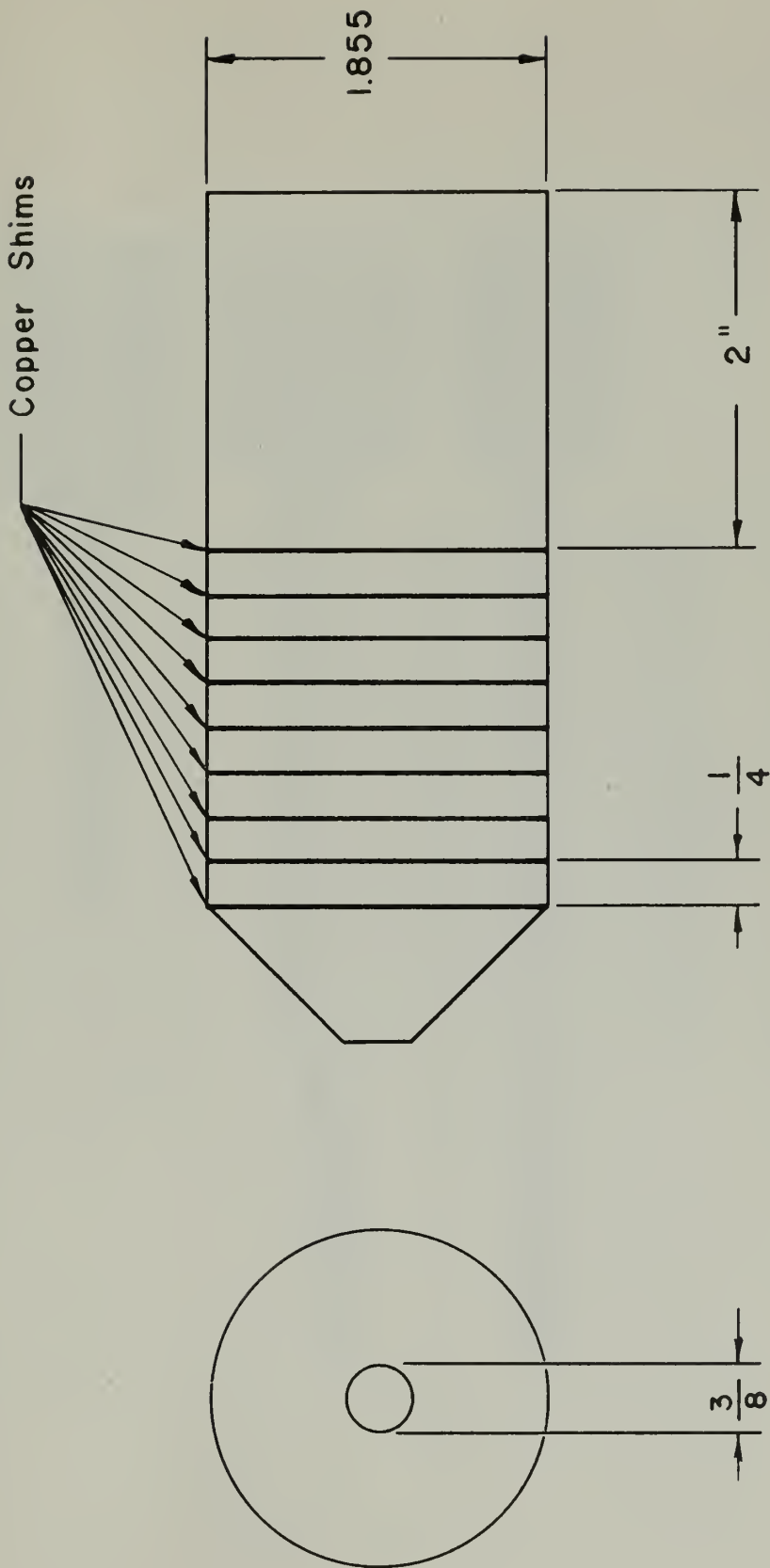


Figure 53 - Cross Section of Naval Brass Billet Components for Series 17 and 18.



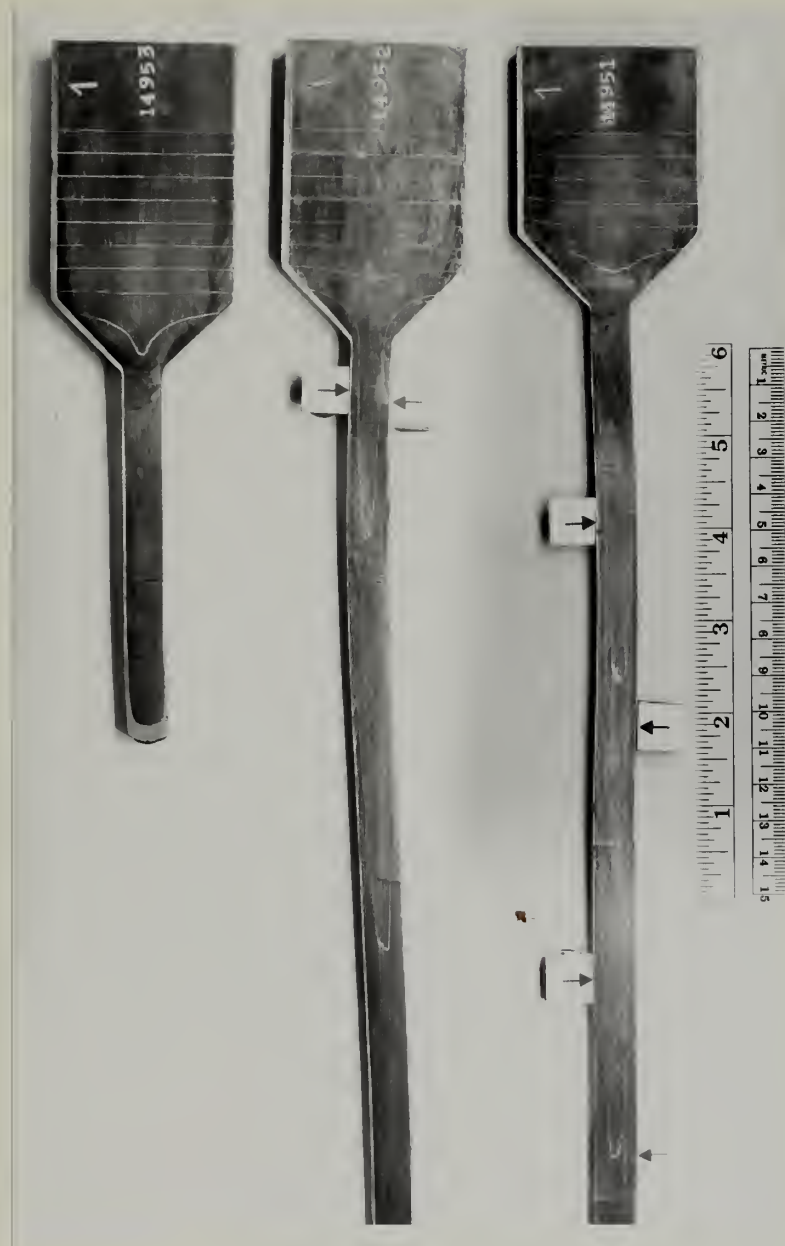


Figure 54 - Series 17 "Defects" (.5X).



identical conditions, and the press was stopped at a different stage of each extrusion to study the progression of metal flow which results in shift.

The billet components are shown in Figure 53. The cones and dies were at 900°F, the liner at room temperature, and the billets at 1150°F. Normal lubrication procedures were used except that only the bottom half of the liner was lubricated in order to induce shift.

Results: The results are shown in Figure 54.

#### Series 18

Objective: To determine the effect of cone lubrication on the shift phenomenon.

Procedure: Three canned multi-element billets similar to those used in Series 17 were extruded under identical conditions, and the press was stopped at different stages of the extrusion process as before.

The billet and liner were completely lubricated with several coats of aquadag, dried out, and heated together to 900°F for 3 hours to maintain "ideal" lubrication conditions as in Series 16. The bottom half of each cone was roughened by machining heavy concentric grooves as shown in Figure 55. The top halves of the cones were evenly coated with aquadag. No lubricant was used on the die in order to maintain the desired lubrication conditions on the cone surface. Cones and dies were heated to 900°F.

Results: The results are shown in Figure 56.

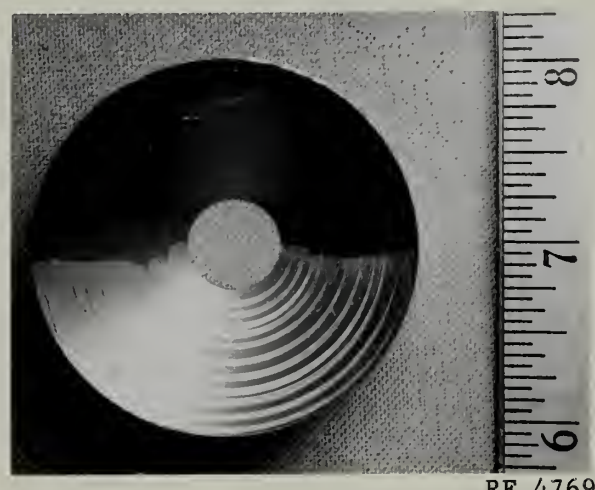
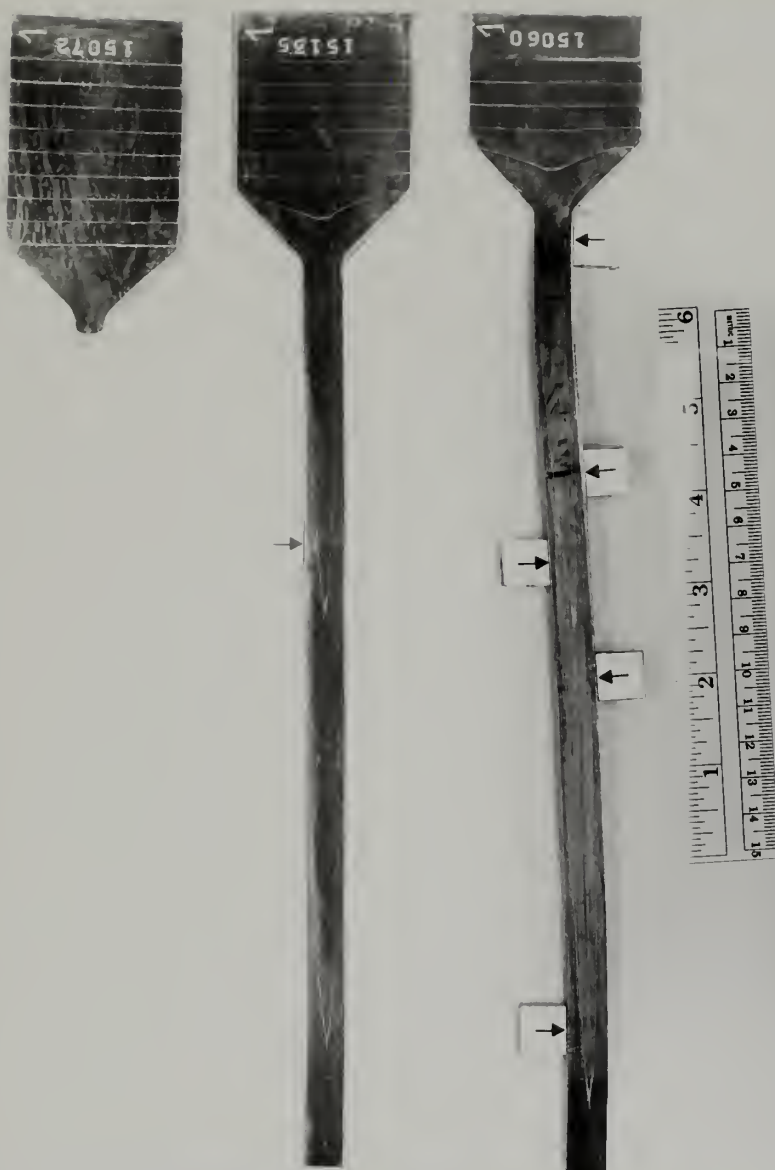


Figure 55 - Preparation of cones for Series 18.



RF 4868

Figure 56 - Series 18 "Defects" (.5X).





## 2. Discussion of Results

The random nature of shift, both in position in the billet and in magnitude, can be seen in Figure 57, which shows shift data from the Main Series experiments. The specimens in each of Series 2-4 were extruded in succession using the same liner. As can be seen from the plots, there is no correlation in shift between defects which were extruded from the same billet, and there is no general preference or trend for top or bottom shift.

It should be pointed out at this time that all shift data was obtained by milling on the diameter which was vertical as the rod was extruded. This was done because it was the simplest and most inexpensive method of examining the "defects" in general, and because it was felt that shift would be most pronounced on the vertical diameter if lubrication was indeed the major factor involved.

The results of sectioning the specimens of Series 16 proved that examination on the vertical diameter will not give reliable data on shift since maximum shift can apparently occur at any angle with the vertical. Although this point should be borne in mind it does not affect the qualitative conclusions which can be drawn from the shift experiments.

In Series 11 one might expect that since the ram bore first on the top of the billet and forced metal to flow into the void at the bottom during upset, bottom shift would predominate and increase with the slant angle. This effect is indicated in specimens 14695 and 14697. In 14696, however, slight top shift resulted. This may have resulted from not having the longest billet dimension exactly on top during extrusion. However, even with the grossly exaggerated slant angles, the observed shift was not unduly long compared to that obtained under normal conditions. It is therefore concluded that uneven initial upset of the billet either has no effect or is at most a second order effect in the shift mechanism.

Since the three billets of Series 12 were extruded under identical conditions and still produced random shift, it is concluded that billet



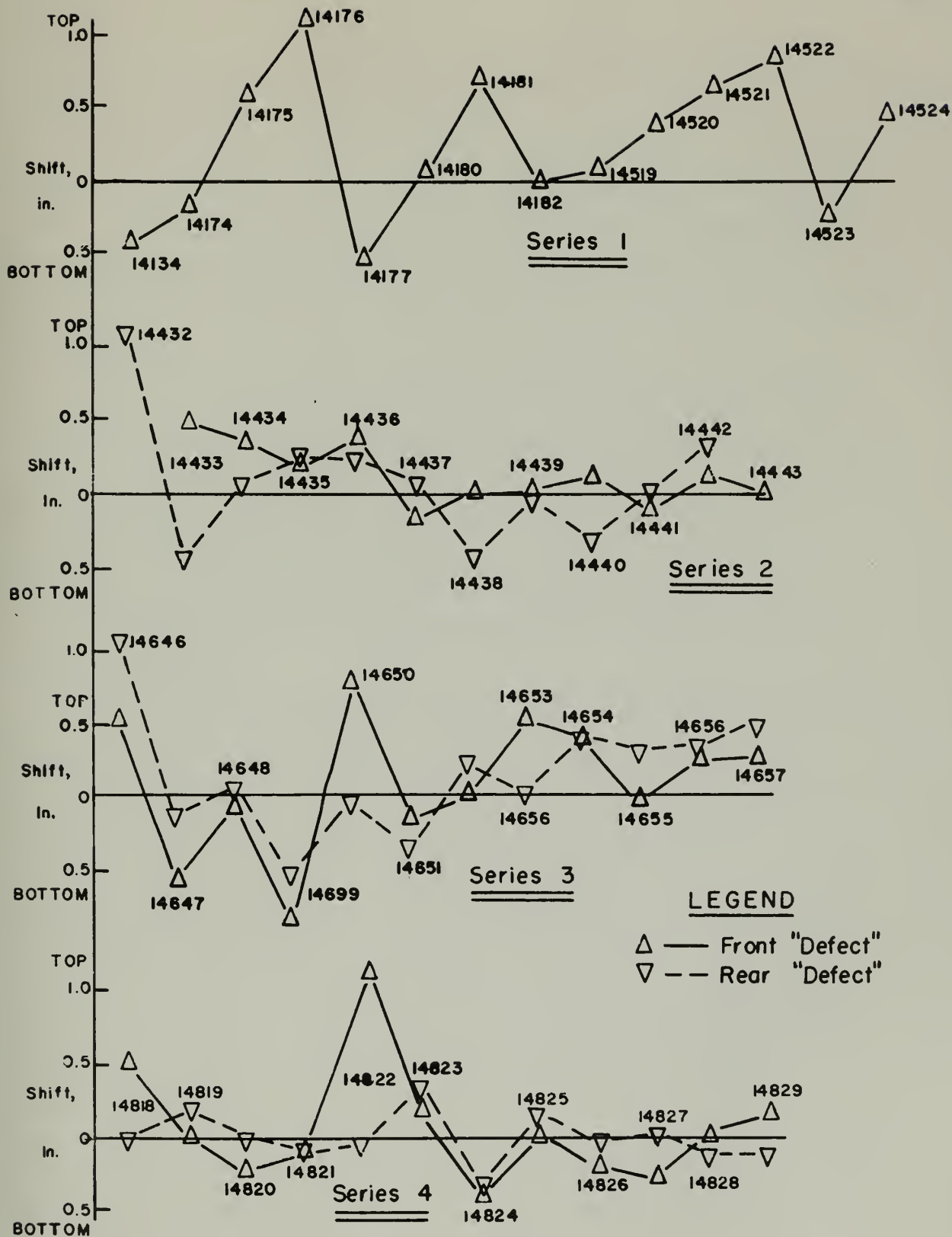


Figure 57 - Shift Data from Series 1-4



alignment with respect to die and cone is not a contributing factor to shift or is at most a second order effect.

In Series 13, the fact that all six specimens show top shift might indicate that relative fit of liner and billet is a factor influencing shift. However, since the amount of shift is within the normal range, it is considered more probable, because of the extremely loose fits chosen, that this factor is of only second order importance in the shift mechanism.

In Series 14, the shift is random and shows no correlation with the exaggerated cooling periods, thus leading to the conclusion that uneven billet cooling is not a contributing factor to shift.

The results of Series 15 indicate that Ore-Lube gives results which are comparable to those with oildag, whereas Hot Die Lube No. 4 is definitely not suitable as a lubricant for extrusion under these conditions. The fact that the latter consistently produced significant shift indicates that lubrication may play an important role in the shift mechanism.

The results of Series 16 confirm the conclusion that lubrication must be the most important factor involved in the shift mechanism. Although slight shift in specimens 14752 and 14863 is indicated by the arrows in Figure 51, subsequent examination under magnification revealed absolutely no shift on the milled diameter and perfect concentricity of the shim when examined on the half section. Although the shift later discovered on a different diameter in specimen 14751 might tend to invalidate the conclusion, the average for these three extrusions is certainly less than would be expected from three normal extrusions, and the fact that "ideal" lubrication conditions actually did produce absolutely no shift in two extrusions out of three is considered significant.

In Series 17, the exaggerated effect of uneven lubrication in the liner is seen to hold back the top of the interface (no lubrication on the top half of the liner) as it approaches the cone. The degree of "hold-back" is apparently a function of billet movement through the



liner. Although very slight in specimen 14953, it is measurable with a square in 14952 and quite pronounced in 14951, which was stopped after the greatest amount of ram travel.

The net effect of this slight shift formation in the liner is to place the interface in the cone unevenly where accelerated metal flow magnifies the disadvantage and produces significant shift in the extruded "defect". As seen in Figure 54, the shift produced in specimen 14951 constitutes about 1/3 of the total "defect" length.

According to the above theory one would expect shift to be larger in rear defects than in front defects because friction effects have had more time to deform the rear interface due to its greater travel through the liner. This is confirmed in the Series 3 and 4 curves of Figure 57, but is not conclusive from the data for Series 2.

The general conclusion to be drawn from Series 17 is that any uneven lubrication in the liner will tend to produce a slight shift of the interface which is greatly magnified in the cone and die due to acceleration of metal flow.

From the nature of the experiments in Series 18 and the results of Series 16, it will be assumed that the shift produced in Series 18 specimens was entirely due to cone effects and was not influenced by any uneven lubrication in the liner. Since the bottom of the cone was unlubricated and rough, it was expected that bottom shift would be produced, as confirmed by the results. It is interesting to note, however, that the effect of cone lubrication was reflected back into the liner as seen by the fact that the tops of the interface in the specimens of Figure 56 have advanced more than the bottoms. As the interface progressed through the cone and die, this "holding back" of the bottoms of the interfaces was accentuated in a striking manner with resulting shift that constituted almost half of the total "defect" length. It is concluded that any uneven lubrication or surface roughness in the cone will contribute significantly to the total shift produced in an extruded specimen. The overall conclusion to be drawn from Series 17 and 18 is that uneven lubrication or roughness in either cone or liner is the most significant contributing factor to the shift phenomenon.



### E. The Whiskers Experiments

#### 1. The Experiments and the Results

All whiskers experiments were performed at an area reduction ratio of 20.4 with liner, cone, and die construction exactly as shown in Figure 8. All billets were heated to 1150°F; and in all cases the die, cone, and liner were at 900°F. Normal lubrication as described in II. General Procedures was used throughout.

Naval brass and copper-nickel were used for all composite billet components in order to obtain sufficient difference in extrusion constant for whiskers to occur. All cladding sleeves had radial dimensions as shown in Figure 58 and were machined from a Cu-9w/o Ni alloy.

Other copper-nickel billet components were a Cu-9.5w/o Ni alloy except in Series 23 and 25 where the nickel percentage was 9.1. All components inside a cladding sleeve had an O.D. of 1.550" except in Series 20 where this dimension was varied.

#### Series 19

Objective: To determine if whiskers can result from so-called "penetration" of soft material into hard material at a point of weakness.

Procedure: Six canned billets were extruded under identical conditions except for different degrees of finish on the mating surfaces of both hard and soft materials.

The billet components are shown in Figure 59. The surface finishes were:

500 RMS - rough grooves  
63 RMS - normal  
2 MU - polished

Results: The results are shown in Figure 60. The surface finish combination for each specimen is given in Table X. (Refer to Figure 59 for surface designation.)



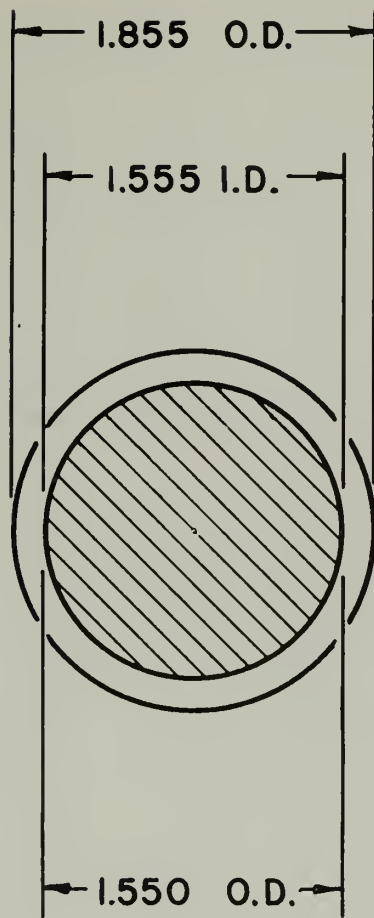
**Sleeve Dimensions****Core and End Seal Dim.**

Figure 58 - Billet Component Dimensions Common to  
Series 20-24



Naval Brass

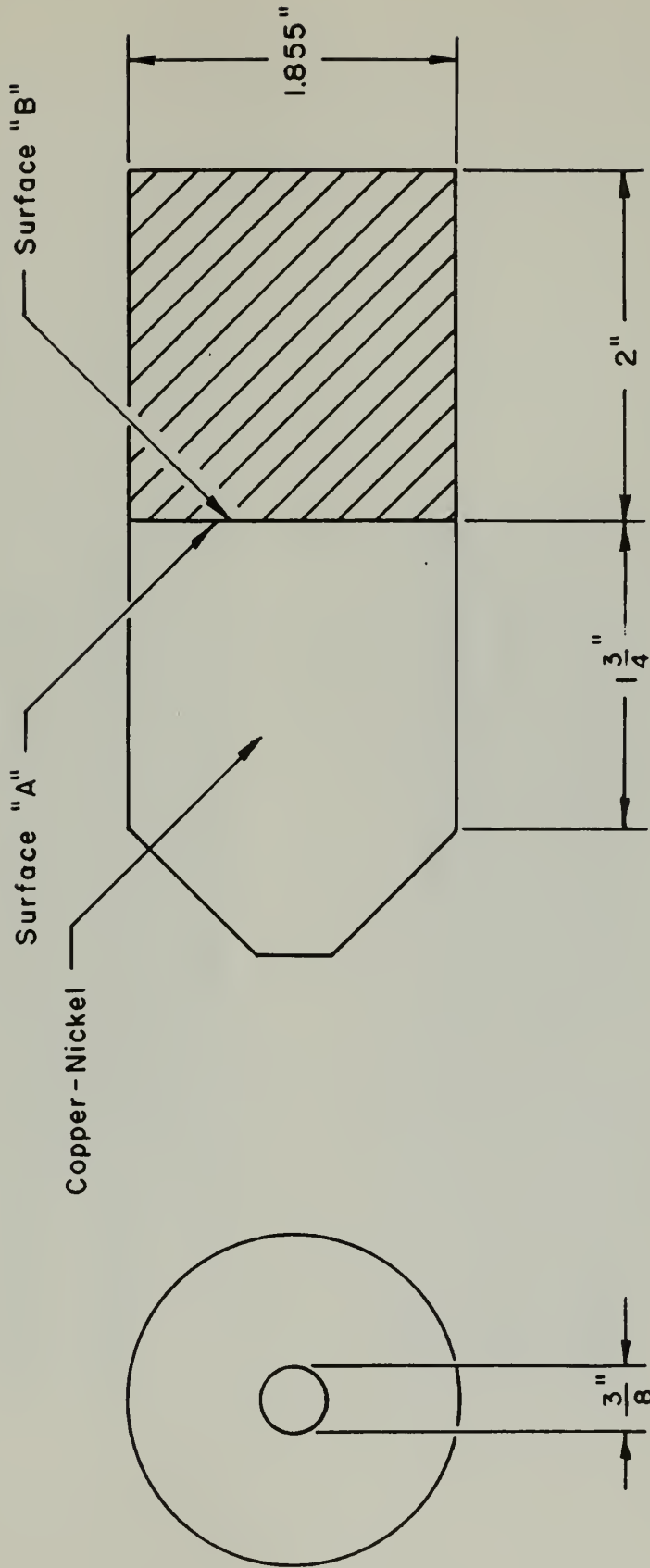
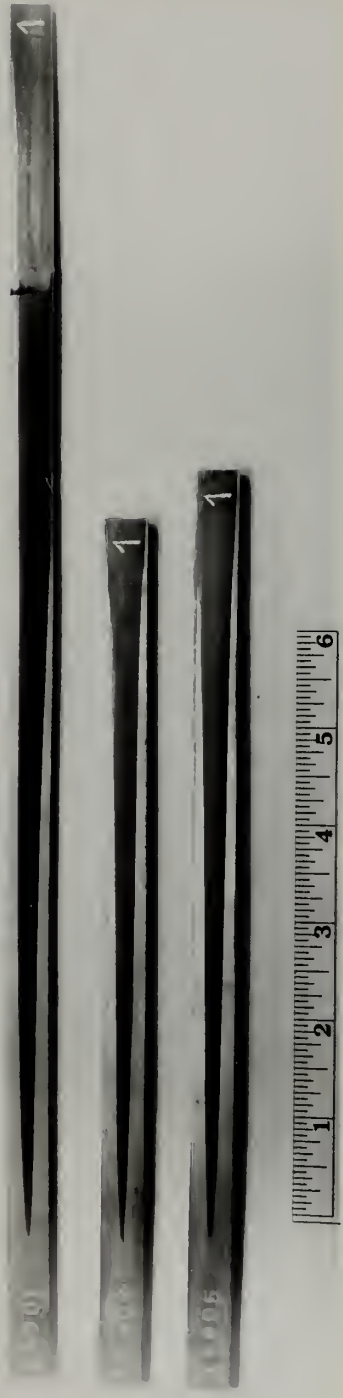


Figure 59 - Gross Suction of Billet Components for Series 19.





a. Surface B - 500 RMS Finish

RF 4786



b. Surface B - 2 MJ Finish

RF 4787

Figure 60 - Series 19 "Defects" (.5X).



Table X. Surface Finish Combinations for Series 19

<u>Specimen No.</u>	<u>Surface A</u>	<u>Surface B</u>
14901	500 RMS	500 RMS
14903	63 RMS	500 RMS
14905	2 MU	500 RMS
14902	500 RMS	2 MU
14904	63 RMS	2 MU
14906	2 MU	2 MU

Series 20

Objective: To determine if the relative fit between cladding sleeve and core and end seal components was a contributing factor to whiskers formation.

Procedure: Three clad and canned billets as shown in Figure 61, were extruded under identical conditions except for the cladding sleeve fit.

Results: The results are shown in Figure 62. The O.D. of components inside the clad was varied as indicated in Table XI.

Table XI. O.D. of Core and End Seal Components for Series 20

<u>Specimen No.</u>	<u>O.D.</u>	<u>Fit to Sleeve</u>
14907	1.559"	Shrink
14908	1.550"	Normal
14909	1.530"	Loose

Series 21

Objective: To determine the effect on whiskers of machining mating chamfered edges on the "core" and "end seal" components.

Procedure: Four clad and canned billets were extruded under identical conditions except that the type and amount of chamfer was varied. Two of the billets were as shown in Figure 63 with 1/4" and 1/8" straight 45° chamfers, and the other two were similar to the billets shown in Figure 70 except that 1/4" and 1/8" radii were used instead of straight chamfers.

Results. The results are shown in Figure 64. The chamfer configurations are listed in Table XII.



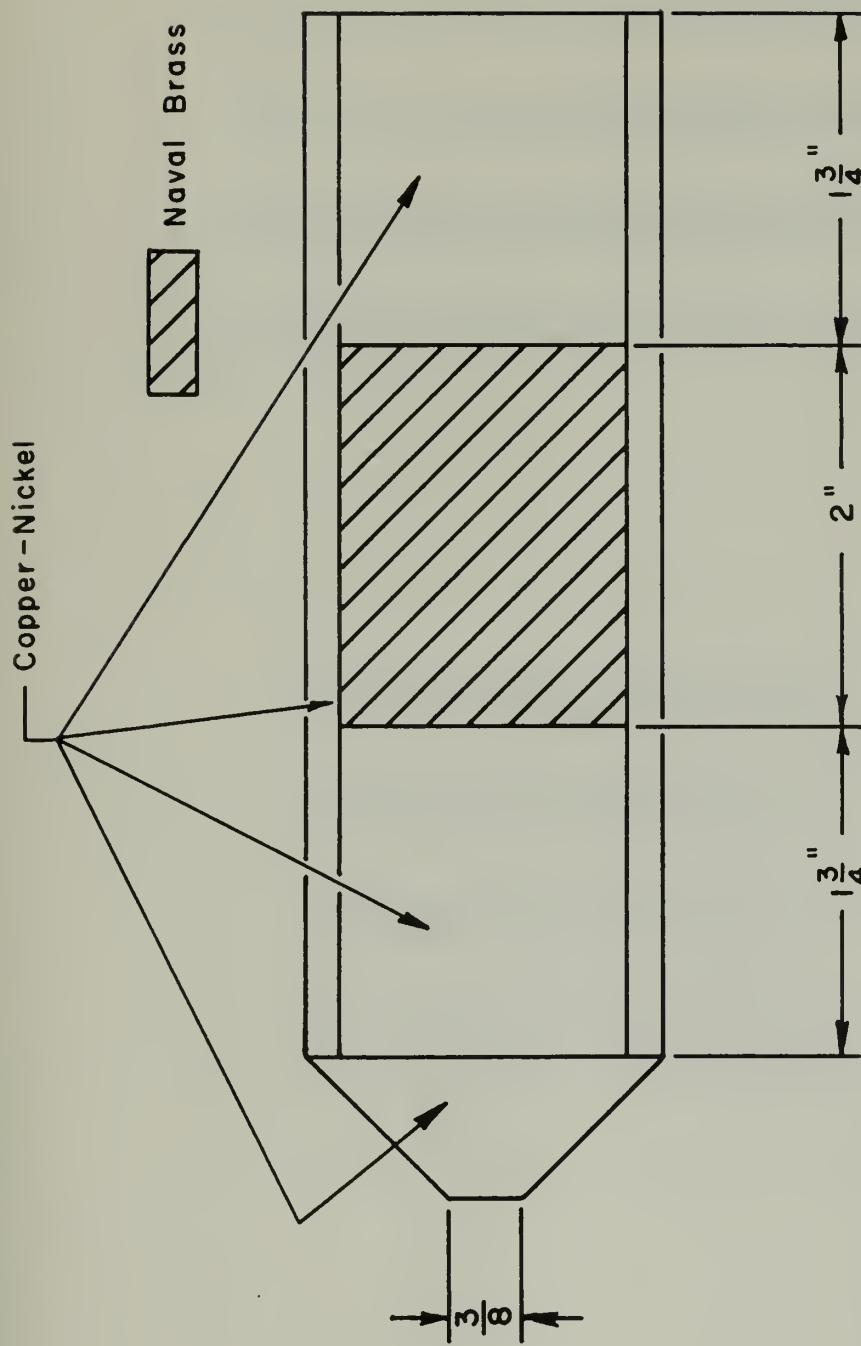


Figure 61 - Gross Section of Billitt Components for Series 20.





a. Front "Defects"

RF 4788



b. Rear "Defects"

RF 4789

Figure 62 - Series 20 "Defects" (.5X).



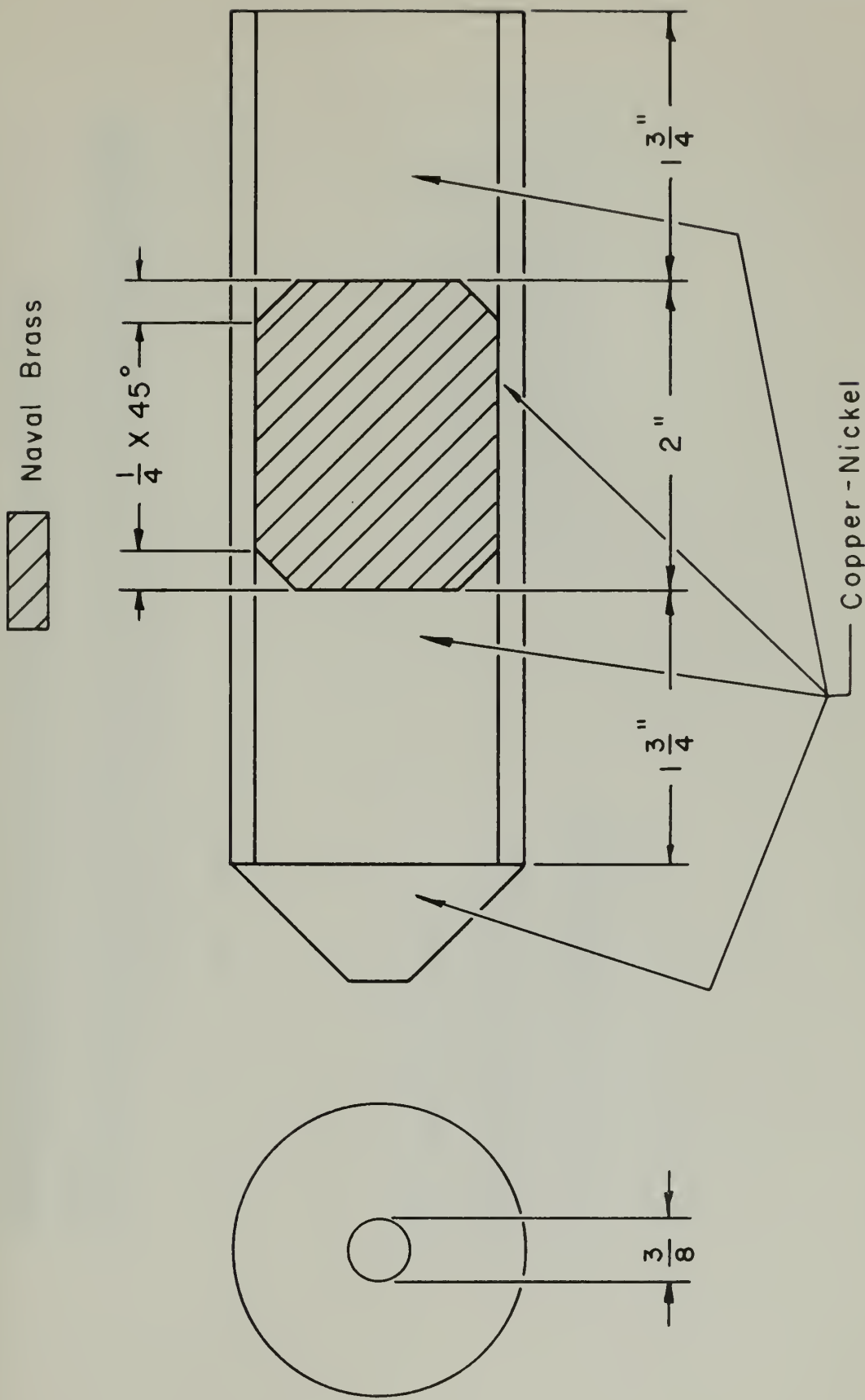
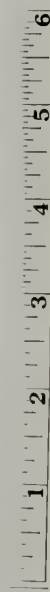


Figure 63 - Cross Section of Billet Components for Series 21.

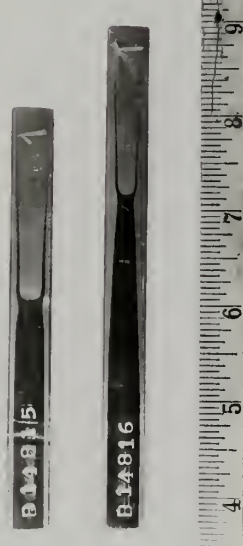




a. Straight Chamfer - Front "Defects".

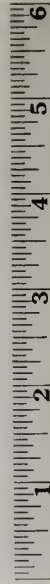


RF 4790



b. Straight Chamfer - Rear "Defects".

RF 4791



RF 4878

c. Round Chamfer - Rear "Defects".

Figure 64 - Series 21 "Defects" (.5X).



Table XII. Chamfer Configurations for Series 21

<u>Specimen No.</u>	<u>Chamfer</u>
14815	1/8" straight (Figure 63)
14816	1/4" straight " "
15184	1/8" round (Figure 70)
15185	1/4" round " "

Series 22

Objective: To extend the results of Series 21 by determining the effect of another billet interface geometry on whiskers formation.

Procedure: One clad and canned billet as shown in Figure 65 was extruded.

Results: The results are shown in Figure 67.

Series 23

Objective: To study the mechanism of whiskers formation in billets with a flat interface.

Procedure: Three clad and canned billets as shown in Figure 66 were extruded under identical conditions, and the press was stopped after different amounts of ram travel.

Results: The results are shown in Figure 68. The completely extruded "defect" at the bottom was taken from specimen 14912 but is representative of the "defects" produced in all three specimens.

Series 24

Objective: To study the mechanism of whiskers formation in billets with a chamfered interface.

Procedure: Three clad and canned billets as shown in Figure 70 were extruded under identical conditions, and the press was stopped after different amounts of ram travel.

Results: The results are shown in Figure 71. A completely extruded defect from these billets would be represented by specimen B 14816 of Figure 64. Figure 72 shows the line of demarcation between the copper-nickel components which is not readily discernable from the photograph in Figure 71.

Series 25

Objective: To study the mechanism of whisker formation when one material in the billet is infinitely stiffer than the other.



Naval Brass

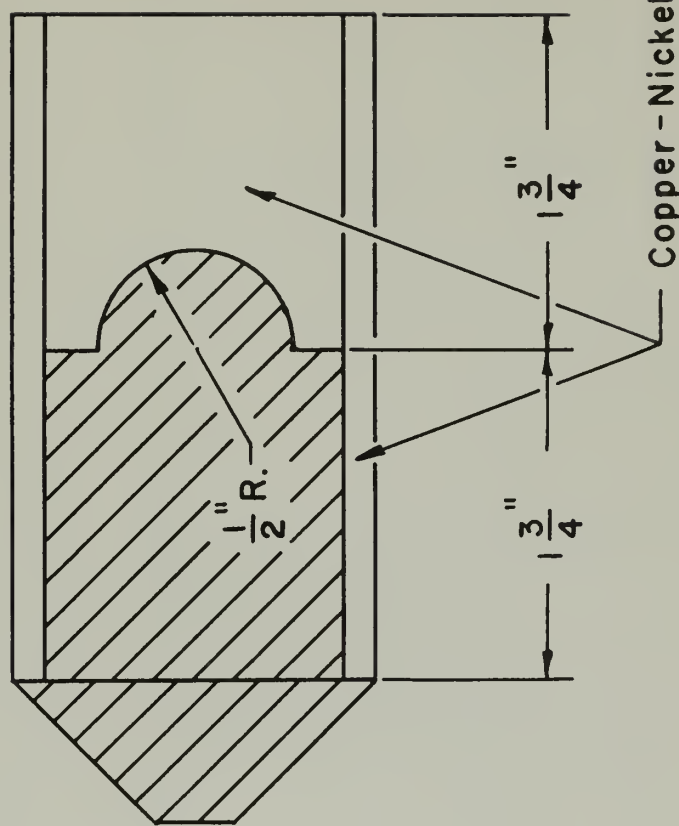
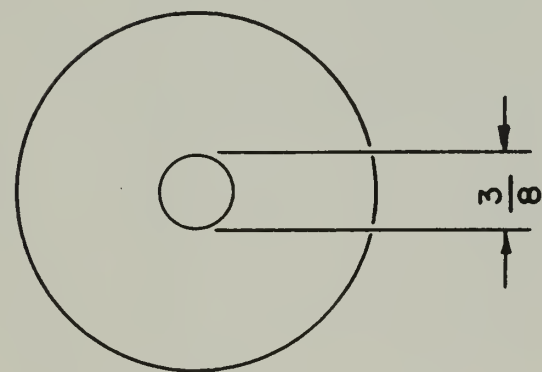


Figure 65 - Cross Section of Billet Components for Series 22.





Naval Brass



Copper-Nickel

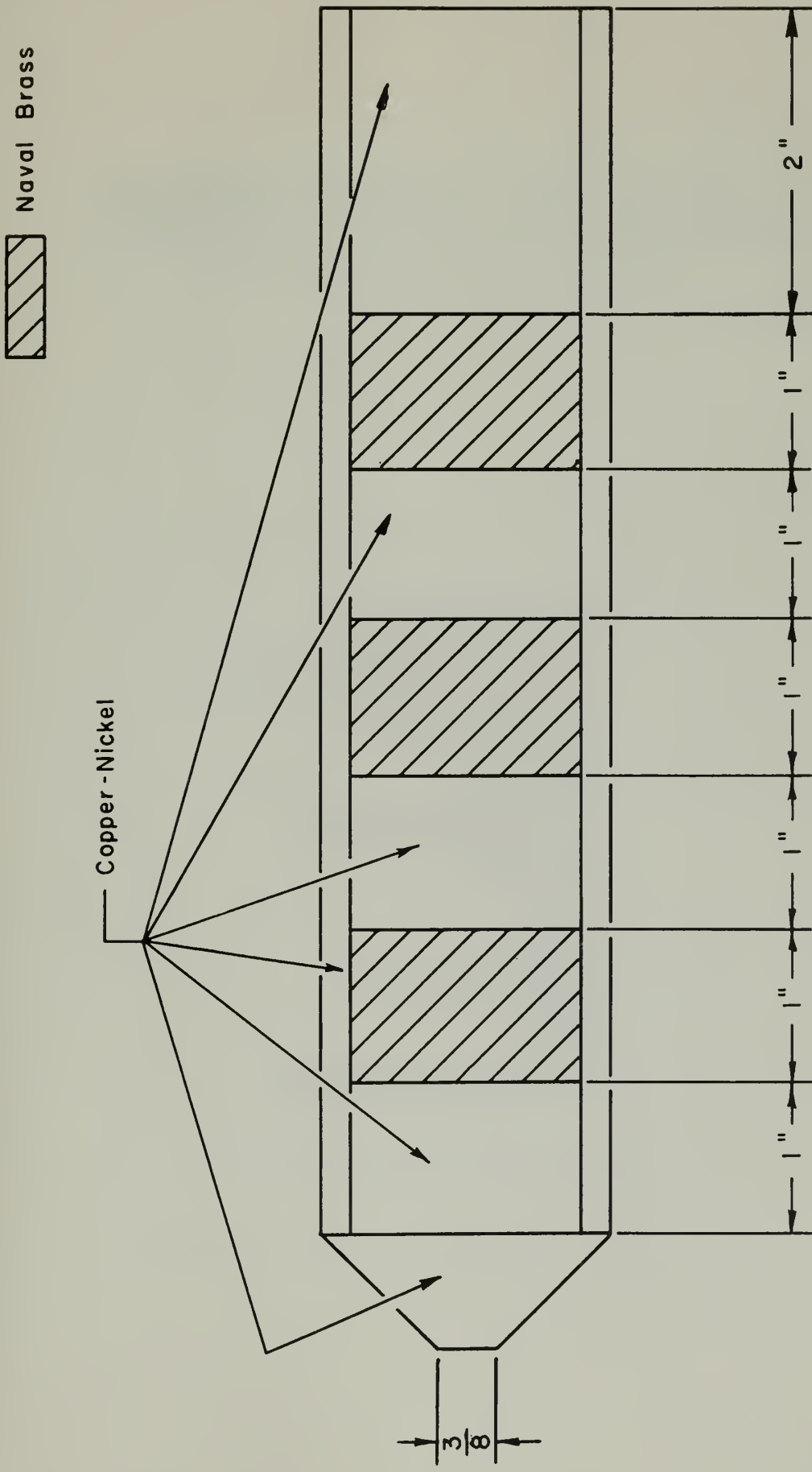
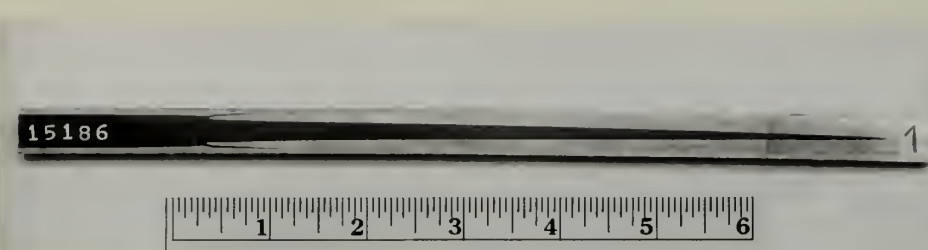


Figure 66 - Cross Section of Billet Components for Series 23.





RF 4879

Figure 67 - Series 22 "Defects" (.5X).



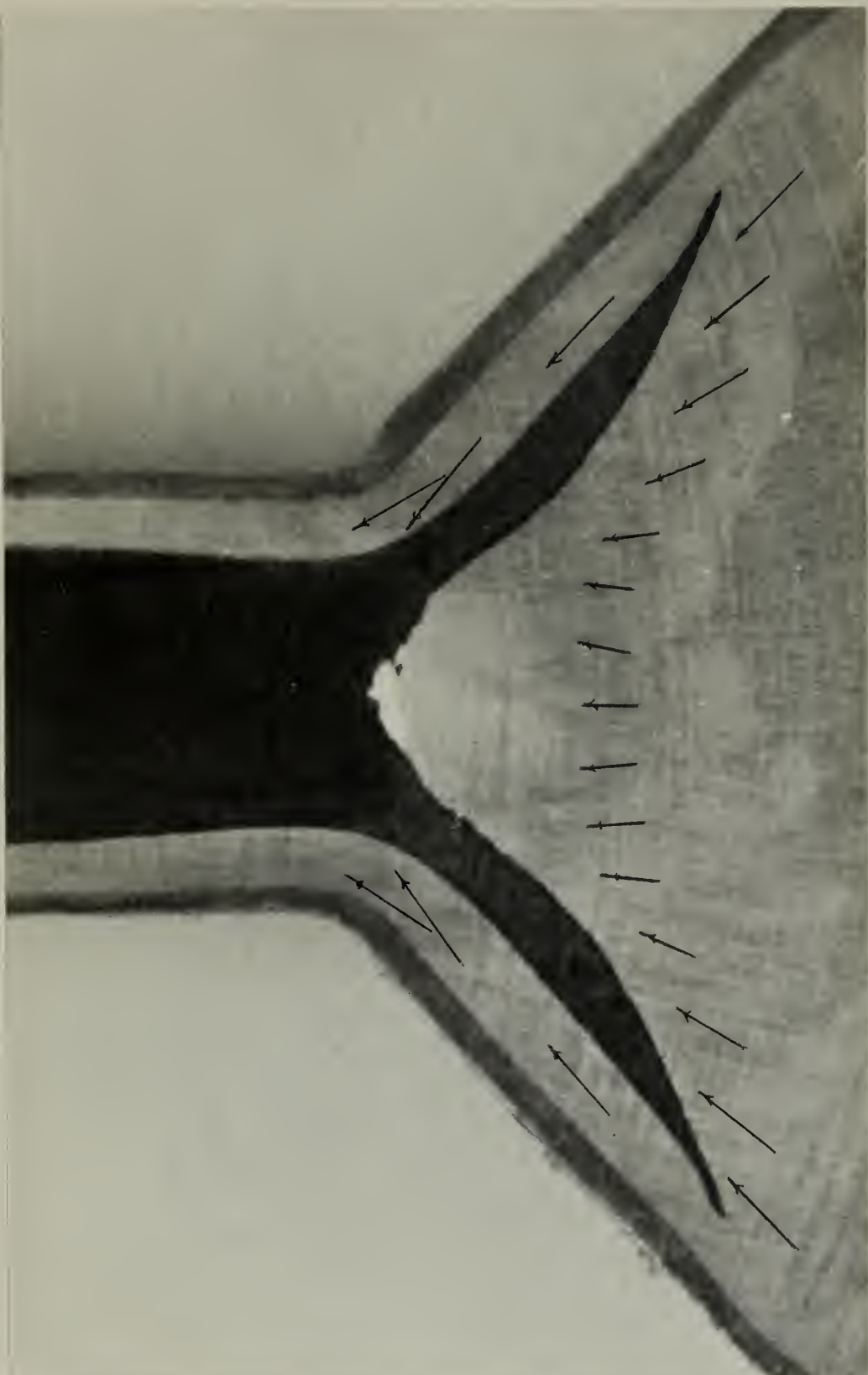
14912



RF 4833

Figure 68 - Series 23 "Defects" (.5X).





RF 4833

Figure 69-Metal Flow During Whiskering (Series 23).



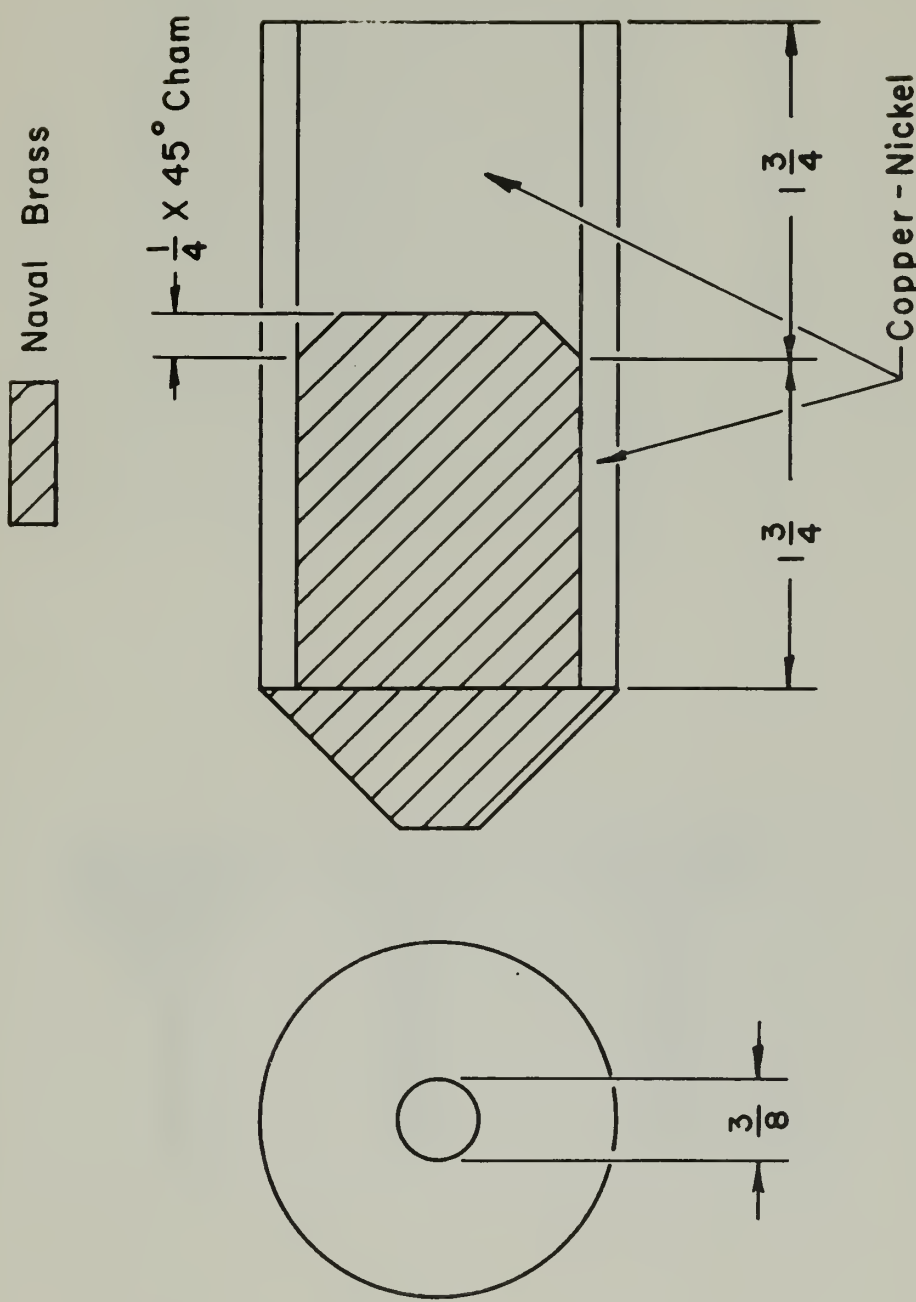


Figure 70 - Cross Section of Billet Components for Series 24.





Figure 72 - Line of Demarcation between  
Copper-Nickel Components in  
Series 24 (1X).

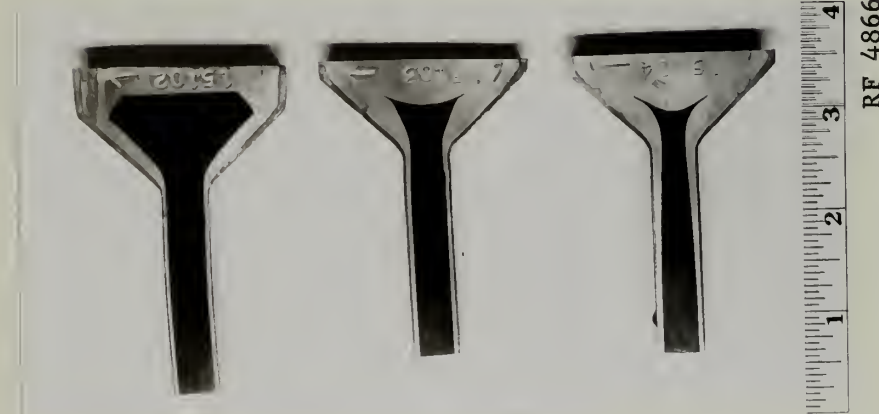


Figure 71 - Series 24 "Defects"  
(.5X).



Procedure: Five unclad and uncanned billets were extruded with air as the "soft" material. The billet geometry is shown in Figure 73. Three billets of type "A" were stopped after different amounts of ram travel. The type "B" and "C" billets were completely extruded.

Results: The results are shown in Figure 74. Specimens 15025 - 15027 were extruded from type "A" billets, 15169 from type "B", and 15168 from type "C".

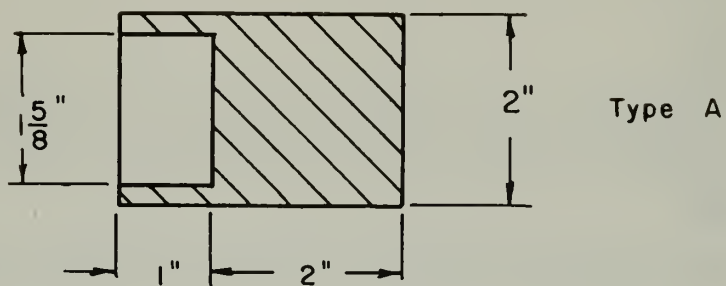
## 2. Discussion of Results

Examination of Main Series results reveals several interesting points about whisker formation. For instance, whiskering occurs only when there is a wide variation in extrusion constants between the core and end seal material. Thus whiskers were produced in Series 2 and 3 where such a condition was met but not in Series 4 where the K's were nearly equal. In addition, whiskers were produced only when the harder material was behind the softer material in the billet (see Figures 14 and 16). The whisker-like projections of naval brass material in some of the specimens of Figures 15 and 16 are not considered to be true whiskers but merely the "reversal" effect which results from overcompensation. In Figures 14 and 16 it can also be seen that whiskers decrease with decreasing cone angle and with increasing interface (preshape) angle.

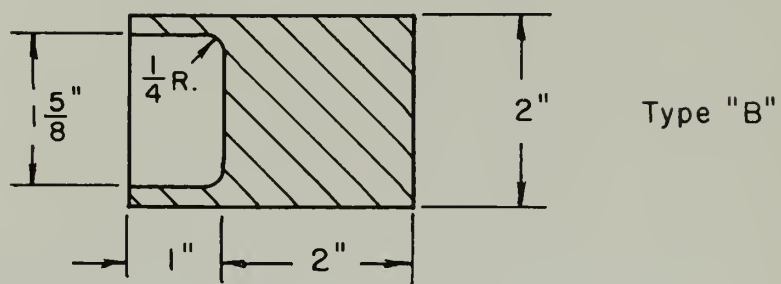
At the beginning of this investigation, it was thought that whiskers might result from "penetration" of the soft material into the hard. Series 19 and 20 reflect this thinking. In Series 19, the attempt was to induce points of weakness by the machining procedure. In Series 20, the natural point of weakness between cladding sleeve and end seal components was exploited. The results of these two series of experiments are considered conclusive proof that no "penetration" phenomenon is involved in whisker formation.

Series 21, though it reflects the "penetration" theory in its original objective, actually introduces a new metal flow concept of whisker formation which is verified in later experiments. It should be noted that straight and radius chamfers produced almost identical

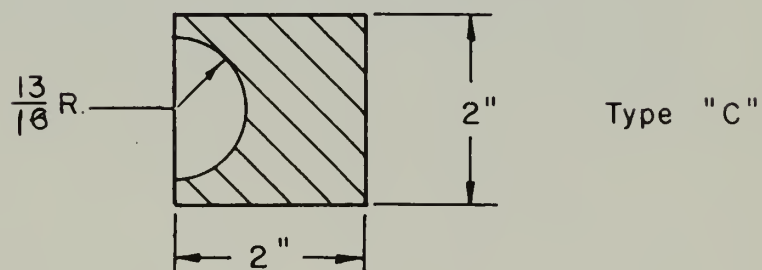




Type A



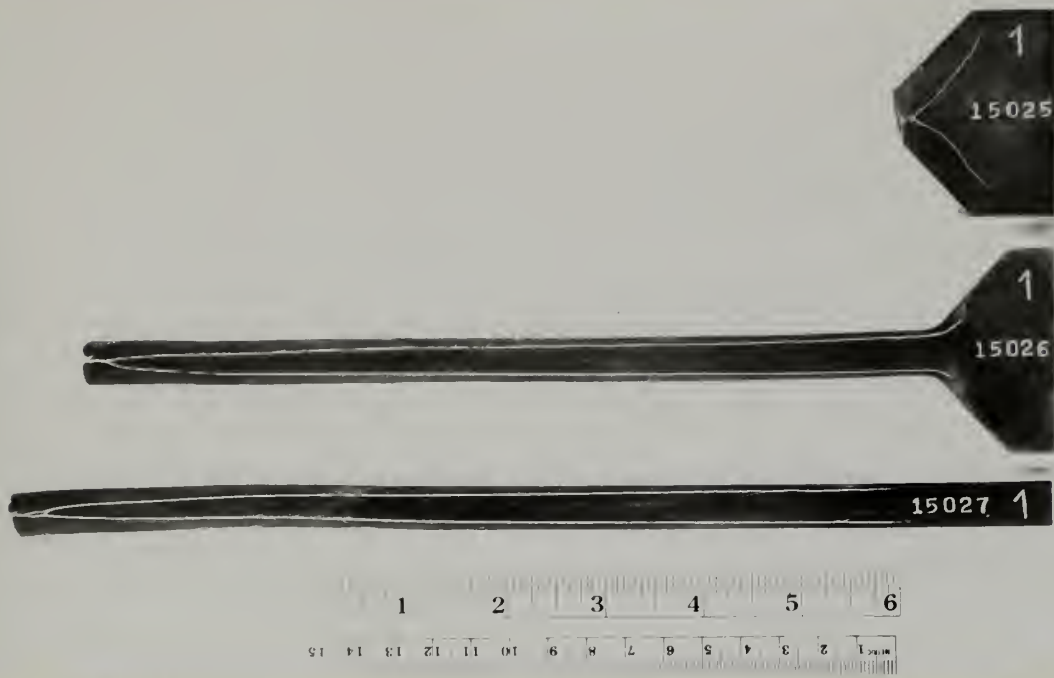
Type "B"



Type "C"

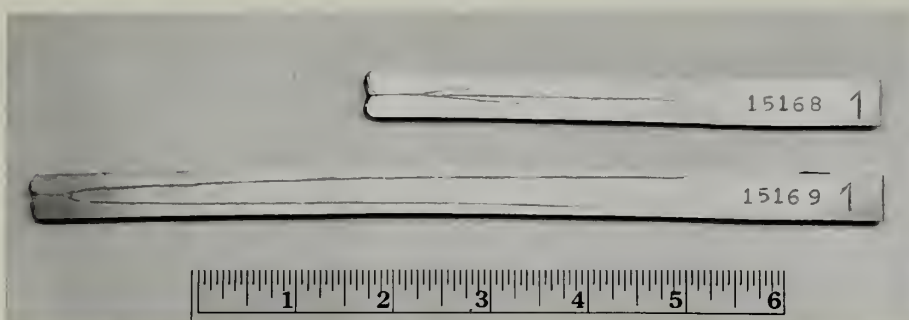
Figure 73 - Cross Sections of Naval Brass Billet Components for Series 25.





a. Type "A" Billets

RF 4831



b. Type "B" and "C" Billets

RF 4867

Figure 74 - Series 25 "Defects" (.5X).



"defects" and that increasing the amount of chamfer always moved the whiskers away from the cladding surface and toward the center of the specimen.

Series 22 is simply an interesting sideline to the whiskers study and shows the effect of overcompensation coupled with the usual whisker formation.

In the results of Series 23, we can begin to obtain a qualitative concept of the mechanism of whisker formation. In specimens 14910 and 14912 of Figure 68, the "defect" was "caught" in two slightly different stages of formation with the typical result shown at the bottom of the photograph. The line of demarcation between the copper-nickel cladding sleeve and "end seal" component can be seen clearly in the upper part of specimen 14910. The whiskers apparently result from a difference in relative flow velocity of the hard and soft metals as they are deformed in the cone. The soft material, having less resistance to deformation, flows faster through the central region of the die opening but is held back around the periphery of the cone by the squeezing effect of the hard material behind. Actually this same mechanism was taking place in the unclad billets of the Main Series. With the presence of a cladding sleeve, however, the relative flow rates of the two materials evidently causes the displacement of the held-back, softer material toward the cone surface as this material moves toward the die opening. Figure 69 shows an estimate of material velocities during whiskering; the length of the vectors indicates relative velocities. The presence of the characteristic void between hard and soft coextruded materials, as seen in Figure 69, and the necking down of the soft material just ahead of the void are associated with the flow system which results in whiskering.

The slight thinning of the can near the tip of the whiskers is thought to be due to the discontinuity between all hard material and hard material with a soft core. This discontinuity thus subjects the can to an abrupt pressure change and produces the thinning effect seen in Figure 68.



In Series 24, the same basic mechanism is operating except that the chamfer acts to some degree as a compensating interface to produce whiskers which are shorter and nearer the axis of the rod. Referring to Figures 71 and 72, the chamfer is seen to fold in toward the axis as it traverses the cone, thus allowing a path for more hard material to move in the periphery of the cone and die openings. The net effect is to place more cladding material between the tip of the whiskers and the surface of the clad and thus restrict the whiskers to a point nearer the axis of the rod. As can be seen, the necking down near the base of the "defect" is more severe with the chamfered billets due to the flow of more hard material to this point of weakness. It should also be noted that thinning of the canning material did not occur with the chamfered billets because the point of discontinuity at the tip of the whisker was further from the can and less likely to produce abrupt pressure changes.

In Series 25 the whisker mechanism has been exaggerated by use of air as the "soft" material, and the effect is as would be expected, with very long whiskers produced and extreme necking down just forward of the base of the "defect". The axial line after the "defect" in specimen 15168 of Figure 74 is a flaw and not to be considered part of the "defect" itself. Rounding the corner of the billet for specimen 15169 had the effect of shortening the "defect" length by about 1/3 that in specimen 15025 - 15027.



IV. CONCLUSIONSA. Main Series

1. Increasing interface angle and decreasing included cone angle both lead to a shorter "defect"; decreasing cone angle reduces the preshaping necessary to optimize "defect" length. As K-ratio increases, the preshaping required for "defect" optimization is increased.

2. Under the conditions of this experiment, the S-curves of "defect" area variation with K-ratio developed by Wegner (19) were not reproduced. "Defect" length behaved in a manner explainable on the basis of the K's of the billet materials.

3. Qualitatively, "defect" length and area show a similar variation with cone angle, interface angle and K-ratio.

4. The "defect" lengths which resulted from Series 1-5 constitute not a single curve but are rather a part of a family of curves, and are therefore spread out over an area on the "defect" length - K-ratio plots.

5. "Defect" length, under conditions of these experiments, is reproducible within about  $\pm 15\%$ , regardless of the position of the "defect" within the billet.

6. A modest amount of overcompensation will reduce or eliminate the voids and dogboning normally associated with coextrusion of materials whose K-ratio is appreciably less than unity.

7. Spherical preshaping yields shorter "defects" than conical preshaping, whenever overcompensation occurs.

B. Double Extrusion

1. Double extrusion is a practical means of fabricating clad fuel rods when the K-ratio is near unity.

2. Small first reduction ratios, near 1.50, must be used if double extrusion is to succeed, since "defect" length is very sen-



sitive to first reduction ratio.

3. On the basis of the experiments conducted, "defect" length resulting from double extrusion with the optimum first reduction ratio is relatively insensitive to overall reduction ratio.

4. The optimum preshape geometry for conventional coextrusion is a severely flattened parabola.

5. Elimination of voids between the nose piece, cut-off, and billet assembly reduces "defect" length, as does providing the ram with a flat bearing surface for second extrusion.

6. The difficulty of producing the same amount of compensation in front and rear "defects" in a double extrusion results from differences in front and rear "defect" length in both extrusions. This difficulty may be met by varying the stiffness of the nose piece and cut-off.

#### C. Shift

1. Initial upset, billet and die alignment, liner and billet fit, and billet cooling have either no effect or a relatively minor effect upon shift.

2. Lubrication is the most significant contributing factor to the mechanism of shift.

3. Uneven lubrication in either the liner or the cone is equally significant to the shift mechanism.

4. Shift can occur at any position with respect to the liner.

#### D. Whiskers

1. Whiskers result from a different flow velocity of the hard and soft materials as they deform in the cone.

2. Penetration of soft material into hard material is not indicated as a mechanism involved in whisker formation.

3. Within limits, cone angle and preshaping can be profitably employed to control whiskers.

4. Chamfer of the billet components, although it will not eliminate whiskers, will direct them away from the surface of the cladding.



V. RECOMMENDATIONSA. Main Series

1. Further tests should be run in order to determine the exact form of the area occupied by "defect" lengths of various combinations of materials, when "defect" length is plotted against K-ratio for various extrusion conditions.

B. Double Extrusion

1. The application of the double extrusion process to tubular and other types of fuel elements should be investigated.

2. Double extrusion of materials with K-ratios appreciably different from unity should be investigated to determine the extent of whiskers and dogboning under these conditions.

3. The feasibility of using first reduction ratios less than unity should be investigated.

4. The degree of bonding between core and clad in double extrusion should be investigated quantitatively.

C. Shift

1. Further studies of the shift problem should be directed toward the development of better lubricants and better lubricating procedures for the coextrusion process.

D. Whiskers

1. Further whiskering studies should be conducted to determine the best type of billet geometry for controlling whiskers.



VI. APPENDIXA. Data SheetSpecimen Numbering:

The prefix before the extrusion number has the following meaning:

Prefix letter: (if included)	A - Front "defect" B - Rear "
Cone angle designation:	9 - 90° included cone angle
	6 - 60° " " "
	3 - 30° " " "
Interface angle designation:	0 - 0° Interface angle
	8 - 8° " " "
	1 - 16° " " "
	2 - 24° " " "

Example: A68-14437 indicates the front "defect" of extrusion 14437, extruded with 60° included cone angle, 8° interface angle.

Shift: The letter after shift length has the following meaning:

T - "Defect" was longer at the top of the rod.  
B - "Defect" was longer at the bottom of the rod.



Series 1 Data

Extrusion Number	K Tsi	"Defect" Area, in. <sup>2</sup>	Gross "Defect" Length, in.	Shift, in.	Net "Defect" Length, in.	Remarks
90.11738	10.9	1.53	5.37	0	5.37	
98.14134	11.0	1.42	4.56	0.44B	4.12	
98.14174	11.5	1.37	4.50	0.19B	4.31	Rerun of 98.14134
91.14177	12.2	0.85	2.94	0.56B	2.38	
92.14180	11.2	0.66	2.31	0.06T	2.25	
60.11903	10.4	1.04	2.81	0	2.81	
68.14175	12.2	0.72	2.31	0.56T	1.75	
68.14519	10.0	0.72	2.19	0.06T	2.12	Rerun of 68.14175
61.14520	10.0	0.50	1.91	0.38T	1.91	
62.14181	12.2	0.90	3.94	0.69T	3.94	
62.14521	10.7	0.92	3.66	0.62T	3.66	Rerun of 62.14181
30.11910	10.4	0.63	2.12	0.25T	1.87	
38.14176	12.4	0.34	1.50	1.12T	1.50	
38.14522	9.2	0.27	1.19	0.81T	1.19	Rerun of 38.14176
31.14523	9.2	0.70	2.16	0.25B	2.16	
32.14182	11.7	0.94	4.75	0	4.75	
32.14524	9.7	1.21	5.53	0.44T	5.53	Rerun of 32.14182



## Series 2 (Front "Defect") Data

Extrusion K <sub>1</sub> , Number	K <sub>2</sub> , T <sub>51</sub> Area, in. <sup>2</sup>	"Defect" 2 Length, in.	Gross "Defect" Length, in.	Shift, in.	Net "Defect" Length, in.	Remarks
A90.14432 12.0 18.6	0.84	2.50	2.50		2.50	Can thickness zero at forward end of "defect". 3/8" conical void between naval brass and CuNi.
A98.14433 11.8 19.2	0.49	1.56	0.50T		1.06	Can thickness zero at forward end of "defect". 1/8" void between naval brass and CuNi.
A91.14434 11.3 18.4	0.53	1.34	0.38T		1.34	Can very thin at forward end of "defect".
A92.14435 11.2 18.8	1.14	3.06	0.19T		3.06	Can very thin at forward end of "defect".
A60.14436 11.3 19.7	0.96	2.34	0.38T		1.96	Can very thin at forward end of "defect". 1/4" long void between naval brass and CuNi.
A68.14437 10.9 18.9	0.25	0.69	0.19B		0.50	Can very thin at forward end of "defect". 1/10" void between naval brass and CuNi.
A61.14438 11.7 19.1	1.08	2.84	0		2.84	Can thin at forward end of "defect", and broken open in several places.
A62.14439 11.2 18.8	0.19	1.78	0.06B		1.72	Can broken open all around at forward end of "defect". CuNi pulled away from naval brass at forward end of "defect".
A30.14440 9.5 18.4	0.17	0.44	0.12T		0.31	Can broke open all around at forward end of "defect".
A38.14441 10.2 19.2	0.53	1.88	0.12B		1.75	Can thinned at forward end of "defect", broken open in several places.
A31.14442 10.6 19.3	1.59	4.66	0.12T		4.54	Can thickened at forward end of "defect".
A32.14443 9.5 19.1	2.10	6.75	0		6.75	Can thickened at forward end of "defect".



## Series 2 (Rear "Defect") Data

Extrusion Number	$K_1$ , Tsi	$K_2$ , Tsi	"Defect" Area, in. <sup>2</sup>	Gross "Defect" Length, in.	Shift, in.	Net "Defect" Length, in.	Remarks
B90.14432	18.6	12.0	2.18	8.62	1.12T	7.50	Can wall thicker at top than bottom due to shift.
B98.14433	19.2	11.8	1.48	5.22	0.44B	4.78	
B91.14434	18.4	11.3	0.88	2.31	0.09T	2.22	
B92.14435	18.8	11.2	0.19	1.44	0.28T	1.44	
B60.14436	19.7	11.3	1.25	4.81	0.25T	4.56	
B68.14437	18.9	10.9	0.69	2.03	0.09T	1.94	
B61.14438	19.1	11.7	0.33	1.66	0.47T	1.25	
B62.14439	18.8	11.2	0.19	1.78	0.06B	1.72	Can thin in vicinity of "defect", broken open in several places.
B30.14440	18.4	9.5	0.66	2.91	0.22B	2.69	
B38.14441	19.2	10.2	0.45	1.19	0	1.19	
B31.14442	19.3	10.6	0.10	1.38	0.31T	1.06	
B32.14443	19.1	9.5	0.44	2.50	0	2.50	



Series 3 (Front "Defect") Data

Extrusion Number	K <sub>1</sub> , T <sub>si</sub>	K <sub>2</sub> , T <sub>si</sub>	"Defect" Area, in. <sup>2</sup>	Gross "Defect" Length, in.	Shift, in.	Net "Defect" Length, in.	Remarks
A90.14646	12.2	15.5	1.15	3.56	0.44T	3.12	Can thin at forward end of "defect". 5/16" void between naval brass and CuZn.
A98.14647	11.7	15.5	0.92	2.38	0.62B	1.75	Can thin at forward end of "defect". 1/8" void between naval brass and CuZn.
A91.14648	10.2	15.8	0.40	1.12	0.25B	1.12	Can thin at forward end of "defect".
A92.14649	10.2	15.3	1.04	3.06	0.84B	3.06	Can thin at forward end of "defect"; broken open in one place, in vicinity of small void between naval brass and CuZn.
A60.14650	11.2	15.8	0.63	2.75	0.69T	2.06	Void 1/8" long between naval brass and CuZn.
A68.14651	11.2	16.1	0.29	0.75	0.19B	0.75	
A61.14652	10.7	15.7	0.99	2.78	0.03B	2.75	Can broke open at one point just ahead of "defect".
A62.14653	10.2	15.3	1.74	5.41	0.38T	5.03	Can broke open at one point in vicinity of small void between naval brass and CuZn.
A30.14654	10.7	16.3	0.31	0.81	0.38T	0.43	Can broke open at one point just ahead of "defect".
A38.14655	10.7	15.7	0.72	2.44	0.06B	2.38	
A31.14656	11.2	16.3	1.39	4.56	0.25T	4.31	Can broke open at one point just ahead of "defect".
A32.14657	11.2	16.5	1.56	5.62	0.25T	5.37	Can thickened at forward end of "defect".



Series 3 (Rear "Defect") Data

Extrusion Number	$K_{Ts}^1$	$K_{Ts}^2$	"Defect" Area, in. <sup>2</sup>	Gross "Defect" Length, in.	Shift, in.	Net "Defect" Length, in.	Remarks
B90.14646	15.5	12.2	2.37	8.38	1.06T	7.31	
B98.14647	15.5	11.7	1.34	4.41	0.19B	4.22	
B91.14648	15.8	10.2	0.73	2.59	0.03T	2.56	
B92.14649	15.3	10.2	0.28	1.75	0.56B	1.19	
B60.14650	15.8	11.2	1.00	3.72	0.09B	3.62	
B68.14651	16.1	11.2	0.69	2.50	0.44B	2.06	
B61.14652	15.7	10.7	0.13	1.09	0.22T	1.09	
B62.14653	15.3	10.2	0.23	2.09	0	2.09	
B30.14654	16.3	10.7	0.76	2.62	0.44T	2.18	
B38.14655	15.7	10.7	0.33	1.50	0.31T	1.19	
B31.14656	16.3	11.2	0.08	1.31	0.38T	1.31	Can thickness reduced to zero in several areas in vicinity of "defect".
B32.14657	16.5	11.2	0.21	2.66	0.50T	2.66	



## Series 4 (Front "Defect") Data

Extrusion Number	$K_1'$ Tsi	$K_2'$ Tsi	"Defect" 2 Area, in. <sup>2</sup>	Gross "Defect" Length, in.	Shift, in.	Net "Defect" Length, in.	Remarks
A90.14818	18.4	15.3	1.45	5.12	0.50T	4.62	
A98.14819	18.9	15.8	1.00	3.12	0	3.12	
A91.14820	18.9	16.0	0.50	2.00	0.34B	2.00	
A92.14821	18.4	16.3	1.00	3.28	0.12B	3.28	
A60.14822	18.9	16.7	1.15	4.00	1.12T	2.88	Cone cracked during extrusion.
A68.14823	18.4	16.8	0.50	1.47	0.16T	1.31	
A61.14824	17.9	16.8	0.45	2.19	0.44B	2.19	
A62.14825	17.9	16.3	1.00	3.75	0	3.75	
A30.14826	17.9	16.8	0.50	1.56	0.25B	1.31	
A38.14827	16.8	16.3	0.25	1.03	0.31B	1.03	
A31.14828	16.8	16.3	0.80	3.25	0	3.25	
A32.14829	17.3	16.3	1.50	6.0	0.12T	5.88	



Series 4 (Rear "Defect") Data

Extrusion Number	$K_1$ , T <sub>Si</sub>	$K_2$ , T <sub>Si</sub>	"Defect" Area, in.²	Gross "Defect" Length, in.	Shift, in.	Net "Defect" Length, in.	Remarks
B90.14818	15.3	18.4	1.49	4.50	0	4.50	
B98.14819	15.8	18.9	1.05	2.75	0.19T	2.56	
B91.14820	16.0	18.9	0.70	1.88	0.03B	1.85	
B92.14821	16.3	18.4	1.15	3.75	0.12B	3.75	
B60.14822	16.7	18.9	0.98	2.94	0.06B	2.88	Cone cracked during extrusion.
B68.14823	16.8	18.4	0.38	1.31	0.34T	0.97	
B61.14824	16.8	17.9	0.99	2.84	0.38B	2.84	
B62.14825	16.3	17.9	1.46	4.97	0.16T	4.97	
B30.14826	16.8	17.9	0.50	1.44	0.06B	1.38	
B38.14827	16.3	16.8	0.42	1.31	0.06T	1.31	
B31.14828	16.3	16.8	1.14	3.94	0.12B	3.82	
B32.14829	16.3	17.3	1.72	6.31	0.12B	6.19	



Series 5 Data

Extrusion Number	$K_1$ , Tsi	$K_2$ , Tsi	Gross "Defect" Length, in.	Shift, in.	Net "Defect" Length, in.	Remarks
14553	18.3	-	4.00	0.19B	3.81	
14564	18.3	-	3.44	0.78T	2.66	
14574	20.4	-	2.66	0.19T	2.47	
14532	21.4	-	3.78	1.25T	2.53	
A14668	9.2	18.4	1.75	0.19B	1.56	Can broke open at forward end of "defect".
B14668	18.4	9.2	7.22	0.62T	6.50	
A14669	14.8	16.8	4.06	0.31B	3.75	
B14669	16.8	14.8	4.88	0	4.88	
A14670	15.3	16.8	4.44	0.56T	3.88	
B14670	16.8	15.3	5.19	0.50T	4.69	



Series 6 Data

Extrusion Number	$K_1$ , T <sub>Si</sub>	$K_2$ , T <sub>Si</sub>	Gross "Defect" Length, in.	Shift, in.	Net "Defect" Length, in.	Remarks
A68.14975	14.8	11.7	3.25	0.50B	2.75	Recorder readings believed inaccurate.
B68.14975	11.7	14.8	0.69	0.25B	0.69	" " "
A61.14976	14.8	10.2	2.06	0.31B	1.75	" " "
B61.14976	10.2	14.8	2.00	0	2.00	" " "
A62.14977	14.8	10.2	1.44	0.19B	1.25	" " "
B62.14977	10.2	14.8	5.19	0	5.19	" " "

Series 7 Data

Extrusion Number	$K_1$ , T <sub>Si</sub>	$K_2$ , T <sub>Si</sub>	Gross "Defect" Area, in.	Shift, in.	Net "Defect" Length, in.	Remarks
A68.15005	9.2	16.9	1.25	1.12T	0.12	Visual pressure gage K data.
B68.15005	16.9	9.2	3.62	1.00T	2.62	" " "
A61.15006	9.2	16.9	1.00	0	1.00	" " "
B61.15006	16.9	9.2	1.56	0.56T	1.00	" " "
A62.15007	8.7	16.4	2.00	0	2.00	" " "
B62.15007	16.4	8.7	1.12	1.00B	0.12	" " "



Series 8 Data

Extrusion Numbers	Extrusion Length, in.	Gross "Defect" Length, in.	Shift, in.	Net "Defect" Length, in.	Remarks
1 14247	0.19	0.06T	0.12	Broken open for inspection after first extrusion.	
2 14248	0.62	0.12T	0.50	Broken open for inspection after first extrusion.	
3 14389	3.38	0.38B	3.00	Milled open for inspection after first extrusion.	
4 14296/14328	1.38	0.38T	1.00		
5 14346/14367	0.50	0.22T	0.50		
6 14384/14503	1.06	0.38T	0.88		
7 14347/14368	3.50	0.38B	3.50		
8 14385/14505	4.88	0.19B	4.88		
9 14386/14504	1.62	0.62T	1.62		
10 14348/14506	2.50	0.81B	2.50		
11 14387/14507	5.88	0.50T	5.88		
12 14388/14508	6.50	0.34T	6.50		
13 14559/14565	0.81	0.56B	0.50	Rerun of 14296/14328 (Extrusion 4)	



Series 9 Data

Extrusion	Extrusion Numbers	Gross "Defect" Length, in.	Shift, in.	Net "Defect" Length, in.	Remarks
1	A <sub>1</sub> 4645/14667	0.81	0	0.81	
1	B <sub>1</sub> 4645/14667	0.31	0.06B	0.25	
2	A <sub>1</sub> 4758/14764	0.78	0.19	0.59	
2	B <sub>1</sub> 4758/14764	0.22	0	0.22	
3	A <sub>1</sub> 4793/14805	0.62	0.38T	0.25	
3	B <sub>1</sub> 4793/14805	0.75	0.31B	0.44	Estimated from appearance of "butt".

Series 10 Data

Extrusion	Extrusion Numbers	Gross "Defect" Length, In.	Shift, in.	Net "Defect" Length, in.	Remarks
1	A <sub>1</sub> 4994/14996	1.00	0.25T	0.75	Under compensated.
1	B <sub>1</sub> 4994/14996	1.12	0.25T	0.75	Over compensated.



Series 11 Data

Extrusion Number	Gross "Defect" Length, in.	Shift, in.	Net "Defect" Length, in.	Remarks
14695	5.84	0.06B	5.78	5° angle on rear billet component.
14696	5.87	0.22T	5.65	10° angle on rear billet component.
14697	6.06	0.50B	5.56	15° angle on rear billet component.

Series 12 Data

Extrusion Number	Gross "Defect" Length, in.	Shift, in.	Net "Defect" Length, in.	Remarks
14707	5.84	0.59T	5.25	Uncanned.
14708	5.87	0.18T	5.69	Uncanned.
14709	5.50	0.22B	5.28	Uncanned.



## Series 13 Data

Extrusion Number	Gross "Defect" Length, in.	Shift, in.	Net "Defect" Length, in.	Remarks
14635	6.81	0.78T	6.03	1.875" O.D. can.
14636	6.68	0.56T	6.12	1.875" O.D. can
14637	6.68	0.62T	6.06	1.875" O.D. can.
14759	7.25	1.00T	6.25	1.75" O.D. can.
14760	6.75	0.25T	6.50	1.75" O.D. can.
14761	6.68	1.06T	5.62	1.75" O.D. can.

## Series 14 Data

Extrusion Number	Gross "Defect" Length, in.	Shift, in.	Net "Defect" Length, in.	Remarks
14700	5.25	0.31B	4.94	Billet cooled 15 sec. in cold liner.
14698	4.94	0	4.94	Billet cooled 30 sec. in cold liner.
14699	4.75	0.38T	4.37	Billet cooled 60 sec. in cold liner.



Series 15 Data

Extrusion Number	Gross "Defect" Length, in.	Shift, in.	Net "Defect" Length, in.	
14692	6.00	0	6.00	Full lubrication with Ore-Lube.
14693	5.88	0.12B	5.75	Full lubrication with Ore-Lube.
14694	6.06	0.34B	5.72	Full lubrication with Ore-Lube.
14783	12.00	1.25T	10.75	Full lubrication with Fiske's Lube.
14784	8.25	1.25T	7.00	Full lubrication with Fiske's Lube.
14785	8.00	2.13T	5.87	Full lubrication with Fiske's Lube.

Series 16 Data

Extrusion Number	Gross "Defect" Length, in.	Shift, in.	Net "Defect" Length, in.	
14571	3.31	0.37	2.94	"Ideal" Lube; shift on side.
14752	4.75	0.06B	4.69	"Ideal" Lube.
14683	4.38	0	4.38	"Ideal" Lube.



VI. APPENDIX (CONT.)B. DETERMINATION OF THE EXTRUSION CONSTANT, K.

One of the most useful relationships which has been evolved to describe quantitatively the extrusion process is the concept of extrusion constant, K, which gives a measure of the resistance to deformation of a metal under specified conditions. Early in the art, it was shown (12) that if the extrusion pressure is plotted against the natural logarithm of the area reduction ratio, straight lines are obtained which pass through the origin, thus indicating the relationship

$$P = K \ln A_1 / A_2$$

where  $P = F / A_1$  = extrusion pressure in tons per square inch

$F$  = Force applied by the ram in tons

$A_1$  = cross sectional area of the liner in square inches

$A_2$  = cross sectional area of the die aperture in square inches

$A_1 / A_2$  = area reduction ratio

$K$  = Extrusion constant in tons per square inch

The extrusion constant is essentially a constant characteristic of a metal under given temperature conditions but also depends upon many other factors and must therefore be determined experimentally for each set of extrusion conditions. Some of the factors which have a second order effect on  $K$  are ram speed, lubrication techniques, die geometry, cone angle, and canning techniques. A complete discussion of these effects is given in reference 18.

During the course of this investigation, all of the above factors were varied depending upon the information being sought in each series of experiments.

Chapter III. states the conditions under which each series of experiments was conducted, and the Appendix, A. Data Sheet lists the  $K$  values which were obtained for the extruded rods.

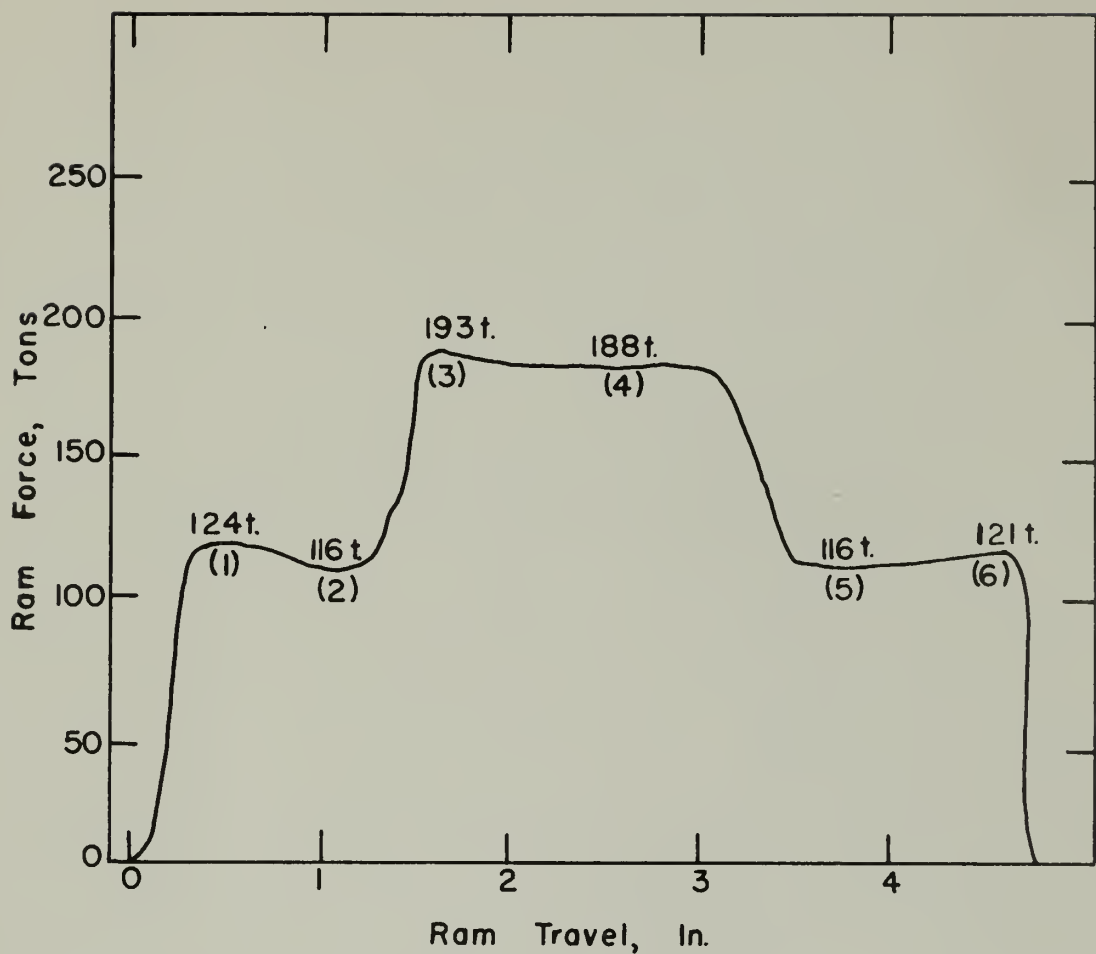


During the actual extrusion process, the force applied by the ram (the quantity  $F$  above) was recorded by means of a revolving drum and stylus. The drum rotation was controlled by the forward movement of the ram, and the stylus was positioned by the hydraulic pressure of the extrusion press acting through a Bourdon tube and suitable linkages. This arrangement resulted in a graph of force in tons versus ram travel. Knowing the cross sectional area of the liner and die, the extrusion constant was calculated by the formula given above.

The matter of judgment entered in the selection of the value of  $F$  from the graph which best characterized the particular conditions of each extrusion. Figure 75, which is typical of the type of curve obtained for a three-element billet (stiffer material in the middle) shows that  $F$  is never absolutely constant during the extrusion process.

Figure 75 is a full size tracing of the graph obtained during extrusion of specimen 14433 (series 2). In this instance, the  $K$ 's were computed from  $F=116$  tons and  $F=188$  tons. These values were selected because they appeared to represent "equilibrium" conditions of ram force. Point (1) on the curve represents non-equilibrium conditions in that initial upset has just been completed, and flow of the softer metal is beginning. Similarly, point (3) occurred just after the front "defect" left the die and flow of the harder material alone was beginning. Points (5) and (6) represent different phenomena: point (5) occurred after the rear "defect" had left the die, and point (6) occurred just as the ram stopped. The gradually rising curve of ram force after extrusion of the rear "defect" is typical and thought to be due to "flash", or the forcing of can material between the liner and the ram as extrusion progresses. Ram force, and apparent  $K$ , is increased because of the resulting increase in friction between ram and liner. For this reason, the





Extrusion 14433, Series 2  
Full Scale

Figure 75 - Typical Graph of Ram Force vs. Ram Travel for a Three-Element Billet.



portion of the curve recorded after extrusion of the rear "defect" was always ignored in the determination of K for the end materials.

In plotting the data for the Main Series experiments, average values of K were used. The values from Series 1-7 were used to compute an average K for each material with the thought that this average value would thus represent a reasonable value typical of the conditions of the experiment. Average K values were computed for cone angles of  $30^\circ$ ,  $60^\circ$ ,  $90^\circ$ ; and as the data below indicates, there was no significant variation in view of the 10% variation in observed K's.

Table XIII - Average K Values (tsi)

Material	All Cones	$30^\circ$ Cones	$60^\circ$ Cones	$90^\circ$ Cones
Naval Brass	10.8	10.9	10.7	11.2
Cu 10 w/o Ni	18.5	18.2	18.7	18.7
Cu 16 w/o Ni	21.95	--	--	--
Cu 5 w/o Zn	16.1	16.4	16.2	15.8

The average K values computed from Series 1-7 for the latter three materials are considerably lower than those anticipated at the beginning of this investigation. Since the exact conditions under which previous investigators obtained K values for these materials did not correspond to the conditions of this investigation, it is believed that this variation is to be expected.

Although graphs were obtained for all extrusions, K values were computed for only the Main Series experiments, for the following reasons:

- Although whiskering is known to be a K dependent phenomenon, K values would normally be ascertained by some simple form of billet geometry such as that used in the Main Series experiments, and therefore these K values were considered satisfactory for analysis of whiskering results



- b. Shift is independent of  $K$ , as may be seen from Figure 57
- c.  $K$  for the double extrusion experiments is of little practical interest because of the low area reduction ratio involved with a preponderance of friction force.

Approximately half way through the experimental work, the recorder gave obviously incorrect results on several occasions. This led to comparison of recorder pressures with those read directly from gauges mounted on the extrusion press. Although the recorder was overhauled, gauge pressures persisted in being 20-30 tsi higher than those of the recorder. The extrusions affected were those of Series 3 and 7, for which gauge pressures were used to calculate  $K$ . It should be noted that the resulting  $K$  values compare well with those from other series.



VI. APPENDIX (Cont.)C. LOCATION OF ORIGINAL DATA

All original data resulting from this investigation is on file at

Nuclear Metals, Inc.  
155 Massachusetts Ave.  
Cambridge, Massachusetts

All specimens are also mounted on display boards at the same location.



VI. APPENDIX (Cont.)D. Literature Citations

- (1) Allen, L. R. and Loewenstein, P., MIT-1086, pp. 39-46, Cambridge, Mass., M.I.T. Metallurgical Project (1952), CONFIDENTIAL.
- (2) Aronin, L. R., Loewenstein, P., and Roll, I.B., NMI-1126, p. 109, Cambridge, Mass., Nuclear Metals, Inc. (1954), CONFIDENTIAL.
- (3) Aronin, L. R. Loewenstein, P., and Pickett, J.J., NMI-1169, pp. 19-25, Cambridge, Mass., Nuclear Metals, Inc. (1956), CONFIDENTIAL.
- (4) Beck, C. J., Lacy, C. E., Ray, W.E., and White, D.W., KAPL-1546, Schenectady, New York, General Electric Co. (1956), CONFIDENTIAL.
- (5) Jaffe, D., KAPL-1578, Schenectady, New York, General Electric Co. (1956), SECRET.
- (6) Loewenstein, P., MIT-1065, pp. 47-52, Cambridge, Mass., M.I.T. Metallurgical Project (1951), CONFIDENTIAL.
- (7) Loewenstein, P., Roll, I. B., and Fitzpatrick, J., MIT-1117, pp. 111-117, Cambridge, Mass., M. I. T. Metallurgical Project (1954), SECRET.
- (8) Paynton, W. C., MIT-1115, pp. 67-79, Cambridge, Mass., M. I. T. Metallurgical Project (1954), SECRET.
- (9) Paynton, W. C., MIT-1117, pp. 118-144, Cambridge, Mass., M. I. T. Metallurgical Project (1954), SECRET.
- (10) Paynton, W. C. Ibid., pp. 145-151, SECRET.
- (11) Paynton, W. C. and Randall, R. N., NMI-1146, Cambridge, Mass., Nuclear Metals, Inc. (1956), SECRET.
- (12) Pearson, C., "Extrusion of Metals", second edition, New York, John Wiley and Sons Inc., (1953).
- (13) Roll, I. B., Loewenstein, P., and Fitzpatrick, J., MIT-1115, pp. 57-66, Cambridge, Mass., M. I. T. Metallurgical Project (1954), SECRET.
- (14) Roll, I. B., NMI-1139, pp. 43-58, Cambridge, Mass., Nuclear Metals, Inc. (1956), SECRET.
- (15) Roll, I. B. NMI-4518, Cambridge, Mass., Nuclear Metals, Inc., (1957), CONFIDENTIAL.
- (16) Sawyer, H. F., Loewenstein, P., Paynton, W. C., and Corzine, P., ANL-5568, Cambridge, Mass., Nuclear Metals, Inc. (1956), CONFIDENTIAL.



- (17) Sawyer, H. F. and Loewenstein, P., NMI-1169, pp. 6-18, Cambridge, Mass., Nuclear Metals, Inc. (1956), **CONFIDENTIAL**.
- (18) Tuer, G. L., MIT-1115, pp. 80-137, Cambridge, Mass., M. I. T. Metallurgical Project (1954), **SECRET**
- (19) Wegner, W., "A Study of Metal Flow During Integral End Closure Extrusion Cladding", M. S. Thesis, Chem. Eng., M. I. T. (1956).











JA 17 58  
7 Sept. 59

BINDERY  
INTERLIB  
AEC

Thesis 35894  
L246 Lakey  
End seal defects in co-  
extruded reactor fuel  
elements.

JA 17 58  
7 Sept. 59

BINDERY  
INTERLIB  
AEC

Thesis 35894  
L246 Lakey  
End seal defects in coextruded  
reactor fuel elements.

thesL246  
End seal defects in coextruded reactor f



3 2768 002 11288 0  
DUDLEY KNOX LIBRARY